Post-transcriptional modification of gephyrin and glycine receptor messenger RNA in temporal lobe epilepsy

Inaugural-Dissertation to obtain the academic degree
Doctor rerum naturalium (Dr. rer. nat.)

Submitted to the Department of Biology, Chemistry and Pharmacy
of Freie Universität Berlin

by

Benjamin Förstera

from Berlin

2011

This work was carried out within 3 years and 7 months (March 2008 to September 2011) under supervision of Prof. Dr. Jochen C. Meier at the Max Delbrück Center for Molecular Medicine (MDC).

1st Reviewer: Prof. Dr. Jochen C. Meier

2nd Reviewer: Prof. Dr. Fritz G. Rathjen

Date of defence: 02.02.2012

Eidesstattliche Erklärung

Hiermit versichere ich, Benjamin Förstera aus Berlin, dass ich die vorliegende Dissertation mit dem Titel „**Post-transcriptional modification of gephyrin and glycine receptor messenger RNA in temporal lobe epilepsy**“ selbstständig und ohne unerlaubte Hilfe angefertigt habe. Alle verwendeten Hilfsmittel und Quellen wurden angegeben.

Des Weiteren erkläre ich, dass die vorliegende Dissertation in keiner anderen Fakultät oder Universität vorgelegt oder veröffentlicht wurde, mit Ausnahme der in PubMed indizierten Publikationen.

Die Promotionsordnung des Fachbereichs Biologie, Chemie und Pharmazie der Freien Universität Berlin ist mir bekannt.

Berlin, 22.09.2011 Benjamin Förstera

Acknowledgements

My thanks go to Jochen Meier for the opportunity to work on this project in his lab at the Max Delbrück Center for Molecular Medicine. His advice and support were invaluable and his direct supervision highly appreciated.

I thank my colleagues Aline Winkelmann, Anne Schäfer, Carola Bernert, Josephine Grosch, Liana Kosizki, Sabrina A. Eichler, Sandra Herms, Sebastian Tausch and Silke Dusatko, which accompanied and supported me throughout this work. I am especially grateful to Caro, for constructive support and introduction into many of the techniques. I want to thank all of them, not only for their work, but also for making the lab a nice place to work - singing made the preparation much more fun.

I also thank Jochen Meier and the co-authors Abdel Ali Belaidi, Birthe Smolinsky, Carola Bernert, Christoph Dehnicke, Günter Schwarz, Michael Fähling, Michael Tsokos, Pascal Legendre, Peter Horn, René Jüttner, Sabrina A. Eichler and Thomas-Nicolas Lehmann for their contribution to the publications this thesis refers to. I thank Jean-Marc Fritschy for providing the GABA(A)R alpha2 antibody used in publication 1, and I also thank him and Brian E. Derrick for helpful comments on that manuscript. I am grateful to Anje Sporbert and Thomas Willnow for access to the confocal microscope.

Furthermore, I thank Fritz Rathjen for acting as reviewer of my PhD thesis. I also thank Thomas Willnow and Udo Heinemann for participation in my PhD committee.

I am grateful for the funding of my project by the Helmholtz Association as well, as funding for material support from the SFB-TR3 of the DFG.

Besonders dankbar bin ich meiner Mutter und meinem Bruder für die persönliche und auch materielle Unterstützung während des Studiums und der Doktorarbeit.

Finally, my thanks go to Tina for her company, for support and motivation.

Table of contents

2. Material and methods

3. Manuscripts

4. Discussion

5. Appendix

1. Introduction

1.1 About the dichotomous nature of chloride signalling in the brain – The chloride equilibrium potential

The chloride equilibrium potential dictates the direction of chloride flux through chloride channels, and it is regulated mainly by the relative expression level of sodium potassium chloride co-transporter 1 (NKCC1), transporting chloride into the cell, and potassium chloride co-transporter 2 (KCC2), which pumps chloride out of the cell. In the developing brain, NKCC1 gene (*SLC12A2* in human, *Slc12a2* in mouse) expression levels are high, while KCC2 expression is low (Rivera *et al.* 2005). Consequently, the intracellular chloride concentration is high, which can render chloride channels excitatory through chloride efflux, depending on the actual membrane potential (Rivera *et al.* 1999). This property facilitates the emergence of giant depolarising potentials (GDPs) in early nervous system development, which is crucial for the establishment of neuronal circuit connectivity (Ben-Ari 2001). This includes the developmental switch of chloride signalling across the plasma membrane from depolarisation to hyperpolarisation as KCC2 expression is regulated by intracellular calcium dynamics, mainly through voltage-dependent calcium channels and not as previously assumed by the neurotransmitter gamma-amino butyric acid (GABA) itself (Ganguly *et al.* 2001; Ludwig *et al.* 2003). On the other hand, expression of the KCC2 gene (*SLC12A5* in human, *Slc12a5* in mouse) can rapidly be down-regulated in response to exposure of neurons to brain-derived neurotrophic factor (BDNF) (Aguado *et al.* 2003), leading to reduced cell surface expression of KCC2 through tyrosin kinase B (TrkB) signalling (Rivera *et al.* 2002; Rivera *et al.* 2004).

1.2 GABA & Glycine

GABA is synthesised from glutamate by glutamic acid decarboxylase (GAD), while glycine is produced by serine hydroxymethyltransferase using serine as a substrate. Both GABA and glycine are loaded into vesicles by the vesicular inhibitory amino acid transporter (VIAAT). Glycine and GABA can be released from separate synapses and co-released from the same synapses in separate vesicles or even from the same vesicle (Jonas *et al.* 1998; Meier 2003). However, VIAAT is more efficient in loading vesicles with GABA than with glycine (Gasnier 2000). Thus, pre-synaptic expression of glycine transporters (GlyT) is required for pre-synaptic vesicle loading with glycine (Aubrey *et al.* 2007).

GABA and glycine are considered the two main neurotransmitters of the ligand-gated ion channel (LGIC) superfamily in the central nervous system, which act at chloride-permeable members. While GABA seems to predominate in the brain, glycine was primarily, but not exclusively, associated with the spinal cord and brain stem (Malosio *et al.* 1991). Large amounts of glycine are stored by astrocytes however, the numerically dominating non-neuronal cell type astrocyte in the brain stores, and this glycine can be released upon depolarisation-induced reversal (e.g. triggered by glutamate release) of GlyT-1 mediated chloride transport (Eulenburg and Gomeza 2010). Moreover, glycine is required as a co-agonist of NR1 subunit-containing NMDARs (N-methyl-D-aspartate receptors) and can be released from glutamatergic nerve endings (Cubelos *et al.* 2005; Raiteri and Raiteri 2010). Thus, glycine may also be a major neurotransmitter in the brain.

1.2.1 Inhibition

The term “inhibition” reflects the reduced ability of neurons to discharge due to “inhibitory” mechanisms. According to this definition, potassium channels are equally well suited to silence neurons as chloride channels. The ability of potassium channels to compensate for loss of a GABA(A) receptor (GABA(A)R) subunit in the alpha 6 knock-out mouse exemplifies the relevance of plasticity mechanisms in the brain (Brickley *et al.* 2001). While both GABAergic and glycinergic inhibition can be mediated by post-synaptic receptors, a major part of it is caused by non-synaptic receptors, and the impact of tonic inhibition can be more than three times as high as that of phasic inhibition (Mody and Pearce 2004). In fact, recent use of most advanced techniques for visualisation of neurotransmitter receptors has revealed that the vast majority of GABA(A)Rs in the hippocampus is actually non-synaptic (Kasugai *et al.* 2010), suggesting that non-synaptic transmission could play a much more significant role than was previously assumed.

The term “shunt inhibition” describes the ability of a neuron to regulate its excitability by exerting ion channel mechanisms irrespectively of sub-cellular localisation issues. Due to a decrease of the membrane resistance upon channel opening at non-synaptic sites, the electrotonic transmission of depolarisation from synapses to the axon initial segment, where neuronal firing initiates, can thus effectively be antagonised due to increased leak current (Mitchell and Silver 2003). Accordingly, shunt inhibition works as a strong determinant of cellular gain control, while GABAergic synaptic transmission provides neurons with narrow time slots required for spike-timing precision and temporal encoding of sensory inputs (Cardin *et al.* 2009).

To underscore the relevance of the chloride equilibrium potential for brain pathology, it should be noted here that chronic silencing of neuronal activity eliminates neurons from the activity-dependent developing nervous system (Tao and Poo 2005) or in pathological conditions when the chloride equilibrium potential returns to an earlier developmental state (Eichler *et al.* 2008). Chronic neuronal silencing does not necessarily provoke neurodegeneration (Shulga *et al.* 2008) in the adult nervous system, when both glutamatergic and GABAergic mechanisms are already established and KCC2 surface expression is not down-regulated, yet it is compensated for by homeostatic regulation of glutamatergic as well as GABAergic synaptic inputs (Eichler *et al.* 2008). This fact highlights chloride signalling as a major determinant of physiological and pathophysiological processes, both early in development as well as at more mature stages.

1.2.2 Glycine Receptor (GlyR)

Glycine receptors are chloride channels, that share structural homology with the nicotinic acetylcholine receptor (nAChR), serotonin receptor (5HT3), GABA(A)R and GABA(C) receptors, all of which belong to the LGIC superfamily of neurotransmitter receptors. Each GlyR subunit has a large extracellular N-terminus, characteristic for the LGIC superfamily, which is involved in ligand binding and requires two disulfide bridges for appropriate protein folding. Furthermore, each subunit has four transmembrane (TM) domains, with TM2 being predicted to line the channel pore, a large intracellular loop between TM3 and 4, and an extracellular C-terminus. There are several phosphorylation, glycosylation and ubiquitination sites (Legendre 2001; Breitinger and Becker 2002).

1. Introduction

Five genes encode GlyR subunits, *GLRA1-4* (Betz and Laube 2006; Lynch 2009) and *GLRB*. However, *GLRA4* is a pseudo-gene that is not expressed (Simon *et al.* 2004), and the beta subunit encoded by *GLRB* is unable to build functional homomeric receptors. GlyR channels are pentameric, either hetero-pentameric involving two alpha and three beta subunits or homo-pentameric consisting of five alpha subunits. The beta subunit of heteromeric receptors modulates ligand binding (Grudzinska *et al.* 2005) and mediates post-synaptic receptor-stabilisation via gephyrin binding (Kirsch *et al.* 1991; Meyer *et al.* 1995; Meier *et al.* 2000; Meier *et al.* 2001; Moss and Smart 2001; Meier and Grantyn 2004). Lacking this property of the beta subunit, homomeric GlyR are mainly excluded from post-synaptic sites (Meier *et al.* 2001).

GlyR have a broad range of action as they are involved in vision (Haverkamp *et al.* 2003; Wassle 2004) and processing of acoustical stimuli (Dlugaiczyk *et al.* 2008), contribute to the generation of motor-rhythms, locomotor behaviour and spinal reflexes (Legendre 2001). Furthermore, they are involved in processing of nociceptive signals in the spinal cord (Harvey *et al.* 2004). Moreover, GlyR are expressed in the hippocampus (Chattipakorn and McMahon 2002; Chattipakorn and McMahon 2003; Kirchner *et al.* 2003; Chattipakorn and McMahon 2004; Song *et al.* 2006; Eichler *et al.* 2008; Eichler and Meier 2008), although their function in this brain region has remained undetermined.

Posttranscriptional processing of GlyR includes alternative splicing of *GLRA1* and *3* mRNA sequences encoding the intracellular loop, as well as in the N-terminal ligand binding domain of *GLRA2*. The exclusion of 8 or 15 amino acids, respectively, turns GlyR alpha1INS (insert) to alpha1deltaINS and GlyR alpha3L (long) to alpha3K

(short), decelerating desensitisation kinetics of the shorter isoforms in both cases (Malosio *et al.* 1991; Nikolic *et al.* 1998). In GlyR alpha2B, an isoleucine and alanine are integrated in place of a valine and threonine of GlyR alpha2A, resulting in increased agonist potency (Kuhse *et al.* 1991; Miller *et al.* 2004).

C-to-U RNA-editing via cytidin-deaminase replaces proline 185 with leucine in GlyR alpha3, which drastically increases the apparent affinity for both glycine and taurine (15- and 60-fold, respectively) and consequently enables the RNA-edited receptors to mediate tonic inhibition at ambient glycine levels (Meier *et al.* 2005). Likewise, proline-to-leucine substitution at corresponding position 192 in GlyR alpha2 has similar effects, and the amount of edited GlyR alpha2 and 3 mRNA in the hippocampus of patients suffering from intractable temporal lobe epilepsy (TLE) correlates with the severity of the disease (Eichler *et al.* 2008).

1.2.3 GABA(A) receptors (GABA(A)R)

While GABA(B) receptors are G-protein coupled, metabotropic receptors, both GABA(A) receptors (GABA(A)R) and GABA(C) receptors are ligand-gated chloride channels, which are permeable for chloride and bi-carbonate (Cossart *et al.* 2005). Similarly to GlyRs, each GABA(A)R subunit has 4 transmembrane domains (TM1-4), an extracellular N-terminus, including the ligand binding site, and an extracellular C-terminus, as well as a large cytoplasmic loop connecting TM3 and 4 and harbouring binding sites for GABA(A)R associated proteins as well as phosphorylation and ubiquitination sites (Moss *et al.* 1992; rancibia-Carcamo *et al.* 2009; Vithlani and Moss 2009).

1. Introduction

There are various subunits (alpha 1-6, beta 1-3, gamma 1-3 and delta) that can assemble into heteropentameric channels with a subunit stoichiometry of 2 alpha, 2 beta and 1 gamma or delta (Moss and Smart 2001). Pentameric GABA(A)R channels consisting of alpha1-3, beta and gamma subunits have low apparent agonist affinities in the millimolar range, according to their preferentially synaptic mode of action (Mody and Pearce 2004). GABA(A)R composed of alpha4-6 and delta subunits, optionaly containing beta subunits, are mainly non-synaptic, have a high apparent agonist affinity in the micromolar range and slow desensitisation kinetics, allowing them to effectively mediate tonic inhibition (Mody and Pearce 2004).

Alternative splicing of the gamma2 subunit produces the short gamma2S and the long gamma2L subunit. Gamma2L contains eight additional amino acids (LLRMFSFK) (Whiting *et al.* 1990) including the protein kinase C (PKC) phosphorylation site S343 (underlined) in the large intracellular loop (TM3-4). Gamma2S and L can likewise be phosphorylated by PKC at S327, and the beta1 subunit can be phosphorylated by cAMP-dependent protein kinase (PKA), as well as PKC at S409 (Moss *et al.* 1992). Phosphorylation of gamma2 contributes to the diversity of synaptic mechanisms as it regulates the number of postsynaptic GABA(A)R channels (Whiting *et al.* 1990; Muir *et al.* 2010), while the role of posttranslational modification of beta subunits awaits clarification. Knock-out of GABA(A)R gamma2 results in loss of synaptic GABA(A)Rs and gephyrin (Essrich *et al.* 1998; Schweizer *et al.* 2003; Alldred *et al.* 2005; Li *et al.* 2005). On the other hand, gephyrin knock-out leads to reduced GABA(A)R clustering (Levi *et al.* 2004; Yu *et al.* 2007), suggesting that both gamma2 and gephyrin are critically involved in regulation of post-synaptic GABA(A)R pools, which is in agreement with most recent data (Muir *et al.* 2010).

An interesting feature of the GABA(A)R alpha2 subunit is its preference in subcellular localisation for the axon initial segment, in addition to its involvement in perisomatic synaptic transmission. Both compartments are of high strategic relevance since GABAergic transmission at the axon initial segment directly controls action potential firing and perisomatic inhibition provides a powerful mechanism for the control of oscillatory hippocampal network activity involved in encoding of sensory inputs.

GABA(A)R alpha2 is able to directly interact with gephyrin (Tretter *et al.* 2008), while direct binding of gephyrin to other GABA(A)R subunits has remained controversial. The GABA(A)R-associated protein (GABARAP), which interacts with GABA(A)R as well as with gephyrin, is a candidate protein for regulation of GABA(A)R-recycling, membrane targeting or both, though it is not present at the synapse itself (Kanematsu *et al.* 2007; Chen and Olsen 2007). Perhaps, the lack of any deficits in GABARAP knock-out animals suggests that other yet unidentified homologues compensate for the inability of GABARAP to regulate post-synaptic GABA(A)R dynamics. On the other hand, GABARAP might selectively regulate intracellular GABA(A)R pools (O'Sullivan *et al.* 2005).

A putative complex for anterograde transport of GABA(A)R to GABAergic synapses involves KIF5C and the GABA(A)R beta2 subunit, but not gephyrin (Smith *et al.* 2006; Kneussel and Loebrich 2007). Retrograde transport of GABA(A)R alpha1 was recently reported to depend on muscelin and dynein (Heisler *et al.* 2011).

1.3 Gephyrin

Gephyrin is the evolutionary fusion product of two bacterial proteins, MogA and MoeA, in vertebrates. Bacteria require MogA and MoeA for molybdenum co-factor (MoCo) synthesis, which is also required in vertebrates for a variety of cellular redox reactions (Schwarz *et al.* 2009). Gephyrin is a highly conserved protein as it has homologues in insects (Cinnamon) and even in plants (Cnx1) (Stallmeyer *et al.* 1995; Stallmeyer *et al.* 1999; Xiang *et al.* 2001). In addition to its metabolic function, gephyrin serves as post-synaptic anchoring protein for GlyR and GABA(A)R at inhibitory synapses (Feng *et al.* 1998). It was first discovered in biochemical studies as a constituent of affinity-purified GlyR preparations (Luscher and Keller 2004; Kirsch 2006; Kneussel and Loebrich 2007).

1.3.1 Gephyrin structure and aggregation

Gephyrin consists of three domains; the 20 kDa N-terminal **G**-domain, homologous to Mo**g**A, the 43 kDa C-terminal **E**-domain, homologous to Mo**e**A, and the 18-21 kDa **c**entral **C**-domain linking these two regions (Lardi-Studler *et al.* 2007). The nomenclature of gephyrin isoforms has suffered from the independent discovery of distinct ‘splice-cassettes’ by different laboratories, so different protein-domains have been attributed the same name. Furthermore, the list of published pseudo-splice variants with C2 and C6 splice-cassettes which in fact are constitutively spliced, was ever growing. Fritschy et al. therefore proposed a new nomenclature system to solve these conflicts and allow explicit discrimination between the different splice-cassettes of the G-, C-, and E-domains (Fritschy *et al.* 2008).

The C-domain contains protein-binding sites for gephyrin interaction partners like collybistin, dynein light chain 1 and 2, and pin1, the peptidyl-prolyl isomerise NIMA interacting protein 1 (Kins *et al.* 2000; Navarro-Lerida *et al.* 2004; Bausen *et al.* 2006; Zita *et al.* 2007); it has also recently been found to be sensitive to proteolytic degradation (Tyagarajan *et al.* 2011). Furthermore, gephyrin contains 2 proline (P), glutamic acid (E), serine (S) and threonine (T) rich peptide (PEST) sequences (Prior *et al.* 1992), which are linked to caspase mediated cleavage and proteasomal degradation of proteins (Dice 1987; Belizario *et al.* 2008). PEST sequences are predicted to be positioned between amino acids 181 and 201 as well as 259 and 271 (Prior *et al.* 1992), *id est* in the C-domain.

In the central nervous system (CNS), the repertoire of splice-variants is characteristic for brain regions as well as neuronal and glial expression patterns (Meier and Grantyn 2004; Paarmann *et al.* 2006; Smolinsky *et al.* 2008). Alternative splicing of several of the 30 exons produces different gephyrin isoforms, with a tissue specific distribution, but only exon 6 in the G-domain has been attributed with a functional impact to date (Meier *et al.* 2000; Meier and Grantyn 2004; Bedet *et al.* 2006) and the majority (~80%) of gephyrin in the brain does not contain exon 6 (Paarmann *et al.* 2006). These delta 6 gephyrins build G-domain trimers, which together with E-domain dimerisation are proposed to lead to a hexagonal structure lattice, resulting in intracellular, globular aggregates in any cell type (Meier *et al.* 2000; Sola *et al.* 2004; Smolinsky *et al.* 2008). G-domain trimerisation crucially relies on the four hydrophobic amino acid residues F90, L113, L128, and L168, while the three mandatory residues necessary for E-domain dimerisation are G483, R523, and A532 (Saiyed *et al.* 2007).

The fore mentioned 20% of G-domains including exon 6 in the brain (Paarmann *et al.* 2006) build dimers leading to spine-like aggregates in tandem with E-domain dimerisation (Meier *et al.* 2000; Smolinsky *et al.* 2008). These exon 6 gephyrins exhibit dominant negative effects on regular gephyrin oligomerisation and post-synaptic GABA(A)R stabilisation (Meier *et al.* 2000; Meier and Grantyn 2004; Bedet *et al.* 2006; Fritschy *et al.* 2008).

1.3.2 GlyR and GABA(A)R binding of gephyrin

Gephyrin is a critical factor for GlyR clustering, cytoskeleton-interaction, intracellular transport, and regulation of lateral mobility in the plasma membrane (Kirsch *et al.* 1991; Meier *et al.* 2001; van Zundert *et al.* 2002; Hanus *et al.* 2004). The E-domain harbours the high affinity binding site for the GlyR beta TM3-4 large cytoplasmic loop in the vicinity of the E-domain dimerisation interface (Bedet *et al.* 2006), involving the crucial residues F330, Y673, and P713 (Schrader *et al.* 2004; Sola *et al.* 2004; Kim *et al.* 2006). Thus, each E-domain of a gephyrin trimer can bind to one of the three beta subunits of a hetoropentameric GlyR chloride channel. GlyR beta binding is enhanced by conformational changes to gephyrin, which are conferred by phosphorylation-dependent interaction with Pin1 (Zita *et al.* 2007). In analogy to GlyRs, gephyrin binds to a hydrophobic motif in the TM3-4 larger cytoplasmic loop of the GABA(A)R alpha2 subunit (Tretter *et al.* 2008; Saiepour *et al.* 2010).

1.3.3 Gephyrin trafficking and synaptogenesis

While gephyrin normally oligomerises specifically at glycinergic, GABAergic and mixed glycinergic/GABAergic synapses in the CNS, gephyrin recruitment to post-synaptic domains facing glutamatergic terminals is possible *in vitro* in the absence of appropriate pre-synaptic input (Christie *et al.* 2002; Brunig *et al.* 2002). In fact, recent

data demonstrates gephyrin interaction with both, neuroligin2 (predominantly found at GABAergic synaptic terminals) as well as neuroligin1 (found at glutamatergic pre-synaptic domains) in immature neurons, regulating both GABAergic and glutamatergic inputs to the same neuron (Varley *et al.* 2011).

Gephyrin serves as an adapter for conventional kinesin (KIF5) motor-proteins that provide a vehicle for anterograde transport of GlyR along microtubules to glycinergic synapses (Dumoulin *et al.* 2009). Furthermore, the gephyrin C-domain binds to dynein light chain1 and 2, which are constituents of motor proteins contributing to the retrograde transport of GlyR from glycinergic post-synapses along microtubules (Navarro-Lerida *et al.* 2004; Bausen *et al.* 2006; Maas *et al.* 2006). *In vitro*, gephyrin does also directly bind to polymerised tubulin, which might be achieved by a peptide-motive in the C-domain (exon 14) as this sequence shares homology with the core repeat sequence of microtubule-binding domains (VQSRCSSKENILRA) in tau and MAP2 (Ramming *et al.* 2000). Moreover, the gephyrin E-domain interacts with profilin1 and 2, as well as with the mammalian enabled/vasodilator stimulated phosphoprotein (Mena/VASP) (Giesemann *et al.* 2003; Neuhoff *et al.* 2005; Bausen *et al.* 2006); both being involved in actin polymerisation and thus interaction of gephyrin with microfilaments.

While GlyR and gephyrin are co-transported to glycinergic post-synapses (Hanus *et al.* 2004), the interaction between gephyrin and GABA(A)R seems to be limited mostly to cell surface receptors (Thomas *et al.* 2005), leaving intracellular GABA(A)R transport to be gephyrin independent (see **1.2.3**). Post-synaptic GABA(A)R clustering is facilitated by direct binding of gephyrin to the alpha2 subunit: However, post-synaptic GABA(A)R recruitment is still possible in the absence of gephyrin, although

the stability of GABAergic synapses is diminished and the number of post-synaptic GABA(A)Rs available for synaptic transmission is reduced (Fischer *et al.* 2000; Levi *et al.* 2004). Lack of GABA(A)R gamma2, on the other hand, leads to dispersion of GABA(A)R and loss of gephyrin clusters at GABAergic post-synapses. Thus and according to the pioneer role of the GABA(A)R in early nervous system development, the gamma2 subunit seems to be involved in establishment of the whole post-synaptic protein scaffold at GABAergic synapses. In fact, the gamma2 subunit could help to establish a molecular link between cell adhesion molecules such as neuroligin2 and gephyrin, hence serving a synapse-organising role (Poulopoulos *et al.* 2009) and providing post-synaptic protein scaffolds with GABA(A)R docking sites. In this context, pre-synaptic alpha-neurexin, and certain beta-neurexin splice variants, could confer specificity of post-synaptic GABA(A)R to GABAergic synapses and likewise contribute to the maturation of GABAergic synapses by inducing clustering of neuroligin2 (Kang *et al.* 2008).

Collybistin is a GDP-GTP exchange factor for G-proteins, which binds to the gephyrin C-domain. This interaction was originally proposed to be necessary for the translocation of gephyrin from cytoplasmic aggregates to sub-membranous accumulations (Kins *et al.* 2000), yet the fact that GlyRs are able to dissolve intracellular gephyrin aggregates and translocate gephyrin to the cell surface has disproved this hypothesis (Meier *et al.* 2001; Hanus *et al.* 2004). Notably, post-synaptic GlyR clustering seems to be completely independent of collybistin (Papadopoulos *et al.* 2007). In fact, the regional specificity in the loss of gephyrin and GABA(A)R clusters in collybistin-deficient mice, which is limited to amygdala and hippocampus, indicates that the situation is far more complex than previously assumed as it might involve yet unidentified gephyrin interaction partners.

Nonetheless, according to a recent publication (Saiepour *et al.* 2010), collybistin seems to be involved in regulation of post-synaptic alpha2-GABA(A)R dynamics.

In addition to these considerations, phosphorylation of gephyrin S270 by glycogen synthase kinase 3beta (GSK3beta) can regulate post-synaptic gephyrin clustering by conferring susceptibility of gephyrin to proteolysis by the calcium-activated cystein protease calpain-1, for which gephyrin is a direct substrate (Tyagarajan *et al.* 2011). Phosphorylation-deficient gephyrin, as well as inhibition of GSK3beta by its specific inhibitor GSK3-IX or the mood-stabilising drug Lithium, and inhibition of calpain-1 by over-expression of its endogenous inhibitor calpastatin (CAST), leads to increased post-synaptic gephyrin pools due to decelerated post-synaptic gephyrin turnover. As a possible mechanism for GSK3beta mediated susceptibility of gephyrin proteolysis, S270-phosphorylation by GSK3beta might lead to conformational changes in gephyrin, exposing one of the two PEST sequences mentioned above, residues 259-271 (DTASLSTTPSESP) in the C-domain, for calpain-1-mediated proteolysis (Tyagarajan *et al.* 2011). Likewise, phosphorylation-defective gephyrin increases mIPSC-amplitudes by 10% and reduces the inter-event interval by 25%. Interestingly, post-synaptic PSD95 cluster size increases at glutamatergic synapses in response to chronic Lithium treatment, which may represent a homeostatic compensatory mechanism of excitatory/inhibitory balance maintenance (Tyagarajan *et al.* 2011).

Beyond its the role of gephyrin in regulation of post-synaptic GABA(A)R pools, it might in fact also be involved in translational control at synapses through interaction with the rapamycin and FKBP12 target (RAFT1) in signal transduction pathways (Sabatini *et al.* 1999).

1.3.4 Molybdenum co-factor synthesis of gephyrin

The molybdenum co-factor (MoCo) is crucial for the function of molybdenum-dependent enzymes like sulphate oxidase, aldehyde oxidase and xanthine oxidoreductase, which are mainly active in the liver where they are involved in metabolic detoxification (Schwarz 2005; Fritschy *et al.* 2008). While MoCo-synthesis in nervous tissue is evident, particularly in glial cells, its relevance for brain function remains unknown (Smolinsky *et al.* 2008). Likewise, gephyrin is also very abundant in other non-neuronal cell types, especially liver and kidney (David-Watine 2001; Paarmann *et al.* 2006). These organs are known to mediate metabolic detoxification due to gephyrin dependent MoCo biosynthesis (Schwarz 2005; Lardi-Studler *et al.* 2007).

MoCo synthesis requires both the G-domain, which catalyses the adenylation of molybdopterin (MPT) to MPT-AMP, and the E-domain, which further catalyses the biosynthesis of MoCo from MPT-AMP (Schwarz *et al.* 2009). Meanwhile the C-domain is not directly involved, but it serves a spacer role in optimising MoCo synthesis through adjustment of the spatial proximity of G- and E-domains. Deficits in MoCo-synthesis lead to neurodegeneration, severe seizures and early childhood death (Feng *et al.* 1998; Reiss and Johnson 2003; Schwarz 2005), indicating that metabolic detoxification is crucial to nervous system integrity.

1.4 Glia cells

Glia cells are the non-neuronal cells of the brain, which are involved in axon-sheathing, synaptogenesis, synaptotrophic and metabolic support of neurons, as well as maintenance of the extracellular chemical milieu.

1. Introduction

There are three broad categories of glia cells, namely astrocytes, first described by Santiago Ramón y Cajal in 1913, microglia and oligodendrocytes, first described by Pio del Rio Hortega in 1921 and 1928 (Kettenmann and Verkhratsky 2008).

Microglia are the immune cells of the brain. They are derived from the immune system (Santambrogio *et al.* 2001) and modulate inflammatory processes. Upon injury, they are transferred from the inactive or scanning state to an active state, migrate to the site of the injury, remove cellular debris (Nimmerjahn *et al.* 2005) and secrete high levels of various cytokines, which amongst other effects, weaken the integrity of the blood-brain barrier (Arnett *et al.* 2001).

Oligodendrocytes are crucial for axon myelination in the central nervous system, similar to the Schwann cells of the peripheral nervous system (Kettenmann and Verkhratsky 2008). Beyond providing trophic support and insulation (Barres 2008), they also influence electrical and structural properties of axons through control of ion channel clustering and regulation of electrotonic transmission of depolarisation (Kettenmann and Verkhratsky 2008).

Astrocytes make up the basal, yet underestimated, connective tissue of the central nervous system. They are involved in metabolic processes, i.e. the glutamine cycle, energy supply to neurons (Magistretti 2006), control of extracellular ion levels such as potassium, and they are important for clearance of neurotransmitters from the synaptic cleft upon synaptic transmission (Barres 2008). Furthermore, they control the formation of the blood brain barrier by endothelial cells (Bundgaard and Abbott 2008) and excert control over the local blood flow (Zonta *et al.* 2003; Mulligan and MacVicar 2004).

1.5 The hippocampus

The hippocampal formation is part of the limbic system. In the human brain, it is situated in the medial telencephalon, beneath the cortical surface, inside the medial temporal lobe. The hippocampus is involved in spacial navigation and short term memory and is one of the first brain-areas damaged in Alzheimer´s disease, which is associated with disorientation and memory deficits or amnesia. It can also suffer damage through encephalitis, anoxia and temporal lobe epilepsy (TLE).

1.5.1 Hippocampal anatomy

The structure of the hippocampus is highly organised and made up of interconnected pyramidal cells, as well as more than 12 different types of interneurons, which employ at least 6 different neurotransmitters, among them acetylcholine (ACh), GABA, glutamate (Glu), glycine (Gly), noradrenalin (NA) and serotonin (5-HT) (Vizi and Kiss 1998; Sanes and Lichtman 1999). It consists of the subiculum (Sub), the cornu ammonis, which is divided into four regions (CA1 to 4), and the dentate gyrus (DG). The closely associated entorhinal cortex (EC), which is connected to many areas of the brain, is central to hippocampal information processing (see **Figure 1**) as EC layer II stellate cells and EC layer III pyramidal cells provide input to the hippocampus, while EC layers IV and V receive output from the hippocampus (Heinemann *et al.* 2000).

1.5.2 The main hippocampal circuit

The main hippocampal circuit (see **Figure 1**) consists of the excitatory projections of the perforant fibre pathway, mossy fibre pathway and Schaffer collateral (Heinemann *et al.* 2000). The hippocampus gets its main input via the perforant fibre pathway

passing through the subiculum, which originates from the large stellate pyramidal cells in layer II of the EC and terminates mainly onto granule cells of the stratum granulare in the DG and to a lesser degree onto CA3 pyramidal cells (Steward and Scoville 1976; Ruth *et al.* 1982; Ruth *et al.* 1988). Information is passed on from the DG granule cell layer to the CA3 pyramidal cells through the mossy fibre tract.

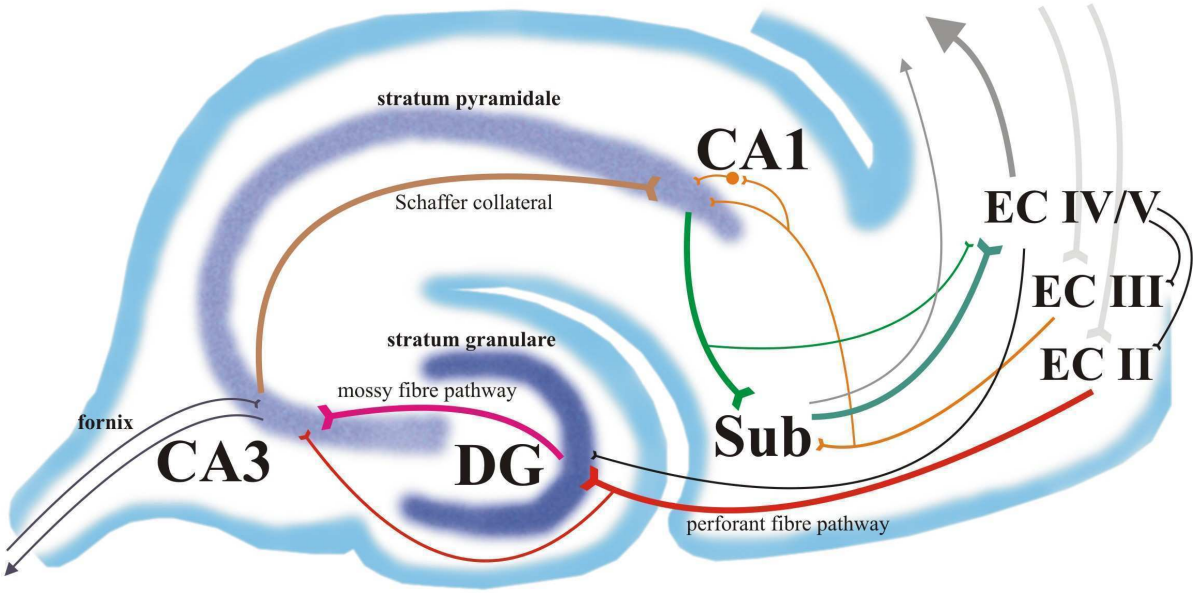

Figure 1: The hippocampal formation. The hippocampal formation consists of the entorhinal cortex (EC), subiculum (Sub), dentate gyrus (DG) and the cornu ammonis (CA) area 1 to 4. The premier input (light gray) to the hippocampus arrives through the entorhinal cortex layers II and III. EC III sends input to the subiculum and mainly via GABAergic interneurons to the CA1, but the main hippocampal circuit consists of the excitatory projections of the perforant fibre pathway (red) from ECII to the DG granule cells (dark purple) and the pyramidal cells (light purple) of CA3 to a lesser degree, the mossy fibre pathway (pink) from the DG to CA3, and the Schaffer collateral (brown) from CA3 to CA1. The CA1 sends projections (light green) directly to the EC and to the subiculum, which in turn projects (dark green) to the EC deep layers IV and V. EC IV/V is the main output relay from the hippocampus (dark gray), but also projects back onto EC II and III and directly to the DG (black). The subiculum also sends projections out of the hippocampus to a lesser degree (dark gray). A secondary in- and output, connecting the septum and mammillary bodies to the hippocampal CA3, passes through the fornix (dark gray).

From the CA3 area, the Schaffer collateral pathway connects to CA1, which delivers hippocampal output directly and relayed through the subiculum to the EC deep layers IV and V (Kohler 1985). The EC layers IV and V distribute hippocampal output to other brain regions (Witter *et al.* 1989), but also connect back to EC layers II and III (Heinemann *et al.* 2000).

Wile these connections constitute the main hippocampal circuit, a second major input comes from the EC layer III pyramidal cells delivering information directly to the CA1 and subiculum (Steward 1976; Witter *et al.* 1988; Witter *et al.* 1989), these nerve-endings predominantly contact interneurons in the CA1 (Empson and Heinemann 1995). Moreover, axonal projections from the EC deep layers IV and V to the DG have been found (Kohler 1985; Deller *et al.* 1996) and the hippocampus is connected through the fornix to the septum and mammillary bodies (Cassel *et al.* 1997), exchanging secondary input and output to and from the hippocampal CA3.

1.6 Epilepsy

Epilepsy is a severe neurological disorder characterised by the periodic occurrence of seizures. It constricts quality of life as seizures occur in an unpredictable way. A seizure is defined as the simultaneous, synchronous and rhythmic firing of many neurons, which may eventually spread by stimulation of neurons in other brain regions. There are currently approximately 50 million people suffering from epilepsy worldwide and though mutations occurring in ligand- and voltage-gated ion channels have been linked to epilepsy, many patients do not have a discernable genetic background (Hauser 1997). Epilepsy exists in many different forms, with diverse types of seizures and varied onset and time courses of the disease. Seizures are divided into several categories, depending on the brain-area involved, impairment of

consciousness and type of manifestation, be it motor, sensory, autonomic or psychic. The main categories are partial, generalised and unclassified seizures (see **Table 1**).

1. Partial seizures

- A Simple seizures (no impairment of consciousness)
  - A1 motor manifestations
  - A2 sensory manifestations
  - A3 autonomic manifestations
  - A4 psychic manifestations
- B Complex seizures (sometime followed by automatism, i.e. smacking)
  - B1 simple partial seizures at onset (1.A) followed by impairment of consciousness
  - B2 impaired consciousness at onset
- C Secondarily generalised
  - C1 Simple partial seizure (1.A) escalating to generalised seizure (2.)
  - C2 Simple complex seizure (1.B2) evolving into a generalised seizure (2.)
  - C3 Simple partial seizure (1.A) evolving to simple complex seizure (1.B1), which further escalates into a generalised seizure (2.)

2. Generalized seizures

- A Absence seizures, typical or atypical
- B Myoclonic
- C Clonic
- D Tonic
- E Tonic-Clonic
- F Atonic

3. Unclassified seizures

Table 1: Classification of epileptic seizures. Epileptic seizures are divided into partial, generalised and unclassified seizures. Generalised seizures are subdivided into 6 types. Partial seizures include simple, complex and secondarily generalised partial seizures, which are further divided into subtypes.

Partial seizures start focally with only one of the brain hemispheres being involved. They can be simple, without impairment of consciousness, or complex, with impaired consciousness. Simple partial seizures can evolve into complex ones, and both complex and simple partial seizures can become secondarily generalised spreading to other brain areas. Generalised seizures always involve both brain hemispheres. These include absence, myoclonic, clonic, tonic, tonic-clonic and atonic seizures.

1.6.1 Temporal Lobe Epilepsy

Temporal lobe epilepsy (TLE) is the most common form of epilepsy, comprising one third of all cases. In TLE, seizures most often emerge from the hippocampus or the amygdala, They can start focally, either in the limbic system or cortex, and subsequently spread to other brain areas (secondary generalisation, as mentioned above). As for other types of epilepsy, the reasons for TLE can be manifold, including atrophy or sclerosis, cranio cerebral injury, inflammation, stroke, benign tumours and vascular deformation. Dispersion of the granule cell layer, occurring in the first four years of TLE development, is a histopathological sign of TLE (Lurton *et al.* 1998). Roughly half of the cases comprise idiopathic TLE, with seizures arising spontaneously from an obscure or unknown cause. Seizures usually last one to two minutes and are starting and ending gradually. They are often followed by automatisms like smacking or licking, and are sometimes accompanied by ten to twenty seconds of akinesia. Impairment of consciousness is common, while lalopathy occurs rarely.

Patients often become resistant to available drug therapy over time, leaving resection of the epileptic focus as an alternative treatment. Histopathological analysis of the resected epileptic hippocampus reveals the degenerative nature of the disease. The

degree of damage to the hippocampus is graded according to the Wyler classification (Wyler *et al.* 1992; Blumcke *et al.* 2007) from W0 with no cell loss to W4 with over 50% cell loss, including reactive proliferation of glia (gliosis) and affecting all hippocampal regions (see **Table 2**).

Wyler Grade	General Description	Pathological Markers
W0	no mesial temporal lesions	no hippocampal sclerosis or cell loss
W1	slight mesial temporal lesions	gliosis with cell loss below 10% effecting CA1, 3 and/or 4, sparing CA2
W2	moderate mesial temporal lesions	gliosis with cell loss of 10 to 50% effecting CA1, 3 and/or 4, sparing CA2*
W3	classical hippocampal sclerosis	gliosis with cell loss over 50% effecting CA1, 3 and 4, sparing CA2
W4	severe hippocampal sclerosis	gliosis with cell loss over 50% total CA sclerosis, effecting CA1 to CA4

Table 2: Wyler classification of hippocampal damage. Hippocampectomies from TLE patients subjected to histopathological analysis are graded according to the Wyler classification of hippocampal damage. Specimens are attributed a Wyler grade from W0 to W4 according to the degree of gliosis and cell loss, and the areas effected by sclerosis. *End folium sclerosis affects CA3 and 4 but not CA1 and 2.

1.6.1.1 Network and cellular mechanisms of TLE

The frequency in neuronal network oscillations is controlled by GABAergic interneurons (Buzsaki 2001; Freund 2003; Gloveli *et al.* 2005), which phase-lock the firing pattern of principal cell populations by feedback inhibition, to synchronise network activity in a wide range of frequencies (Monyer and Markram 2004; Gloveli *et al.* 2005; Gloveli *et al.* 2005). Interneurons are classified into fast or slow spiking according to characteristic discharge frequencies.

One example for slow spiking interneurons is the oriens-lacunosum moleculare (O-LM) cell (Gloveli *et al.* 2005; Gloveli *et al.* 2005). O-LM cells are cholecystokinin (CCK)-positive, which can be used for their identification with molecularbiological and immunochemical methods, and due to their slow spiking characteristic they promote network oscillatory activity in the theta range (4 to 7Hz).

Basket cells are an example of fast spiking interneurons, which can be identified by their expression of the calcium binding protein parvalbumin. Due to their fast spiking properties this cell type promotes high frequency oscillations in the gamma range (>30Hz). Oscillation of hippocampal network activity in the theta and gamma frequency ranges is critically involved in cognitive functions as deregulation of the gamma power impairs information processing through the hippocampal loop between EC layers II and III on one end, and layers IV and V on the other.

1. Introduction

The auto-associative network in area CA3 has an important function within the hippocampus as it connects entorhinal and frontal input (septum, associative and commissural fibres) via the hippocampal fornix (see **Figure 1**). Because of the recurrent glutamatergic connectivity within the auto-associative network in area CA3 functional GABAergic inhibition is ultimately required for control of the gamma power. In addition, dentate gyrus granule cells can easily discharge CA3 pyramidal cells via the so-called mossy fibre “detonator synapses” (Henze *et al.* 2002). Likewise, seizures in TLE are often preceded by focal increases in gamma power (Fisher *et al.* 1992; Dugladze *et al.* 2007; Bragin *et al.* 2007).

In fact, deficits in GABAergic neuronal mechanisms were observed in TLE (Baulac *et al.* 2001; Palma *et al.* 2005; Kumar and Buckmaster 2006; Stief *et al.* 2007; Eichler and Meier 2008), and a decrease of only 20% in amplitude and decay time constant of inhibitory post-synaptic potentials (IPSPs) may suffice for seizure onset (Eugene *et al.* 2007). Reasons that underlie reduced GABAergic inhibition include changes in excitability of CCK-positive interneurons, for example arising from increased firing of glutamatergic afferent fibres (Dugladze *et al.* 2007) and transforming interneuronal discharge from theta to higher frequencies. Another reason for decreased GABAergic inhibition can be a reduction of post-synaptic gephyrin and GABA(A)R alpha2 (Knuesel *et al.* 2001), the latter being mainly involved in interneuronal transmission in the theta frequency range (Freund and Katona 2007).

1.7 Aim of the PhD work

The involvement of gephyrin in hyperexcitability disorders has been postulated due to the observation that gephyrin immunoreactivity is decreased in the epileptic hippocampus in mice, and reduced post-synaptic gephyrin mirrors reduced GABA(A)R alpha2 in the epileptic hippocampus (Bouilleret *et al.* 2000; Kneussel *et al.* 2001; Kumar and Buckmaster 2006). Moreover, gephyrin was recently shown to be gradually down-regulated during epileptogenesis in an animal model of TLE (Fang *et al.* 2011). However, the mechanisms underlying diminished gephyrin expression have remained enigmatic; notably, gene mutations can be ruled out as wild-type animals are used in animal studies of epileptogenesis. Therefore, the aim of this PhD thesis was to identify and characterise cellular mechanisms responsible for loss of post-synaptic gephyrin in TLE.

2. Material and methods

2.1 Preface

2.1.1 Chemicals

Acetic acid, glacial (Carl Roth GmbH & Co. KG, Karlsruhe, Germany)
Agar-Agar (Carl Roth GmbH & Co. KG, Karlsruhe, Germany)
Agarose (Invitrogen GmbH, Karlsruhe, Germany)
Antibiotic-Antimycotic (Gibco - Invitrogen GmbH, Karlsruhe, Germany)
Ammonium chloride (Carl Roth GmbH & Co. KG, Karlsruhe, Germany)
Ampicillin (Sigma-Aldrich Logistik GmbH, Schnelldorf, Germany)
AraC: Arabinofuranosyl Cytidine (Sigma-Aldrich Logistik GmbH, Schnelldorf, Germany)
B27-Supplement (Gibco - Invitrogen GmbH, Karlsruhe, Germany)
Calcium chloride di-hydrate (Carl Roth GmbH & Co. KG, Karlsruhe, Germany)
Chloroform (Carl Roth GmbH & Co. KG, Karlsruhe, Germany)
DAKO Pen (Dako Deutschland GmbH, Hamburg, Germany)
DEPC: Diethylpyrocarbonate (Sigma-Aldrich Logistik GmbH, Schnelldorf, Germany)
Diethyl ether (Carl Roth GmbH & Co. KG, Karlsruhe, Germany)
DMF: N,N-Dimethyl formamide (Carl Roth GmbH & Co. KG, Karlsruhe, Germany)
DMSO: Dimethyl sulfoxide (Serva Electrophoresis GmbH, Heidelberg, Germany)
dNTPs (Bioline GmbH, Luckenwalde, Germany)
dTTPs (Fermentas Life Science, St. Leon-Rot, Germany)
EDTA (Carl Roth GmbH & Co. KG, Karlsruhe, Germany)
ECL: Enhanced chemiluminescence Immun-Star-WesternC (BioRad, Munich, Germany)
Ethanol (Carl Roth GmbH & Co. KG, Karlsruhe, Germany)
Ethidium bromide (Carl Roth GmbH & Co. KG, Karlsruhe, Germany)
FCS: Fetal calf serum (Gibco - Invitrogen GmbH, Karlsruhe, Germany)
Gelatine (VWR International GmbH, Germany)
D-(+)-Glucose (Sigma-Aldrich Logistik GmbH, Schnelldorf, Germany)
L-Glutamine (Invitrogen GmbH, Karlsruhe, Germany)
Glycine (Carl Roth GmbH & Co. KG, Karlsruhe, Germany)
HEPES: *N*-(2-hydroxyethyl)piperazine-*N*′-(2-ethanesulphonic acid) (Carl Roth GmbH & Co. KG, Karlsruhe, Germany)

Horse serum (Gibco - Invitrogen GmbH, Karlsruhe, Germany)
Hydrochloric acid (VWR International GmbH, Germany)
IPTG (Carl Roth GmbH & Co. KG, Karlsruhe, Germany)
Isopropanol (Carl Roth GmbH & Co. KG, Karlsruhe, Germany)
Kanamycin (Gibco - Invitrogen GmbH, Karlsruhe, Germany)
Magnesium chloride hexa-hydrate (Carl Roth GmbH & Co. KG, Karlsruhe, Germany)
Magnesium sulphate hepta-hydrate (Carl Roth GmbH & Co. KG, Karlsruhe, Germany)
beta-Mercaptoethanol (Sigma-Aldrich Logistik GmbH, Schnelldorf, Germany)
Methanol (Carl Roth GmbH & Co. KG, Karlsruhe, Germany)
O.C.T TissueTec (Sakura Finetec Inc., Torrance, CA, USA)
Oligo dT12, 15, 18 (BioTeZ Berlin Buch GmbH)
PFA: paraform aldehyde (Sigma-Aldrich Logistik GmbH, Schnelldorf, Germany)
Penicillin-Streptomycin (Gibco - Invitrogen GmbH, Karlsruhe, Germany)
Peptone (Carl Roth GmbH & Co. KG, Karlsruhe, Germany)
Poly-DL-ornithine hydrobromide (Sigma-Aldrich Logistik GmbH, Schnelldorf, Germany)
Potassium chloride (VWR International GmbH, Germany)
Potassium di-hydrogen phosphate (Carl Roth GmbH & Co. KG, Karlsruhe, Germany)
Sodium chloride (Carl Roth GmbH & Co. KG, Karlsruhe, Germany)
Sodium hydrogen carbonate (Carl Roth GmbH & Co. KG, Karlsruhe, Germany)
di-Sodium hydrogen phosphate di-hydrate (Carl Roth GmbH & Co. KG, Karlsruhe, Germany)
Sodium hydroxide (VWR International GmbH, Germany)
Sodium pyruvate (Sigma-Aldrich Logistik GmbH, Schnelldorf, Germany)
Sucrose (VWR International GmbH, Germany)
SuperSignal West Pico Chemiluminescent Substrate (Thermo Fisher Scientific, Waltham, MA, USA)
TRIS (Carl Roth GmbH & Co. KG, Karlsruhe, Germany)
Triton X-100 (Sigma-Aldrich Logistik GmbH, Schnelldorf, Germany)
TRIzol Reagent (Invitrogen GmbH, Karlsruhe, Germany)
Vectashield Mounting Medium (Vector Laboratories, Inc., Burlingame, CA, USA)
Vitamin B12 (Sigma-Aldrich Logistik GmbH, Schnelldorf, Germany)
X-Gal (Carl Roth GmbH & Co. KG, Karlsruhe, Germany)
Yeast extract (Carl Roth GmbH & Co. KG, Karlsruhe, Germany)

2.1.2 Enzymes

2.1.2.1 Enzymes for cell culture:

DNase Type I (Sigma-Aldrich Logistik GmbH, Schnelldorf, Germany)

RNase-free DNase (Roche Applied Science, Mannheim, Germany)

Trypsin inhibitor Type I-S, soybean (Sigma-Aldrich Logistik GmbH, Schnelldorf, Germany)

Trypsin Type XII-S, bovine pancreas, 12000 to 16000U/mg (Sigma-Aldrich Logistik GmbH, Schnelldorf, Germany)

2.1.2.2 Polymerases:

Phusion Hot Start High-Fidelity DNA polymerase (New England Biolabs, Hertfordshire, UK)

RedTaq DNA polymerase (Sigma-Aldrich Logistik GmbH, Schnelldorf, Germany)

TTH-Pyrophosphatase (Invitek Stratec GmbH Berlin-Buch, Germany)

2.1.2.3 Restriction enzymes:

BamHI (New England Biolabs GmbH, Frankfurt, Germany)

BspEI (New England Biolabs GmbH, Frankfurt, Germany)

EcoRV (New England Biolabs GmbH, Frankfurt, Germany)

HindIII (New England Biolabs GmbH, Frankfurt, Germany)

KpnI (New England Biolabs GmbH, Frankfurt, Germany)

2.1.3 Kits

Effectene Transfection Reagent (Qiagen GmbH, Hilden, Germany)

GeneEditor (Promega, Madison, WI, USA)

Matrix Gel Extraction System (Marligen Biosciences, Ijamsville, MD, USA)

Rapid DNA Ligation Kit (Fermentas Life Science, St. Leon-Rot, Germany)

RNeasy Protect Mini Kit (Qiagen, Hilden, Germany)

Superscript II reverse transcriptase (Invitrogen GmbH, Karlsruhe, Germany)

2.1.4 Media and solutions

DMEM (Gipco - Invitrogen GmbH, Karlsruhe, Germany)

MEM with Earle's salts (Gibco - Invitrogen GmbH, Karlsruhe, Germany)

MEM with Hanks' salts (Gibco - Invitrogen GmbH, Karlsruhe, Germany)

NB (Gibco - Invitrogen GmbH, Karlsruhe, Germany)

PBS (Gibco - Invitrogen GmbH, Karlsruhe, Germany)

2.1.4.1 Primary hippocampal cell culture

NB-B27:
NB, 25µM beta-Mercaptoethanol, 2% B27-Supplement, 0.25mM L-Glutamine, 0.05% Penicillin-Streptomycin, pre-warmed and equilibrated 2 h at 37°C and 5% CO_2

DMEM-FCS:
DMEM, 10% FCS

DNase-Ovomucoid:
MEM with Hanks' salts, 1380U DNase/ml, 1.8g/l D-(+)-Glucose, 25mM HEPES, 0.44mM $MgCl_2$ x $6H_2O$, 50mM $MgSO_4$ x 7 H_2O, Trypsin inhibitor 0.3% (m/v)

PBS-CMF:
PBS, 1x Antibiotic-Antimycotic, 3.6g/l Glucose, 15mM HEPES

PBS-CMF-EDTA:
PBS, 1x Antibiotic-Antimycotic, 1mM EDTA, 3.6g/l Glucose, 15mM HEPES

Poly-DL-ornithine hydrobromide (PO):
0.005% Poly-DL-ornithine hydrobromide in ddH_2O (w/v)

Standard salt solution (SSS):
ddH_2O, 1x Antibiotic-Antimycotic, 1.25mM $CaCl_2$ x $2H_2O$, 4.5g/l Glucose, 10mM HEPES, 5mM KCl, 135mM NaCl, 1mM $NaHCO_3$, 0.5mM $MgCl_2$ x $6H_2O$, 0.5mM $MgSO_4$ x $7H_2O$

Transfection NB (transfection medium for neurons):
NB, 0.25mM glutamine, prewarmed and equilibrated 2h at 37°C and 5% CO_2

Transfection MEM (glycine-free expression medium for neurons):
MEM with Earle's salts, 25mM D-(+)-Glucose, 10mM HEPES, 230µM Sodium Pyruvate, 0.2µM Vitamin B12, 250µM L-Glutamine, 25µM beta-Mercaptoethanol, 0.05% Penicillin-Streptomycin, B27 supplement, pH 7.3, prewarmed and equilibrated 2h at 37°C and 5% CO_2

2.1.4.2 Media and solutions for HEK293 cells

$CaCl_2$, 250mM $CaCl_2$ x $2H_2O$ in ddH_2O

2x HBS (pH 7.05):

2.16g/l Glucose, 40mM HEPES, 10mM KCl, 274mM NaCl, 1.4mM Na_2HPO_4 x $2H_2O$

HEK-MEM (Culture medium for HEK293 cells):

MEM with Earle´s salts, 10% FCS, 1% Penicillin-Streptomycin, 30mM D-(+)-Glucose, 10mM HEPES, 0.25mM L-Glutamine, 230µM Sodium Pyruvate; pH 7.3]

Trypsin: 0.1% Trypsin in PBS-CMF-EDTA (w/v)

2.1.4.3 Substances for pharmacoloigical manipulations (stock solutions)

DNQX (Tocris, Bristol, UK): 10mM in ddH_2O and NaOH

K252a (Sigma-Aldrich, Deisenhofen, Germany): 200µM in DMSO

KCl: 2M in ddH_2O

MK801 (Tocris, Bristol, UK): 2mM in ddH_2O

Nifedipine (Sigma-Aldrich Logistik GmbH, Schnelldorf, Germany): 15mM in DMSO

TEA (Sigma-Aldrich Logistik GmbH, Schnelldorf, Germany): 1.5M in ddH_2O

2.1.4.4 RHC whole-cell patch-clamp recording

Extracellular solution: 105mM NaCl, 3mM KCl, 10mM HEPES, 5mM glucose, 2mM $CaCl_2$ and 1mM $MgCl_2$. Osmolarity was adjusted to that of the culture medium (240mosmol/kg).

Recording pipette solution: 90mM KCl, 3mM NaCl, 5mM HEPES, 5mM glucose, 0.5mM $CaCl_2$ and 4mM $MgCl_2$; buffered to pH 7.3 (210mosmol/kg).

2.1.4.5 HEK293 whole-cell patch-clamp recording

Extracellular solution: 145mM NaCl, 2.5mM KCl, 20mM HEPES, 10mM glucose, 2mM $CaCl_2$, 1mM $MgCl_2$, adjusted to pH 7.3.

Recording pipette solution: 4mM NaCl, 130mM KCl, 5mM EGTA, 10mM HEPES, 10mM glucose, 0.5mM $CaCl_2$, 4mM $MgCl_2$, adjusted to pH 7.3.

2.1.4.6 HEK293 outside-out patch-clamp recording

Extracellular solution: 147mM NaCl, 2.4mM KCl, 2mM $CaCl_2$, 2mM $MgCl_2$, 10mM HEPES, 10mM glucose (pH 7.2, osmolarity 320mosmol).

Recording pipette solution: 130mM CsCl, 4mM $MgCl_2$, 4mM Na_2ATP, 10mM EGTA, 10mM HEPES (pH 7.2, osmolarity 290mosmol).

2.1.4.7 Solutions for immunofluorescence

PBS-Gelatine: 0.12% Gelatine in PBS (w/v)
95% Methanol / 5% Acetic acid glacial (v/v)
50mM NH_4Cl in 1x PBS (w/v)
PFA-succrose: 4% PFA / 4% Sucrose in PBS (w/v)
8% Sucrose in PBS (w/v)
Triton X-100: 0.12% Triton X-100 in PBS-Gelatine (v/v)

2.1.4.8 Media and solutions for bacterial cultures

Agar plates: 1.5% Agar-Agar in LB-Medium (w/v), with 0.1mg/ml ampicillin or 40µg/ml kanamycin.
Ampicillin: 100mg/ml ampicillin in ddH_20
IPTG: 100mM IPTG in ddH_20
Kanamycin: 40mg/ml kanamycin in ddH_20
LB-Medium: 0.5% Yeast extract (w/v), 1% Peptone (w/v), 1% NaCl (w/v)
X-Gal: 3% X-Gal in DMF (w/v)

2.1.4.9 Solutions for molecular biology

DEPC-water: ddH_2O incubated with DEPC (1:2000) under constantly stirring over night, autoclaved 3 times 20 min.
DEPC-ethanol: 70% un-denatured ethanol in DEPC-water
nit-1-buffer: 50mM sodium phosphate, 200mM NaCl, 5mM EDTA
TBS: 100mM Tris/HCl pH 7.4, 154mM NaCl, 0.05% Tween-20
wash-buffer: 15mM sodium phosphate, 200mM NaCl, 2.5% (v/v) Tween-20

2.1.5 Antibodies

Antibody	Host	Dilution	Source
c-myc-tag 9E10	ms m	1:200	Sigma Aldrich, Deisenhofen, Germany
EGFP	ch p	1:300	Chemicon, Temecula, CA, USA
GABA(A)R alpha2	gp p	1:200	Jean-Marc Fritschy, University of Zurich, Switzerland
GAD65	ms m	1:200	Chemicon, Temecula, CA, USA
Gephyrin E-domain mAb3B11	ms m	1:1000	Synaptic Systems GmbH, Göttingen, Germany
Gephyrin mAb7a	ms m	1:50	Synaptic Systems GmbH, Göttingen, Germany
Gephyrin pAb	rb p	1:500	Synaptic Systems GmbH, Göttingen, Germany
GlyR alpha3L	rb p	1:100 and 1:750	Sigma Aldrich, Deisenhofen, Germany
HA-tag	ch p	1:2000	BETHYL Lab. Inc., Montgomery, TX, USA
NeuN	ms m	1:200	Chemicon, Temecula, CA, USA
Ubiquitin UB N-19	gt p	1:50	Santa Cruz Biotechnology Inc., Heidelberg, Germany
VGluT 1/2	gp p	1:600 and 1:200	Synaptic Systems GmbH, Göttingen, Germany
VIAAT	rb p	1:200	Synaptic Systems GmbH, Göttingen, Germany

Table 3: Overview of antibodies. Host denotes species (ch for chicken, gp for guinea-pig, gt for goat, ms for mouse or rb for rabbit) and monoclonal (m) or polyclonal (p). All secondary antibodies for immunofluorescence were purchased from Jackson ImmunoResearch Laboratories (West Grove, PA, USA), made in donkey, affinity purified and multiple labelling declared. Secondary antibodies were applied at a dilution of 1:200, and antibodies coupled with aminomethylcoumarin (AMCA), carboxymethyl indocyanine (Cy3 and Cy5), fluorescein isothiocyanate (FITC) and tetramethylrhodamine isothiocyanate (TRITC) were combined for multi-labelling. For western-blot, a horse-radish peroxidase conjugated anti-mouse IgG or anti-rabbit IgG, respectively, produced in donkey (Dianova - Jackson ImmunoResearch Laboratories, West Grove, PA, USA) was applied at a dilution of 1:10000 in TBS.

2.1.6 Plasmids

pEGFP-N1 expression vector with cytomegalovirus (CMV) promoter (BD Biosciences Clontech, Franklin Lakes, NJ, USA): Basis for all gephyrin splice-reporter and GlyR expression constructs.

pDsRed Express-C1 expression vector with a CMV promoter (BD Biosciences Clontech, Franklin Lakes, NJ, USA): Basis for all gephyrin single-exon expression constructs.

EGFP-tagged delta 6 gephyrin construct (Lardi-Studler 2007), based on eukaryotic pEGFP-C2 expression vector with a CMV promoter (Clontech, Mountain View, CA, USA): Basis for all TLE-gephyrin expression constructs.

2.1.7 Oligonucleotides

Target	Oligonucleotide Sequence
GABA(A)R subunits (2.5.5.5)	
alpha1 forward reverse	5'-CTG TTT GCC TGC TCT TCG TGT-3' 5'-CCC ATC TTC TGC CAC AAC CAC-3'
alpha2 forward reverse	5'-AAT CGT CTT AGA CCA GGA CTG-3' 5'-GAG CCA CTG ACT TTT TCC CGT-3'
alpha3 forward reverse	5'-TCA AGA CGA CAA GAA CCT GGG-3' 5'-TAT CAG TGT CTG ACA CAG GGC-3'
alpha5 forward reverse	5′-AAT CTG TCC CAG CTA GGA CAG-3′ 5′-TGG GAT GTT TGG AGG ATG GGT-3′
beta2 forward reverse	5'-CAG GTT CTT ATC CCA GAT TGT CC-3' 5'-GGT CCA TCT TGT TGA CAT CCA GG-3'
beta3 forward reverse	5'-CTT TTC GGC ATC TTC TCG GC-3' 5'-TCC ACG CCA GTA ACA GCC TTG-3'
gamma2 forward reverse	5'-CAA GGT CTC CTA TGT CAC AGC-3' 5'-AAG GCG GTA GGG AAG AAG ATC-3'
Genomic gephyrin DNA (2.5.6)	
GPHN exon 3 forward reverse	5′-AAA TAA ATC AAT AGT AAT GTT TGG G-3′ 5′-AAT ATG TGT AAA ACG CAT TAT TAG A-3′
GPHN exon 4 forward reverse	5′-CTA CCT CTT TTA AAC TAA TAC ATG G-3′ 5′-ATC TGA TGG TGA TTA TCT GAT ACA-3'
GPHN exon 5 forward reverse	5′-GAT CAA GAG TGA AAC TGT TCC AT-3′ 5′-CAA GTC ATT TGT TAT GCC TAG CA-3′
GPHN exon 8 forward reverse	5′-TTC CAA TTT GCC ATA CTA ACC AT-3′ 5′-TCC ATT GAA TTA CTG AAC CCA AG-3′
GPHN exon 9 forward reverse	5′-AAC ATT GTA GCA CTG TAG TTC C-3′ 5′-CAA ATC TTC AAG TTC ATC ATG C-3′
GPHN intron 8 forward reverse	5′-GAG TCT CAC TGT GTC ACC CTG-3′ 5′-TGC AGT GTA TAC CTC TCG GTG-3′
Gephyrin constructs (2.5.7.1)	
delta4-8 forward reverse (BspEI site bold)	5'-GGG **TCC GGA** GGA ATG CTT TCA GTT CAT-3' 5'-CCC **TCC GGA** GTG ACA TCT CGT G-3'
other TLE sequences forward reverse (BspEI and AflII site bold)	5′-AGA AGA CCA C**TC CGG A**AT AAA TCT CAA-3′ 5′-CAA TGG CAT CA**C TTA AG**A GGT CAA TGG-3′
BspEI insertion forward reverse (BspEI site bold)	5′-GGG **TCC GGA** ATA AAT CTA AAA GAT CTC GTC-3′ 5′-GGG **TCC GGA** GCG GTC TTC TGC AAG ATT C-3′
AflII insertion forward reverse (AflII site bold)	5′-GAG **CTT AAG** AGA TGC CAT TGT AAA AGT AAA-3′ 5′-GGG **CTT AAG** AGG TCA TGG CAT GAG GTA-3′
DsRed exon 1-3 forward reverse (XhoI and BamHI site bold)	5′-GGG **CTC GAG** TGA TGG CGA CCG AGG GAA TGA TC-3' 5'-CC**G GAT CC**T ACA AAG AAG GGT CTT GGA CAA GA-3'
DsRed exon 4 forward reverse (XhoI and BamHI site bold)	5′-GG**C TCG AG**T GTT GGG TGG GAC TAT ATC GG-3′ 5′-CC**G GAT CC**T ACT TGA TTT CTT CTA TTT CAT CTG G-3′
DsRed exon 5 forward reverse (XhoI and KpnI site bold)	5′-GG**C TCG AG**A GGA AAC ACT CAT AGA CTG GTG-3′ 5′-CC**G GTA CC**T ACT CT GGA GTG ACA TCT CGT G-3′
DsRed exon 7 forward reverse (XhoI and BamHI site bold)	5′-CG**C TCG AG**A GGC CAC AAA AGA AGT AAT AG-3′ 5′-CC**G GAT CC**T ATC TAG AGA GCA TGC CCA GAG-3′
DsRed exon 8 forward reverse (XhoI and BamHI site bold)	5′-GG**C TCG AG**G ACC AGT GTG TGG AAT AAG GG-3′ 5′-CC**G GAT CC**T ACT GAG ACC CTT TCT TGC TAC CA-3′
Gephyrin RNA (2.5.5.2)	
G-domain (exon 1-9) forward reverse	5′-GGA GGT GCA TGA TGA ACT TGA-3′ 5′-TTG CTG CTG CAC CTG GAC TG-3′
C-domain (exon 9-16) forward reverse	5′-GAG TCC TCA CAG TGA GTG ATA-3′ 5′-TCA AGT TCA TCA TGC ACC TCC-3′
E-domain (exon 18-24) forward reverse	5′-GCA TCA GTA AAA GAT GGC TAT G-3′ 5′-GGT CAT CTT CAG GAT TTA GTA G-3′

Target	Oligonucleotide Sequence
GlyR alpha2 RNA (2.5.5.3)	
alpha2A forward alpha2B forward reverse	5'-ATC AAC AGT TTT GGA TCA GTC A-3' 5'-TCA ACA GCT TTG GGT CAA TAG-3' 5'-CCT TCA GCA ACT TGC ACT GG-3'
GlyR alpha3 RNA (2.5.5.4)	
alpha3 forward alpha3 human & mouse reverse alpha3 rat reverse	5'-GGG TAC ACA ATG AAT GAT CTC-3' 5'-AGA GAC TTA ATC TTG CTG CTG ATG-3' 5'-TTA GCC CTG TCG ATG AAG ACC-3'
GlyR mutagenesis (2.5.7.3)	
alpha1-191mut	5'-GGA CTG ACC CTG CTG CAG TTT ATC CTG AAG G-3'
Household gene RNA (2.5.5.1)	
beta-actin forward reverse	5'-CGC TCG TTG CCA ATA GTG ATG-3' 5'-TTG TAA CAA ACT GGG ACG ATA TGG-3'
human GAPDH forward reverse	5'-ATG GCA CCG TCA AGG CTG AG-3' 5'-CGA CGC CTG CTT CAC CAC C-3'
mouse GAPDH forward reverse	5'-CCA CTC ACG GCA AAT TCA ACG-3' 5'-AGC CCA AGA TGC CCT TCA GTG-3'
rat GAPDH forward reverse	5'-CAG TAT GAC TCT ACC CAC GG-3' 5'-CTC AGT GTA GCC CAG GAT G-3'
pBluescript Vector (2.5.7)	
T7 forward	5'-GTA ATA CGA CTC ACT ATA GGG C-3'
T3 reverse	5'-CGC AAT TAA CCC TCA CTA AAG-3'

Table 4: Oligonucleotide Primers. Unless noted otherwise, oligonucleotides were used at a final concentration of 0.2µM. In semi-quantitative PCR the oligonucleotide concentration for GAPDH and for beta-actin primers was set to 0.025µM and 0.1µM, respectively, to yield band intensities comparable to the gene of interest.

2.1.8 Human control RNA, Bacteria and Animals

Human post mortem hippocampus RNA (Clontech/Takara Bio Europe, St.-Germain-en-Laye, France)

JM109 Competent Cells, high efficiency (Promega GmbH, Mannheim, Germany)

male C57/BL6 mice, $\geq$ 1 month (Charles River Laboratories, Sulzfeld, Germany)

NMRI-mice, adult (Charles River Laboratories, Sulzfeld, Germany)

Wistar Han rats, E19 (Charles River Laboratories, Sulzfeld, Germany)

2.1.9 Equipment and software

2.1.9.1 Epifluorescence microscopy

Systemmikroskop BX 51 (Olympus Life Science Europa GmbH, Hamburg, Germany):
Filters:
U-MSP100v2 MFISH DAPI Filter
U-MSP101v1 MFISH FITC Filter
U-MSP102v1 MFISH Cy3 Filter
U-MSP104v1 MFISH Cy5 Filter
Objectives:
UPLFLN40xPH/0.75 UPlan Semi Apo Phase, 40x phase contrast
UPlanApo 40x/1.00 oil immersion objective
Camera:
14bit-CCD camera system Spot PURSUIT
Lamp:
X-Cite-120W metal halide lamp

2.1.9.2 Confocal microscopy

DM TCS SP2 Laser scanning microscope (Leica, Solms, Germany)
HCX PL APO 40x oil immersion objective, optical aperture 1.25 (Leica Mikrosysteme, Wetzlar, Germany)

2.1.9.3 Microtome

CM 1850 UV Microtome (Leica, Solms, Germany)
Superfrost Plus slides (Menzel GmbH & Co. KG, Braunschweig, Germany)
Glascuevettes (Carl Roth GmbH & Co. KG, Karlsruhe, Germany)

2.1.9.4 Molecular- and microbiology

Advanced Primus 96 cycler (PeqLab Biotechnologie GmbH, Erlangen, Germany)
Biofuge Pico Heraeus (Thermo Fisher Scientific, Inc., Waltham, MA, USA)
Biofuge 28RS Heraeus (Thermo Fisher Scientific, Inc., Waltham, MA, USA)
BioPhotometer (Eppendorf, Hamburg, Germany)
ChemiDoc XRS Molecular Imager (BioRad, Munich, Germany)
Chemolumineszenz DeVision R2000 (Decon Science Tec GmbH, Hohengandern, Germany)
GeneAmp PCR System 2400 cycler (Perkin Elmer, Inc., Waltham, Massachusetts, USA)
KL1 shaker (Edmund Buhler, Tübingen, Germany)
PerfectBlue Gelsystem (PeqLab Biotechnologie GmbH, Erlangen, Germany)
Zentrifuge 5415R (Eppendorf, Hamburg, Germany)

2.1.9.5 Cell culture

CB 150 Incubator (Binder GmbH Labortechnik, Tuttlingen, Germany)
Fuchs-Rosenthal counting chamber (Carl Roth GmbH & Co. KG, Karlsruhe, Germany)
Microscope slides (Carl Roth GmbH & Co. KG, Karlsruhe, Germany)
13mm glass cover slips, (Glaswarenfabrik Karl Hecht KG, Sandheim, Germany)
35mm cell culture dishes (TPP AG, Trasadingen, Switzerland)
T25 cell culture flasks, (TPP AG, Trasadingen, Switzerland)
24-well cell culture plates (TPP AG, Trasadingen, Switzerland)

2.1.9.6 Electrophysiology

Axopatch 1D amplifier (Axon Instruments, Foster City, USA)
Borosilicate glass tubing (Harvard Apparatus, Kent, UK)
Brown-Flaming puller (Sutter Instrument Co., Navato, USA)
EPC-9 (HEKA Electronics, Lambrecht/Pfalz, Germany).
2mm thin-wall glass theta tube (Hilgenberg, Malsfeld, Germany)
8-pole bessel filter (Frequency Devices, Haverhill, USA)
P245.30 piezo-electric translator (Physik Instrument, Waldbronn, Germany)
P-97 puller (Sutter Instruments, Novato, CA, USA)

2.1.9.7 Computersoftware

Gel-Pro Analyser (MediaCybernetics, Bethesda, MD, USA)
ImageQuant (Molecular Dynamics, Sunnyvale, CA, USA)
LCS (Leica Microsystems Heidelberg GmbH, Germany)
Origin (OriginLab, Northampton, MA, USA)
MetaMorph (Visitron Systems GmbH, Puchheim, Germany)
MiniAnalysis (Synaptosoft Inc., Decatur, GA, USA)
pClamp software 10.1. (Axon Instruments, Foster City, USA)
ScionImage (Scion Corporation, Frederick, MD, USA)
TIDA 5.1 software (HEKA Electronics, Lambrecht, Germany)
WinTida 5.0 (HEKA Electronics, Lambrecht/Pfalz, Germany)

2.2 Legal information

Analysis of resected TLE hippocampi was performed according to the rules laid down by the Ethical Committee (Charité, EA1/142/05), and informed consent was obtained according to the Declaration of Helsinki (BMJ, 1991; 302: 1194). All animals were sacrificed according to the permit (LaGeSo, 0122/07) given by the Office for Health Protection and Technical Safety of the regional government of Berlin and in compliance with regulations laid down in the European Community Council Directive of 24 November 1986 (86/609/EEC).

2.3 Tissue preparation

2.3.1 Human patient hippocampectomies

All TLE patients included in this study were classified pharmaco-resistant, meaning that at least two different medications failed (see **3.2, Publication 1, Supplementary Table 1**). Christoph Dehnicke performed the presurgical evaluation at the Epilepsy Centre Berlin-Brandenburg. To identify the type of seizure, the ictal onset zone, the irritative zone, and the epileptogenic zone, neuropsychological diagnostic, video-EEG-monitoring and MRI were used (see **3.2, Publication 1, Supplementary Table 1**). The epileptogenic zone has previously been defined as the area of the brain necessary and sufficient for habitual generation of seizures, and whose disconnection or removal will precipitate a cure (Luders *et al.* 1993). If required, invasive intracranial recordings were employed (e.g. TLE Patient #2.47.5, see **3.2, Publication 1, Supplementary Figure 1, Table 1** and **Electrocorticogram**).

In all cases the mesial temporal lobe structures were shown to be part of the epileptogenic zone. It must be noted that, while epileptic seizures may originate from other areas of the brain and only spread to the hippocampus initially, the hippocampus can start to generate seizures on it's own in the later course of the disease.

At the Epilepsy Centre Berlin-Brandenburg, the resection of the temporal pole with an amygdalahippocampectomy is the standard operative procedure for patients with isolated pharmacoresistant mesial TLE. When a lesion was detected inside the temporal lobe but outside the mesial structures and presurgical diagnostic confirmed both structures as part of the epileptogenic zone, the lesion as well as the mesial temporal structures were removed. Surgery was performed at the Charité Virchow Clinical Centre by Peter Horn and Thomas-Nicolas Lehmann.

Patient material for isolation of total RNA, extraction of genomic DNA and western blot was frozen in liquid nitrogen, immediately after resection in the operation theatre. For further processing of the specimen see **2.5.3**, **2.5.6** and **2.6.1** respectively. For immunohistochemistry, 3 to 5mm thick hippocampal cross sections were immersed in PFA-succrose, an ice cold mix of PFA (4%) and sucrose (4%) in phosphate-buffered saline (PBS), on wet ice for 1h directly after resection in the operation theatre, for further processing see **2.3.3** and **2.6.2**.

2.3.2 Mouse brain tissue

Diethyl ether anesthetized male C57/BL6 mice (at least 1 month old; Charles River Laboratories) were killed through cervical dislocation and the brain was isolated. For immunohistochemistry (**2.6.2**) brains were prepared for cryosectioning (**2.3.3**), for analysis of GlyR alpha3K and L expression (**2.5.5.4**), the mouse brain was sepparated into cerebellum, hippocampus, frontal cortex, residual cortex, thalamus and midbrain. Isolated mouse brain regions were transferred into an RNase free Eppendorf tube and shock frozen immediately in liquid nitrogen and stored in liquid nitrogen until processed further for isolation of total RNA (**2.5.3**). For western blot analysis, the hippocampus was resected from the brain of 4 months and 1 year old mice and frozen in Aceton/trichloroacetic acid (9:1) at −80°C, before proteins were extracted (see **2.6.1**).

2.3.3 Cryosections

Approximately 3-5mm thick human hippocampal cross sections and mouse-brain cross sections were fixed in PFA-succrose for 1h on wet ice or at 4°C respectively. After fixation, the tissue was washed 3 times for 5 minutes with PBS in petri dishes on a KL1 shaker (Edmund Buhler) at room temperature and then cryoprotected with 8% sucrose in PBS at 4°C over night.

On the following day, the tissue was embedded in OCT TissueTek (Sakura Finetec) on dry ice. 12µm cryosections were obtained at -20°C using a CM1850 cryostate (Leica Microsystems) and mounted on Superfrost Plus microscope slides (Menzel GmbH). Cryosections were further processed for immunohistochemistry on the same day (see **2.6.2**) or stored at -20°C for later use.

2.4 Cell culture

2.4.1 Primary rat hippocampal neuron cell culture

2.4.1.1 Preparation

Hippocampal cultures from E19 Wistar rats were prepared as described previously (Meier and Grantyn 2004). Neurons were cultured on 13mm glass coverslips in 24 well plates. These were previously coated over night with 5mg/ml Poly-DL-Ornithin in water at 37°C and 5% CO_2, dried for 20 minutes at room temperature after removal of the Poly-DL-Ornithin solution, and then coated with 10% foetal calf serum in DMEM (DMEM-FCS) for 30 to 90 minutes at 37° C and 5% CO_2. The serum proteins and the positively charged ornithin facilitate the adhesion of neurons to the surface of the glass coverslips.

At day E19 diethyl ether anesthetised mother rats were sacrificed and the uterus with the embryos was excised and transferred to ice cold standard salt solution (SSS). After detachment of the scalp and skull cap, brains were removed from the skull and stored on ice in fresh SSS. All brains were collected on ice within less then 20 minutes from the mother animals' time of death. The cerebellum was severed from the brain, the cortex was separated along the corpus callosum, and the thalamus was cut out from each hemisphere, giving access to the hippocampi. After removal of the pia mater, hippocampi were excised from the brain and collected in fresh SSS on ice. The hippocampi were then sliced into 2 to 4 pieces, each, and transferred to 4°C cold calcium and magnesium free phosphate buffer solution (PBS-CMF). This step was completed within maximally 60 minutes of the mother animals' time of death.

After disposal of PBS-CMF supernatant, leaving only a small volume to cover the hippocampal material, 1mg trypsin was dissolved in 3.5ml 4°C cold PBS-CMF-EDTA, applied to the hippocampal material and incubated for 5 minutes at 37°C. After careful removal of supernatant, trypsination was stopped by DNase-Ovomucoid solution (trypsin inhibitor). Supernatant was again discarded and hippocampal neurons were isolated by trituration in 1ml NB-B27 (Brewer and Cotman 1989) in 3 steps. Supernatant cell suspension was collected in a fresh falcon tube after debris had settled and cell count was obtained using a Fuchs-Rosenthal cell counting chamber with a chamber factor of 5000. After disposal of DMEM-FCS, cells were plated with an initial cell density of 68000/cm^2 and maintained in 1ml NB-B27 per well at 37°C and 5% CO_2.

Neurons were transfected on *in vitro* Days 6–8 (**2.4.1.2**), experimental cell stress procedures (**2.4.1.3**) were performed over night from *in vitro* Days 8 to 9, and neurons were processed for immunochemistry (**2.6**) and molecular biology (**2.5**) or used for electrophysiological experiments (**2.7**) on *in vitro* Day 9.

2.4.1.2 Effectene based cell transfection

Effectene transfection reagent (Qiagen) was used for transfection of gephyrin variants on *in vitro* Days 6–8 (delta6–8 and delta4–8 on *in vitro* Day 6, delta6 control on *in vitro* Day 7, and delta5–7* and delta4* on *in vitro* Day 8), of gephyrin splice reporter on *in vitro* Day 7 and of GlyR on *in vitro* Day 6, as described previously (Meier *et al.* 2005). To ensure moderate protein expression at *in vitro* Day 9 in ~1% of hippocampal neurons, incubation times were reduced to 30min for delta6 control, 1h for delta4–8 and delta5–7*, 90min for delta4* and delta6–8 for gephyrin, and to 1h for GlyR and the RNA splice reporter. Otherwise, the Qiagen transfection protocol

was followed. For transfection, coverslips were transferred to fresh wells containing 500µl transfection NB medium. For each coverslip, 60µl of EC-buffer were mixed and gently vortexed for 10 seconds with 300ng DNA and 1.6µl Enhancer. After 5 minutes of incubation at room temperature, to facilitate DNA condensation, 5µl of Effectene were added and vortexed shortly. After another 15 minutes at room temperature, to allow complex formation of Effectene and DNA, 200µl of transfection medium were added and 270µl of the mix were applied carefully to the coverslips in small drops. Coverslips were incubated at 37°C and 5% CO_2 for 30 to 90 minutes (depending on the expression construct, see above).

After transfection, gephyrin transfected coverslips were transferred back into the original culture medium. In GlyR transfections, coverslips were transferred to fresh wells containing 1ml of glycine- and serum-free culture medium (transfection MEM) after incubation time, as described previously (Eichler *et al.* 2008). In co-transfections of myc-tagged GlyR beta subunits and HA-tagged GlyR alpha3 splice variants, a ratio of 1mol alpha to 5mol beta DNA was used, to facilitate assembly of heteropentameric alpha3/beta-GlyRs.

2.4.1.3 Experimental cellular stress procedures

To investigate the effect of cellular stress on gephyrin RNA splicing, rat hippocampal neurons were subjected to increased temperature or alkalisation for a period of 16h, which minimised cell death, from *in vitro* day 8 to 9. DAPI (4′,6-diamidino-2-phenylindole) staining was employed to judge the amount of cell death by the number of pyknotic nuclei and neurons with pyknotic nuclei were exempted from analysis of immunocytochemistry. Neurons were exposed to high-temperature cellular stress, by setting the incubator temperature to 39°C. To subject the cells to

alkalisation, the incubator CO_2 level was set to 0%, effecting a change of pH in the extracellular milieu (pH[e]) to a value of a value of 7.94 ± 0.06 at the end of the alkalosis stress period (for a time-course of pH change over 16h, see **3.1, Publication 1, Figure 9A**). A sub-set of cellular stress experiments was carried out with neurons previously transfected with the gephyrin RNA splice reporter construct (see **2.5.7.2**). Stressed neurons and untreated controls from the same batch were processed for immunocytochemistry and isolation of total RNA (see **2.6.3** and **2.5.3** respectively).

2.4.2 Human embryonic kidney cell culture and transfection

2.4.2.1 HEK293 cell cultivation

Human embryonic kidney (HEK293) cells were cultivated in T25 cell culture flasks at 37°C and 5% CO_2 with 5ml of HEK-MEM. Medium was changed approximately twice per week. Flasks with a confluent mono-layer of cells (after approximately 1 week of cultivation) were trypsinated with 0.1% trypsin solution and plated 1:20 in fresh flasks or on 13mm coverslips in 35mm cell culture dishes with 2ml HEK-MEM for transfection.

2.4.2.2 Calcium phosphate based transfection

A standard calcium phosphate precipitation protocol was followed for HEK293 cell transfection. For each cell culture dish, 2µg of DNA were mixed with 100µl $CaCl_2$ buffer. 100µl of 2x HBS buffer were added slowly in small steps (approximately 10µl each) and the mixture was incubated at room temperature for 15 minutes, before application. Cells were used for electrophysiology 2 to 3 days after transfection (see **2.7**) or processed for molecular biology and immunocytochemistry (see **2.5** and **2.6.3**) 4 days after transfection.

2.5 Molecular biology

2.5.1 Gel extraction

Gel extraction was done with the Matrix Gel Extraction System (Marligen Biosciences) following the standard protocol, except that 10 to 20µg silica gel was used for plasmids and 5µl silica gel was used for samples, and the pellets were re-suspended in 5-20µl (according to silica gel) of 10mM Tris buffer (pH 8.0).

2.5.2 TA vector

The in-house TA-cloning vector used for this study was obtained by digestion of pBluescript II SK (pBSK) with the restriction enzyme EcoRV for 2h at 37°C. The blunt ended, linearised pBSK was purified by gel extraction (**2.5.1**) and then incubated for 2h at 37°C, with dTTPs and RedTaq DNA-polymerase (Sigma-Aldrich), to add a single strand T-overhang to the 3'-end. The usable TA vector was obtained by purification in another gel extraction. The T-overhang of the TA vector could then be ligated with an overhanging A at the 3'-end of inserts amplified by polymerases lacking a 3'-5' exonuclease activity.

2.5.3 RNA isolation

Trizol reagent (Invitrogen) was used to isolate total RNA from primary rat hippocampal neurons, isolated mouse brain regions and whole hippocampectomies of patients suffering from intractable TLE. To avoid contamination with RNases, fresh gloves and sterile, RNA free pipette tips and Eppendorf reaction tubes were used. DEPC treated ddH_2O was used exclusively, to ensure the inactivation of any RNases by covalent binding to histidine residues in the catalytic domain.

Frozen patient material was dissolved in 1ml of Trizol reagent by triturating repeatedly. For RNA isolation from cell cultures, culture medium was removed and cells were dissolved in Trizol by washing repeatedly. Material from 12 wells in a 24-well plate was harvested with 1ml of Trizol reagent. After 5 minutes of incubation at room temperature, samples were stored on wet ice until processed further. Samples were then mixed vigorously with 200µl of chloroform each for 15 seconds, to create a uniform emulsion and incubated for 2 to 3 minutes at room temperature. Next, samples were centrifuged with 13000rpm (15700rcf) at 4°C for 15 minutes. The clear supernatant was transferred to a fresh Eppendorf reaction tube, avoiding the white interphase, mixed with 500µl isopropanol, incubated at room temperature for 10 minutes and centrifuged with 13000rpm (15700rcf) at 4°C for 10 minutes. Supernatant was discarded and 1ml of DEPC treated 75% ethanol was added to the pellet and mixed gently. After another 10 minutes of centrifugation at 4°C, with 13000rpm (15700rcf), supernatant was discarded again and the RNA pellet was air-dried and dissolved in 10 to 20µl of DEPC H_2O. The RNA concentration was determined, by measuring the optical density at 260nm, using an Eppendorf BioPhotometer.

2.5.4 Synthesis of complementary DNA

As for the RNA isolation, fresh gloves and sterile, RNA free pipette tips and Eppendorf reaction tubes were used, to avoid contamination with RNases. Superscript II (Invitrogen) was used for reverse transcription of 2µg RNA with a mixture of 3′-anchored poly-T oligonucleotide primers (oligo dT12/15/18) in a GeneAmp PCR System 2400 cycler (Perkin Elmer), to obtain complementary DNA (cDNA) for PCR analysis. The use of 3′-anchored poly-T oligonucleotides ensured an optimised yield and length of cDNAs containing open reading frames, as the reverse

transcriptase would skip the poly-A tails, due to primer binding at the beginning of the poly-A tail. For each sample, 2µg RNA were mixed in an RNase free PCR reaction tube with 1.33µl oligo dT12/15/18 (0.5µg/µl of 13-,16- and 19-mer oligo dTs, each) and filled up with DEPC treated H_2O to 12.5µl total volume. The RNA samples were heated to 70°C for 10 to 15 minutes, to break up secondary structures, while the premix was prepared with 4µl of 5 x 1st standard buffer, 2µl DTT and 1µl dNTP´s. The RNA samples were cooled at 4°C for 2 minutes and 7µl of premix was added to each sample. The samples were then heated up to 42°C, 0.5µl Super Script II reverse transcriptase (Invitrogen) was added to each tube and the samples were incubated for 60 minutes at 42°C. After the incubation time, the samples were heated to 70°C for 10 minutes, to inactivate the enzyme, and finally stored at -20°C.

2.5.5 Polymerase chain reaction

Unless otherwise noted, polymerase chain reaction (PCR) was performed as described here. Oligonucleotide primers applied in this work (see **Table 4** for a comprehensive list of primers with corresponding sequences) were used at a final concentration of 0.2µM. PCR was performed using RedTaq DNA polymerase (Sigma-Aldrich), with 1min elongation at 72°C and 1min of annealing at oligonucleotide-corresponding temperatures. For samples derived from human patient material, post-mortem hippocampus RNA pooled from 20 healthy Caucasians (Clontech) was used for control purposes. PCR products were separated with agarose gel electrophoresis and ImageQuant software (Molecular Dynamics) was used to quantify the mean pixel intensity of bands.

2.5.5.1 Semi-quantitative PCR

Glyceraldehyde 3-phosphate dehydrogenase (GAPDH) or beta-actin messenger RNA was amplified in the same PCR reaction tube with the gene of interest for semi-quantitative PCR. To determine GlyR beta expression relative to GAPDH, samples were subjected to 35 cycles of PCR with an annealing temperature of 54°C. The oligonucleotide concentration for GAPDH primers was set to 0.025µM, to produce comparable band intensities. For analysis of KCC2 expression levels in comparison to beta-actin, 30 cycles with 58°C annealing temperature were run, and the oligonucleotide concentration for beta-actin primers was set to 0.1µM, to yield comparable band intensities. Expression levels were calculated by dividing the mean pixel intensity of PCR product bands of GlyR beta by that of GAPDH and the intensity of KCC2 bands by that of beta-actin.

2.5.5.2 Isolation of irregularly spliced *GPHN* transcripts

To screen TLE patient cDNAs, oligonucleotide primers binding up- and downstream from the alternatively spliced regions of the gephyrin G-, C- and E-domain, respectively, were used (for oligonucleotide sequences, see **Table 4**). The PCR was run with manual hot start for 45 cycles (1min annealing at 50°C). Amplification of post-mortem control hippocampus cDNA with our low stringency PCR protocol resulted in the PCR band pattern including regular (delta6) gephyrin and the G2 splice variant (Fritschy *et al.* 2008), that has previously been observed (Meier and Grantyn 2004; Smolinsky *et al.* 2008). Thus, this PCR protocol is suitable for screening TLE patient material. Agarose gel regions containing G-domain PCR products of unusual size (there were no unusual bands for C- and E-domain) were purified (see **2.5.1**) and ligated with the in-house TA cloning vector (see **2.5.2**).

The relative expression of unusually sized G-domain PCR-products was determined as the ratio between mean pixel intensities of unusually and regularly sized G-domain PCR products. 25 clones of unusual PCR products were DNA sequenced and 4 different TLE-specific gephyrin G-domains could be identified.

2.5.5.3 Detection of GlyR alpha2A and GlyR alpha2B splice variants

This experiment was performed by Sabrina A. Eichler in the lab of Jochen Meier (MDC Berlin). To investigate the relative expression of GlyR alpha2A and GlyR alpha2B, PCR was run with 30 cycles at 58^{o}C annealing temperature. To discriminate the resulting PCR products of similar size, PCR for both splice variants was run in parallel in two separate reaction tubes. The ratio of band intensity between 2A and 2B was used to determine the predominantly expressed splice variant.

2.5.5.4 Detection of GlyR alpha3L and GlyR alpha3K splice variants

This experiment was performed by Sabrina A. Eichler in the lab of Jochen Meier (MDC Berlin). The relative expression of GlyR alpha3 long (L) and short (K) splice variant was analysed via PCR with oligonucleotides flanking the alternatively spliced exon 8A. PCR was run wit 40 cycles at 52^{o}C annealing temperature for human samples and 35 cycles at 54^{o}C annealing temperature for mouse samples. The amount of alternatively spliced GlyR alpha3 was expressed as the ratio of GlyR alpha3K band intensity divided by GlyR alpha3L band intensity. PCR products obtained from human and mouse samples were identified by DNA sequencing at Invitek Stratec GmbH (Berlin, Germany).

2.5.5.5 Detection of GABA(A)R subunits

RNA isolated (see 2.5.3) from primary hippocampal rat neurons (see 2.4.1) at *days in vitro* 9 was analysed by semi-quantitative PCR of GAPDH with oligonucleotides specific to $GABA_A$ receptors alpha1, alpha2, alpha3, alpha5, beta2, beta3 and gamma2 (see Table 4). The PCR was run with manual hot-start at an annealing temperature of 58°C for 30 cycles.

2.5.6 DNA extraction and sequencing of genomic regions

Invisorb Spin Tissue Midi Kit (Invitek Stratec GmbH) was used, according to the manufacturer's instructions, to extract genomic DNA from frozen TLE patient hippocampectomies. Oligonucleotide primers framing *GPHN* exons 3, 5, 8 and 9, including the flanking intron sequences approximately 200bp up- and down-stream of the exons, were used for amplification of genomic DNA sequences by PCR. Intron sequences were included, to verify consensus sequences required for formation of 'lariat' structures during RNA splicing. Intron 8 was likewise amplified using appropriate oligonucleotide primers. For oligonucleotide sequences see **Table 4**. The resulting PCR products were purified using the Invisorb Spin DNA Extraction Kit (Invitek Stratec GmbH) according to the manufacturer's instructions, and directly sequenced using the oligonucleotides mentioned above. Upon detection of composite sequences, the respective PCR products were ligated with in-house TA cloning vector and 4–6 recombinant clones were sequenced. Sequencing was performed at Invitek Stratec GmbH (Berlin, Germany).

2.5.7 Expression constructs

All cDNA-clones employed in the course of this work were DNA-sequenced at Invitek Stratec GmbH (Berlin, Germany). A eukaryotic pEGFP-N1 expression vector with a cytomegalovirus (CMV) promoter (BD Biosciences Clontech) was used as a basis for the HA-GlyR alpha3K and L, c-myc-GlyR beta, GlyR alpha1^{185L}, GlyR alpha1^{185P}, GlyR alpha3K^{185L} and GlyR alpha3K^{185P} expression constructs and the gephyrin splice-reporter constructs. Gephyrin single-exon expression constructs were based on a eukaryotic pDsRed Express-C1 expression vector with a CMV promoter (BD Biosciences Clontech). All TLE-gephyrin expression constructs were derived from an EGFP-tagged delta 6 gephyrin construct (Lardi-Studler *et al.* 2007), which was based on eukaryotic pEGFP-C2 expression vector with a CMV promoter (Clontech).

2.5.7.1 Gephyrin expression constructs

For control purpose and as a basis for TLE gephyrin expression constructs, the enhanced green fluorescent protein (EGFP)-tagged, regular delta6 gephyrin (Lardi-Studler *et al.* 2007) was used. Fusion PCR on EGFP-tagged delta6 gephyrin was employed, to generate the delta4–8 expression construct, using Phusion Hot Start High-Fidelity DNA polymerase (New England Biolabs) with 5% dimethylformamide and oligonucleotide primers including BspEI restriction sites. The restriction sites introduced into the nucleotide sequence are silent with respect to the deduced amino acid sequence. A touch-down PCR protocol was run with 7 minutes elongation at 68^{o}C and five cycles at 53^{o}C, followed by five cycles at 49^{o}C and finally 32 cycles at 45^{o}C annealing temperature. The TLE-specific region spanning exons 4–8 was excised in-frame, due to self-ligation of the PCR product after digestion with BspEI.

The remaining three TLE-gephyrin constructs were obtained by PCR amplification of sequenced G-domains (see **Table 4** for oligonucleotide sequences), running 32 cycles at 58^{o}C annealing temperature with Phusion polymerase. PCR products were digested with BspEI and AflII and ligated with EGFP-tagged delta6 gephyrin. To this end, PCR-based silent mutagenesis (fusion PCR, as described above) was employed, to introduce BspEI and AflII sites in two consecutive rounds (see **Table 4** for oligonucleotide sequences).

DsRed-Express-tagged gephyrin exon expression constructs were likewise created by PCR amplification of EGFP-tagged delta6 gephyrin with corresponding oligonucleotide primers including XhoI and BamHI restriction sites and including stop codons at the 3'-end of reverse primers (see **Table 4**). Subsequently, PCR products were digested with XhoI and BamHI and inserted in-frame into pDsRed-Express C1 (Clontech). In case of exon 5, KpnI was used in lieu of BamHI.

2.5.7.2 Gephyrin RNA splice reporter constructs

To investigate skipping of the gephyrin G-domain exon 4 in the course of gephyrin RNA splicing, a reporter construct consisting of the two fluorescent proteins tdTomato and EGFP separated by gephyrin exons 3 to 5 was generated. The gephyrin based part of the construct was derived from sequence-verified DNA clones of genomic DNA from TLE patient hippocampectomies. The exon 3, including the downstream flanking intron sequence, exon 4 including both adjacent intron sequences, and exon 5 including the upstream flanking intron sequence were amplified by PCR with oligonucleodide primers introducing restriction enzyme sites for molecular assembly of the splice reporter (for oligonucleotide primer sequences see **Table 4**).

Using site-directed mutagenesis (GeneEditor, Promega), a sequence encoding the 2A peptide from *Thosea Asigna* virus (EGRGSLLTCGDVEENPG / P) was introduced between fluorescent protein- and gephyrin-specific sequences. This ensured reliable co-expression of heterologous proteins, due to cleavage at the indicated (/) position (Tang *et al.* 2009).

pEGFP-N1 served as a vector backbone for the construct, which was assembled using the following restriction enzymes: NheI and XhoI for tdTomato-2A, XhoI and EcoRI for gephyrin exon 3 including 3'-flanking intron, EcoRI and KpnI for exon 4 including 5'- and 3'-flanking intron, KpnI and BamHI for exon 5 including 5'-flanking intron. After site-directed mutagenesis to introduce 2A up-stream of EGFP the resulting 2A-EGFP was inserted into pEGFP-N1 using BamHI and NotI. The generated construct turns EGFP expression off when exon 4 is skipped during RNA splicing. To obtain a construct that turns EGFP expression on upon exon skipping, a single additional nucleotide (G) was inserted into the open reading frame of exon 5.

Total RNA isolated from splice reporter transfected HEK293 cells (see **2.5.3**) was subjected to PCR analysis (see **2.5.5.2**), to control excision of intron sequences during reporter construct expression. 50µg of isolated RNA was digested with 10 units RNase-free DNase (Roche Applied Science) at 37°C for 20 minutes to eliminate remaining plasmid DNA, and purified with RNeasy Protect Mini Kit (Qiagen). cDNA synthesized from purified, DNA-free RNA (**2.5.4**) was amplified by PCR with 2A sequence-matched oligonucleotides. To ensure that samples were in deed free of plasmid DNA, a plasmid-matched oligonucleotide in combination with the 2A-matched oligo was amplified in parallel.

2.5.7.3 Epitope tagged and high affinity GlyR expression constructs

Molecular cloning and epitope tagging of other GlyR subunits were described previously (Meier *et al.* 2000) and expression constructs provided by Jochen Meier (MDC Berlin). Briefly, total RNA was isolated from adult mouse hippocampus (see **2.5.3**), to obtain open reading frames of GlyR alpha2B, GlyR alpha3K, GlyR alpha3L and GlyR beta messengers. The hemagglutinin (HA) epitope (YPYDVPDYA; (Hamsikova *et al.* 1987)) or myc epitope (EQKLISEEDL; (Evan *et al.* 1985)) were inserted in the cDNA using site-directed mutagenesis (Promega GeneEditor). The epitopes were positioned upstream of base sequences coding for SGKHPS (alpha2), SRSAPM (alpha3) and KSSKKG (beta), respectively, i.e. following predicted signal peptide cleavage sites. The cDNA sequences of epitope-tagged receptor subunits were then subcloned into a eukaryotic expression vector with a CMV promoter, which was derived from pEGFP-N1 (Clontech). High affinity GlyR alpha1^{185L} constructs were likewise produced by site-directed mutagenesis of GlyR alpha1^{185P}.

2.5.8 Molybdenum cofactor synthesis assay

Analysis of MoCo synthesis was performed by Abdel Ali Belaidi in the laboratory of Günter Schwarz (University of Cologne). The *in vitro* nit-1 reconstitution assay, based on the transfer of MoCo to the nitrate reductase apoprotein of the *Neurospora crassa* nit-1 mutant (Nason *et al.* 1971), was used to quantify biologically active MPT and MoCo. EGFP-tagged regular gephyrin (delta6) and TLE-gephyrins, respectively, (see **2.5.7.1** for details) were expressed in HEK293 cells (see **2.4.2.2**). Cells were harvested 48h after transfection, washed in PBS twice and sonicated in 100–200µl nit-1-buffer (see **2.1.4.9**). For each sample, 1–20µl of crude cell extract was then incubated with 20µl of *Neurospora crassa* nit-1 extract supplemented with reduced glutathione (2mM). The assay used reconstitution of nit-1 nitrate reductase over night

in the presence of 5mM sodium molybdate to determin MPT, and in the absence of molybdate to detect MoCo, respectively, as described previously (Reiss *et al.* 2001).

2.6 Immunochemistry

For all antibodies used in immunochemistry see **Table 3**.

2.6.1 Western blot analysis

Western blot for human hippocampal gephyrin expression was done by Abdel Ali Belaidi in the laboratory of Günter Schwarz (University of Cologne). Frozen tissue samples were thawed at room temperature and washed with acetone 3 times. After the tissue was air dried, proteins were extracted under vigorous shaking at 95°C for 30min in buffer containing 25mM Tris, 200mM glycine and 0.1% sodium dodecyl sulphate (SDS). Hippocampal protein extracts of TLE patient material were re-suspended in 100–200µl PBS and sonicated. 100µg ofprepared protein were separated by SDS-PAGE (polyacrylamid gel electrophoresis) on an 8% gel alongside PageRuler™ Prestained Protein Ladder (Fermentas GmbH) and proteins were transferred to a polyvinylidene difluoride (PVDF) membrane with 75mA for 1h. Membranes were immersed in tris-buffered saline (TBS) blocking solution containing 5% milk powder for 1h, to block non-specific binding sites, and subsequently incubated with the monoclonal 3B11 antibody (see **Table 3**; dilution 1:1000 in TBS) against the gephyrin E-domain at room temperature for 1h. The membrane was washed 3 times with PBS, once with wash-buffer and once more with PBS for 10min each, before incubation with horseradish peroxidase-conjugated anti-mouse IgG antibody (see **Table 3**; diluted 1:10000 in TBS) for 1h at room temperature. After secondary antibody incubation, the membrane was washed again with PBS, wash-

buffer and PBS. Blots were developed by 2min of incubation with SuperSignal West Pico Chemiluminescent Substrate (Thermo Fisher Scientific), visualized in a Chemolumineszenz DeVision R2000 (Decon Science Tec GmbH) and proteins were quantified with Gel-Pro Analyser (MediaCybernetics).

Western blot analysis of GlyR alpha3L expression in the mouse hippocampus was performed by Sabrina A. Eichler (laboratory of Jochen Meier, MDC Berlin) as described above, except that SDS-PAGE was transferred to a Hybond-P membrane. Rabbit polyclonal antibody (pAb) against GlyR alpha3L served as a primary antibody with a dilution of 1:750 and incubation overnight at 4^{o}C under mild shaking.
A horseradish peroxidase-conjugated secondary antibody against rabbit IgG was used (see **Table 3**; dilution 1:10000). Both antibodies were incubated in TBS with 2% bovine serum albumin (BSA). Enhanced chemiluminescence (ECL) Immun-Star-WesternC (BioRad) was used to develop blots and Molecular Imager ChemiDoc XRS (BioRad) was employed to visualize the blots.

2.6.2 Immunohistochemistry

Unless otherwise stated, all washing steps and all incubations for immunohistochemistry were carried out in glass cuvettes on a magnetic stirrer at room temperature. Directly after cryosectioning (see **2.3.3**), sections were post-fixed in PFA-sucrose for 5 minutes, washed with PBS 3 times for 5 minutes, then incubated with NH_4Cl (50mM in PBS) and washed with PBS 2 more times. To block unspecific antibody binding, cryosections were incubated for 2h in PBS-gelatine (0.1%) at 4^{o}C without stirring. Antibodies were applied in a humidity chamber on parafilm. Object slides were dried carefully around the tissue and cryosections were circled with a glycerol DAKO pen. All primary antibodies for immunohistochemistry

(see **Table 3**) were diluted in PBS-gelatine with 0.12% Triton X-100 for permeabilisation. The dilution factors for primary antibodies were optimised individually for signal strength and specificity (**Table 3**). All secondary antibodies were diluted 1:200. 50µl of primary antibody mix were applied to each cryosection and incubated in the humidity chamber sealed with parafilm at 4°C over night (approximately 16h). A styrofoam cover was placed on the chamber lid, to avoid water condensation. After incubation with primary antibodies, cryosections were washed 3 times with PBS-gelatine, before 50µl of secondary antibody mix in PBS-gelatine (without Triton X-100) were applied for an incubation time of 1h at room temperature in a humidity chamber with an opaque lid. After incubation with secondary antibodies, cryosections were washed 3 times with PBS-gelatine and once with PBS at room temperature for 5 minutes. Object slides were shortly submersed in ddH_2O and carefully dried with a soft cosmetic tissue paper around cryosections. 6µl VectaShield with DAPI (Vector Laboratories, Inc.) were applied to each cryosection, and they were sealed with glass coverslips and clear nail-polish.

2.6.3 Immunocytochemistry

2.6.3.1 Surface staining

All primary antibodies for surface-staining were diluted in cell-culture medium, dilution factors were optimised individually for signal strength and specificity (see **Table 3**). Coverslips were transferred to 500µl cell-culture medium on parafilm in a humidity chamber. Medium was removed from the coverslips without letting them run completely dry and 30µl of antibody mix was added to each coverslip. The incubation time of 5 minutes was carried out in a cell-culture incubator at 37°C and 5% CO_2. Afterwards, antibody mix was diluted with 500µl cell-culture medium and washed 3 more times with 500µl medium before fixation (see **2.6.3.2** and **2.6.3.3**).

2.6.3.2 Methanol fixation and permeabilisation

For methanol fixation and permeabilisation, coverslips with cells were transferred to a 24-well plate with 1ml of -20°C cold mix of 95% methanol and 5% glacial acetic acid and then incubated at -20°C for 10 minutes. To keep the temperature during transfer of coverslips to and from the fixation solution, the plate was placed on a cooled aluminium block. After incubation, the coverslips where transferred into 1ml PBS on parafilm, in a humidity chamber and washed 3 times with 1ml of PBS. Afterwards, PBS was exchanged for 1ml PBS-gelatine (0.1%) and incubated at room temperature for 2 to 3 minutes, to block unspecific antibody binding. Finally coverslips where washed 2 more times with 1ml PBS-gelatine.

2.6.3.3 Paraformaldehyde fixation and Triton-X permeabilisation

For Paraformaldehyde (PFA) fixation, coverslips with cells were transferred to a 24-well plate with 1ml of ice cold PFA-sucrose per well and then incubated at room temperature for 15 minutes. After incubation, the coverslips where transferred into 1ml PBS on parafilm, in a humidity chamber and washed 3 times with 1ml of PBS. To reduce fluorescence background of PFA for stainings including EGFP expressing cells or FITC, coverslips were incubated for 15 minutes at room temperature with 1ml of NH_4Cl (50mM in PBS) and washed another 2 times with PBS. Afterwards, PBS was exchanged for 1ml PBS-gelatine (0.1%) and incubated at room temperature for 2 to 3 minutes, to block unspecific antibody binding. For permeabilisation, PBS-gelatine was exchanged for 500µl 0.12% Triton X-100 (Sigma-Aldrich Logistik GmbH) in PBS-gelatine and incubated for 4 minutes at room temperature. Finally, coverslips were washed 2 more times with 1ml PBS-gelatine.

2.6.3.4 Intracellular staining

All secondary and primary antibodies for immunocytochemistry (except for surface staining, see **2.6.3.1**) were diluted in PBS-gelatine. The dilution factors for primary antibodies were optimised individually for signal strength and specificity (see **Table 3**), all secondary antibodies were diluted 1:200. For incubation with antibodies, PBS-gelatine was removed from the coverslips without letting them run completely dry and 30µl of antibody mix was added to each coverslip. For incubation the humidity chamber was closed. After incubation, antibody mix was diluted with 1 ml PBS-gelatine and then removed by washing 3 times with 1ml PBS-gelatine. Primary antibodies were incubated for 1h and secondary antibodies were incubated for 45 minutes, respectively, at room temperature in a humidity chamber with an opaque lid. After incubation with secondary antibodies washing with PBS-gelatine, coverslips were washed 2 times with 1ml PBS, shortly immersed in ddH_2O and dried quickly and carefully, with a soft cosmetic tissue paper from the side and bottom, mounted up-side down on glass microscope slides with 3µl VectaShield with DAPI (Vector Laboratories, Inc.), and sealed with clear nail-polish.

2.6.4 Microscopy and image analysis

2.6.4.1 Fluorescence microscopy

Images of labelled primary hippocampal neurons and HEK293 cells were obtained with an Olympus BX51 standard epifluorescence microscope (Olympus) using a U Plan Apo 40x oil objective with a numerical aperture of 1.00 and U Plan S Apo 60.0× oil objective with a numerical aperture of 1.35 (Olympus). Fluorescence signals were separated using appropriate excitation and emission filter sets (U-MSP100v2 MFISH for DAPI; U-MSP101v1 MFISH for EGFP and FITC; U-MSP102v1 MFISH for DSRed, Cy3 and TRITC; U-MSP104v1 MFISH for Cy5; Olympus). Signals were detected with

a 14-bit cooled charge couple device (CCD) camera (Spot PURSUIT, Visitron Systems GmbH) and acquired using Metamorph software (Universal Imaging Corp.).

2.6.4.2 Confocal microscopy

Confocal laser scanning microscopy was employed, using a DM TCS SP2 (Leica Microsystems), to visualise fluorescence signals of granule and pyramidal cell layers in human hippocampal dentate gyrus and CA3 region, as well as mouse brain sections. To avoid cross-talk between fluorescent signals, fluorochromes were excited sequentially with an argon laser at 488nm (EGFP and FITC) and two helium-neon lasers at 543nm (DSRed, Cy3 and TRITC) and 633nm (CY5) respectively. Through an HCX PL APO 40.0x UV oil objective (Leica Microsystems) with a numerical aperture of 1.25. To minimize background noise, 6 frames from multiple scans were averaged, while acquiring images using LCS software (Leica Microsystems).

2.6.4.3 Splice reporter assays

Metamorph software (Universal Imaging Corp.) was used to measure the ratio between red and green fluorescence within 15µm diameter circular regions of interest projected on the centre of the neuronal soma. Images were not auto-scaled, and the same exposure times were used, both for cellular stress and control conditions. Prior to measurement of supra-threshold pixel grey levels, images were thresholded to 50% in the red channel and 10% in the green channel.

2.6.4.4 Co-localisation analysis

Fluorescent signals on minimum-maximum threshold images of triple- or quadruple-stained transfected neurons (see **2.6.3** and **2.4.1.2**) were acquired along proximal

dendrites in a circular region of interest (ROI). The ROI with a diameter of 100µm was projected on a transfected neuron, the centre of the ROI roughly coinciding with the centre of the soma. The number of receptor clusters and co-localisation with pre-synaptic markers or gephyrin was quantified manually. Assuming a round shape of the contact, a size criterion was applied in synaptic terminal counts, to avoid false positives. A true positive synaptic terminal was defined as an area of supra-threshold intensity with a 0.5 to 2µm diameter. The threshold intensity was set to average intensity in ROI ± 3 times standard deviation (3σ criterion; (Meier and Grantyn 2004)).

2.6.4.5 Receptor cluster analysis

Scion Image (Scion Corp.) and Origin (Microcal) software were employed for receptor cluster analysis in GlyR alpha3K or L transfected neurons. Pixel grey levels of GlyR immunofluorescence along proximal dendrites were acquired via line scans, and plotted against the scanned distance. Pixels were considered part of a receptor cluster, if pixel grey levels were at least 3 times standard deviation below mean pixel grey level across the entire line scan (3σ criterion; (Meier and Grantyn 2004)). An inverse grey scale was applied with a maximum grey scale value of 255 representing black, thus increasing white perception results in declining grey scale values. To calculate the diameter of a receptor cluster the distance between threshold-determined cluster edges was measured. The cluster slope, defined as the relative change of consecutive pixel grey scale values, and calculated as current divided by previous pixel grey scale value, was determined for analysis of GlyR alpha3L cluster shape. Again, an inverse grey scale was applied and therefore the cluster slope was calculated from a cluster's declining phase of grey scale values.

Mathematical image processing was applied to corresponding pairs of images of HA-alpha3 and myc-beta GlyR signals, to rule out bias of quantitative morphometric analysis of heteromeric alpha3/beta-GlyR by non-overlapping signals. For cluster and co-localisation analyses, only congruent HA-alpha3 and myc-beta GlyR signals in the resulting images were used.

2.7 Electrophysiology

All electrophysiological recordings were performed in a continuously perfused recording chamber at room temperature. See **2.1.4** for a detailed description of extracellular and recording pipette solutions.

2.7.1 Whole-cell patch-clamp

Whole-cell patch-clamp recordings were performed by René Jüttner (laboratory of Fritz Rathjen, MDC Berlin). A P-97 puller (Sutter Instruments) was used to fabricate patch electrodes from borosilicate glass capillaries tubing. All whole-cell patch-clamp recordings were performed with a holding potential of -70mV using an EPC-9 (HEKA Electronics).

In whole-cell patch-clamp recordings from primary hippocampal neurons, the same cell-culture batches, which provided neurons for electrophysiological experiments, were also analysed via immunocytochemistry. Post-synaptic currents were recorded from neurons expressing delta4* TLE gephyrin or EGFP, as well as un-transfected neurons at *in vitro* Day 9 (**2.4.1.2**). The series resistance of 5–20MOhm was monitored throughout the entire experiment and compensated up to 70%.

Recordings lasted for at least 300s. To pharmacologically isolate miniature GABAergic post-synaptic currents, glutamatergic synaptic transmission was blocked by application of 20µM DNQX (6,7-dinitroquinoxaline-2,3-dione) and 50µM DL-APV (DL-2-Amino-5-phosphonopentanoic acid), and 1µM TTX (tetrodotoxin) was applied to block generation of action potentials. Electrophysiological signals were sampled at a rate of 10kHz, post-synaptic currents were filtered at 3kHz and analysed off-line using WinTida 5.0 (HEKA Electronics) and MiniAnalysis (Synaptosoft Inc.).

In HEK293 cells whole-cell patch-clamp recordings were performed 2 to 3 days after co-transfection with EGFP and GlyR alpha1 expression constructs (see **2.4.2.2**). A gravity-driven 5-channel superfusion system was employed to locally apply glycine or taurine for 3s. Different agonist concentrations were tested in random order and a minimal interval of 60s was observed between successive applications to allow receptors to recover from desensitisation. Signals were recorded at a sampling rate of 5kHz and filtered at 1kHz. Signal analysis was performed off-line with TIDA 5.1 software (HEKA Electronics). Origin 7.0 software (OriginLab) was used to plot and fit peak currents obtained with different glycine or taurine concentrations to the Hill equation to determine the EC_{50} value for agonists.

2.7.2 Outside-out patch-clamp

Outside-out patch-clamp recordings were performed by Pascal Legendre (University Pierre et Marie Curie, Paris) 2 days after transfection of HEK293 cells (see **2.4.2.2**) with GlyR alpha3K^{185P} or alpha3K^{185L} constructs. A Brown-Flaming puller (Sutter Instrument Co.) was used with thick-wall borosilicate glass (Harvard Apparatus), to fabricate patch-clamp electrodes (5–10MOhm). The bath chamber was perfused at a rate of 2ml/min, and the membrane potential was held at -50mV during experiments.

A fast-flow operating system (Legendre 1998) was used to evoke outside-out single-channel currents. The application pipette was manufactured from a thin-wall glass theta tube (2mm outer diameter; Hilgenberg) that was pulled and broken to obtain a 200µm tip diameter. The glass theta tube was moved using a piezo-electric translator (model P245.30, Physik Instrument) and positioned 100µm away from the outside-out patch. Drug (glycine or GABA) and control solution, were gravity-fed into 1 channel of the application pipette, respectively, and the solution exchange was performed by rapid movement of the solution interface across the patch pipette tip. Agonist concentration steps were applied with a minimal interval of 10s. Prior to each set of experiments the exchange time solution (<100µs) was determined. To this end a 10%-diluted control solution was applied to the open patch pipette tip, and the evoked change in the liquid junction potential was monitored. Signals were acquired at a sampling rate of 50kHz using an Axopatch 1D amplifier (Axon Instruments), filtered at 10kHz using an eight-pole bessel filter (Frequency Devices), and analysed off-line using pClamp software 10.1. (Axon Instruments).

2.8 Statistical data analysis

Unless stated otherwise, numerical data is presented as mean ± standard deviation (SD), and statistical analysis was performed using Origin software (Microcal). Pooled data from GlyR stainings (see **2.6.4.4** and **2.6.4.5**) is presented as mean ± standard error of mean (SEM). Unpaired Student's *t*-test was employed for comparison of 2 groups, for comparison of 3 or more groups, Nevene's test for equal variance and one-way analysis of variance (ANOVA) were performed, followed by *post hoc* Bonferroni's test. Significance levels are indicated in tables and figures with asteriscs (*$P < 0.05$, **$P < 0.01$, ***$P < 0.001$), and refer to either Student's *t*-test or *post-hoc* Bonferroni's test.

All hippocampal cell culture experiments were repeated at least once using different cell cultures, and accordingly neurons were sampled from at least 2 cultures. In immunohistochemistry of mouse tissue, brain slices of 3 different animals were processed, and at least 5 view fields per hippocampus were analysed.

In GlyR stainings data from multiple view fields or coverslips was pooled, after securing the absence of significant differences between means of view fields or coverslip by ANOVA. To ensure ANOVA was applicable, means of coverslips or view fields were tested for normal distribution with Shapiro-Wilk's test against a significance level of 0.05.

As stated above (**2.7.1**), peak currents obtained with different glycine or taurine concentrations were plotted and fitted to the Hill equation to determine the EC_{50} value for agonists. For details on receptor cluster analysis and co-localisation see **2.6.4.4** and **2.6.4.5**, respectively.

3.1 Publication 1

Förstera B, Belaidi AA, Jüttner R, Bernert C, Tsokos M, Lehmann TN,
Horn P, Dehnicke C, Schwarz G, Meier JC.

Irregular RNA splicing curtails post-synaptic gephyrin in the *cornu ammonis* of patients with epilepsy.

Brain. 2010 Dec;133(Pt 12):3778-94. Epub 2010 Nov 10.

Publication is available online:
http://dx.doi.org/10.1093/brain/awq298

3.2 Publication 1, Supplementary Data

Förstera B, Belaidi AA, Jüttner R, Bernert C, Tsokos M, Lehmann TN,
Horn P, Dehnicke C, Schwarz G, Meier JC.

Irregular RNA splicing curtails post-synaptic gephyrin in the *cornu ammonis* of patients with epilepsy. Supplementary Data

Brain. 2010 Dec;133(Pt 12):3778-94. Epub 2010 Nov 10.

Supplementary data is available online:
http://dx.doi.org/10.1093/brain/awq298

3.3 Publication 2

Legendre P, Förstera B, Jüttner R, Meier JC.

Glycine receptors caught between genome and proteome - Functional implications of RNA editing and splicing.

Front Mol Neurosci. 2009;2:23. Epub 2009 Nov 9.

Publication is available online:
http://dx.doi.org/10.3389/neuro.02.023.2009

3.4 Publication 3

Eichler SA, Förstera B, Smolinsky B, Jüttner R, Lehmann TN, Fähling M, Schwarz G, Legendre P, Meier JC.

Splice-specific roles of glycine receptor alpha3 in the hippocampus.

Eur J Neurosci. 2009 Sep;30(6):1077-91. Epub 2009 Sep 1.

Publication is available online:
http://dx.doi.org/10.1111/j.1460-9568.2009.06903.x

4. Discussion

4.1 GABA(A)R, Gephyrin & TLE

While this study encompasses post-transcriptional modification of GlyR and gephyrin, the primary aim of this work was to elucidate the hitherto unknown mechanisms that underlie loss of gephyrin immunoreactivity and the role it plays in TLE pathophysiology. Kainat-injected epileptic mice exhibit reduced gephyrin immunoreactivity in the hippocampal cornu ammonis region (Knuesel *et al.* 2001) and gephyrin expression gradually decreased during acute and latent periods of TLE in experimental rats (Fang *et al.* 2011). Given the role of gephyrin in GABA(A)R clustering, this observation fits the involvement of anomalous GABAergic inhibition in TLE (Kumar and Buckmaster 2006; Stief *et al.* 2007; Eichler and Meier 2008).

This study reveals pathological gephyrin expression as a cause of curtailed GABA(A)R alpha2 scaffolds in the cornu ammonis of TLE patients. The incidence of these findings irrespective of hippocampal sclerosis rules out neuronal drop out as a cause of this development (see **3.1, Publication 1**). Furthermore, the absence of genome sequence modifications in TLE patients (see **3.2, Publication 1, Supplementary Figure 8**), and *in vitro* experiments with primary hippocampal neurons of a wild type background, support the notion that the synthesis of aberrant gephyrin is based on inhibition of gephyrin RNA splicing due to cellular stress like alkalosis and hyperthermia (see **3.1, Publication 1, Figure 9**), which have been related to epileptogenesis before (Church and Baimbridge 1991; Hartley and Dubinsky 1993; Ben-Ari *et al.* 2007; Qu and Leung 2008).

On the contrary, down-regulation of post-synaptic gephyrin in TLE could also result from enhanced protein turn-over in response to increased calcium and calpain mediated gephyrin proteolysis (Tyagarajan *et al.* 2011). It is reasonable to assume that both impaired de-novo synthesis and increased gephyrin turn-over apply to pathogenesis of TLE, given that mice expressing an RNA-editing deficient glutamate receptor (GluR) with increased calcium permeability develop severe epilepsy (Brusa *et al.* 1995).

4.1.1 Gephyrin oligomerisation is essential for the post-synaptic enrichment & stabilisation of GABA(A)R

The C-terminal gephyrin E domain provides GABA(A)R alpha2 binding sites (Tretter *et al.* 2008; Saiepour *et al.* 2010) and controls the enrichment and stabilisation of receptors by regulating the size of post-synaptic receptor scaffolds (Kneussel *et al.* 1999; Meier *et al.* 2000; Meier *et al.* 2001; Levi *et al.* 2004). Gephyrin oligomerisation plays an important part in this mechanism, as it allows a multiplication of receptor docking sites, and accordingly, any impairment of gephyrin aggregation will in turn reduce the availability of GABA(A)R alpha2 binding sites.

Structural and functional data indicates a hexagonal protein lattice as a result of G domain trimerisation and E domain dimerisation (Sola *et al.* 2001; Schwarz *et al.* 2001; Schrader *et al.* 2004; Sola *et al.* 2004; Lardi-Studler *et al.* 2007). The potential of alternative splicing to impact gephyrin aggregation was revealed by the properties of the gephyrin G2 splice variant (Fritschy *et al.* 2008), which incorporates exon 6 and exerts dominant negative effects (Meier *et al.* 2000; Meier and Grantyn 2004; Smolinsky *et al.* 2008). This exon 6 gephyrin disrupts G domain trimerisation (Schwarz *et al.* 2001) and produces filamentous gephyrin aggregates upon E domain

dimerisation (Meier *et al.* 2000; Smolinsky *et al.* 2008). Moreover this work reveals that the G2 splice variant is catalytically inactive in molybdenum co-factor (MoCo) synthesis (see **3.1, Publication 1, Figure 5A** and **B**), which takes place in brain astrocytes (Smolinsky *et al.* 2008). The expression of gephyrin with exon 6 was thence investigated as a prime suspect for the cause of impaired post-synaptic GABA(A)R scaffolds in TLE. This investigation did not turn up any evidence for an up-regulation of exon 6 gephyrin in hippocampectomies from patients with TLE, however (see **3.1, Publication 1, Figure 4B**).

4.1.2 TLE patients express irregularly spliced TLE gephyrins

While exon 6 gephyrin was not found to be up-regulated in the hippocampus of TLE patients, 4 abnormally spliced gephyrin G domains were identified. All of these irregularly spliced TLE gephyrins omitted exon 7 and were aggregation-deficient (see **3.1, Publication 1, Figure 4** and **3.2, Publication 1, Supplementary Figure 6**). Exon 7 constitutes an integral part of the G domain trimerisation interface (Sola *et al.* 2001; Schwarz *et al.* 2001), the loss of which is the probable cause for abolishment of regular aggregation. Delta4-8 gephyrin produced filamentous aggregates reminiscent to G2 gephyrin containing exon 6 (Meier *et al.* 2000; Bedet *et al.* 2006; Smolinsky *et al.* 2008), while the remaining 3 TLE gephyrins featured a diffuse distribution. Expression of TLE gephyrin in TLE hippocampectomies was also indicated by curtailed postsynaptic gephyrin (see **3.1, Publication 1, Figure 8E, F** and **G**) in combination with filamentous and diffuse mAb7a immunoreactivity, overlapping signals of gephyrin, ubiquitin and the neuronal splice factor NeuN, as well as gephyrin cleavage products in western blot analysis, which correspond to the expected size of cleavage products after PEST sequence processing (see **3.1,**

Publication 1, Figure 2 and **3,** compare control **3.2, Publication 1, Supplementary Figure 2**).

Besides the aggregation deficits of TLE gephyrins, the diffuse gephyrin distribution could also be due to expression of solitary E-domains arising from PEST sequence processing. The protein bands detected by western blot exhibited a different size pattern compared to calpain mediated gephyrin proteolysis (Tyagarajan *et al.* 2011). Thus, irregularly spliced gephyrins may not pass quality control of de-novo synthesised proteins and directly enter the proteasome pathway. On the other hand, this result does indicate that calpain mediated proteolytic processing plays a minor role in TLE.

4.1.2.1 Dominant negative effects can be attributed to irregularly spliced TLE gephyrins

To determine whether TLE gephyrins interact with and exert dominant negative effects on regular gephyrin, 3 experimental approaches were pursued. The catalytic activity in molybdenum co-factor synthesis was used to determine TLE gephyrin interaction with regular gephyrin in HEK293 cells. The inhibition of regular gephyrin's catalytic activity regarding G domain mediated molybdopterin synthesis, as well as E domain dependent molybdenum co-factor synthesis, upon co-expression with truncated TLE gephyrins possessing only fragmental G domains, indicated interaction between regular and TLE gephyrins (see **3.1, Publication 1, Figure 5A** and **B**). Likewise, a co-localisation of regular gephyrin with N- and C-terminal parts of TLE gephyrin G domains was observed in HEK293 cells (**3.1, Publication 1, Figure 5C**). Thirdly, TLE gephyrins depleted regular endogenous post-synaptic gephyrin and GABA(A)R alpha2 in primary hippocampal neurons *in vitro*, as was indicated by a

decline of gephyrin and GABA(A)R alpha2 immunoreactivity adjacent to VIAAT positive pre-synaptic terminals (**3.1, Publication 1, Figure 6**) and a reduced mean frequency of miniature post-synaptic GABAergic currents (**3.1, Publication 1, Figure 7A, B** and **C**). Moreover, concomitant reduction of the amplitude of large scale miniature GABAergic postsynaptic currents in delta4* transfected neurons (**3.1, Publication 1, Figure 7D** and **E**) suggests two different types of GABAergic synapses; one where the entire pool of postsynaptic gephyrin is subject to rapid turn-over and experiences GABA(A)R alpha2 and gephyrin depletion when de-novo synthesis is compromised, and another type that maintains a basic pool size of post-synaptic gephyrin. This matches the observation that not all synapses lost post-synaptic gephyrin upon cellular stress. In summa, these 3 experimental strategies clearly revealed the dominant negative effects of TLE gephyrin variants.

4.1.2.2 Cellular stress is sufficient to disrupt regular gephyrin RNA splicing

Modifications of gephyrin genome sequences have been ruled out as a cause of TLE gephyrin expression, as sequencing of G domain exons with flanking intron sequences in genomic DNA from TLE patient hippocampectomies did not reveal any aberrations from database entries (see **3.2, Publication 1, Supplementary Figure 8A**).The Nova CLIP tag consensus sequence in intron 8, which is involved in gephyrin splicing through Nova-2 signaling (Ule *et al.* 2003) was also highly conserved (**3.2, Publication 1, Supplementary Figure 8B**). To validate that the sequenced genomic regions were a sufficient base for the conclusion that TLE gephyrin expression was not based on genome mutations, a novel fluorescence reporter construct was used to investigate skipping of exon 4 upon cellular stress.

4. Discussion

In these experiments, hyperthermia as well as alkalosis proved to be sufficient to trigger exon skipping as expression of the reporter protein EGFP was turned on while EGFP expression was negligible under control conditions (see **3.2, Publication 1, Supplementary Methods** and **Figure 9**), indicating that the sequenced intron regions were sufficient to allow RNA splicing of exon 3, 4 and 5. Furthermore, cellular stress elicited overlapping NeuN, ubiquitin and gephyrin immunoreactivity *in vitro*, mirroring the observations in TLE patient hippocampal CA3 area, but not dentate gyrus (**3.1, Publication 1, Figure 3** and **9**). In concordance with these findings, decreased GABAergic synaptic transmission to pyramidal cells of the cornu ammonis, but not to dentate gyrus granule cells, was recently reported to occur upon hyperthermia (Qu and Leung 2009). Likewise, increased neuronal excitability and epileptiform activity *in vitro* and *in vivo* have been linked to the rise of intracellular pH by a large body of evidence (Aram and Lodge 1987; Balestrino and Somjen 1988; Jarolimek *et al.* 1989; Lee *et al.* 1996; Kaila and Ransom 1998), and seizure-induced rebound alkalosis was shown to elevate intracellular pH up to a value of 8.0 (Hartley and Dubinsky 1993) following a massive rise of extracellular glutamate concentration during epileptic seizures (During and Spencer 1993). The experimental cellular stress paradigms thus proved appropriate and sufficient to effect exon skipping in gephyrin RNA associated with synthesis of dominant negative TLE gephyrins, confirming a direct impact of cellular stress on GABAergic postsynaptic domains. Although abnormal processing of RNA in astrocytes was shown to correlate with TLE pathogenesis, for example in case of GluR (**4.1**; also see (Seifert *et al.* 2002)), alteration of posttranscriptional processing of gephyrin RNA was not observed in gephyrin RNA splice reporter expressing astrocytes (not shown), revealing a particular vulnerability of pyramidal neurons to cellular stress induced exon skipping in gephyrin RNA.

4.1.2.3 Consequences of impaired gephyrin clustering in TLE

The data collected so far indicates impaired delivery of de-novo synthesised gephyrins to post-synaptic domains due to interaction of TLE gephyrins with regular gephyrin, resulting in a reduction of post-synaptic gephyrin pool size. The role gephyrin plays in post-synaptic GABA(A)R recruitment and stabilisation has been under debate for over 10 years (Kneussel *et al.* 1999; Fischer *et al.* 2000; Kneussel *et al.* 2001; Levi *et al.* 2004), but this work (**3.1, Publication 1,** and **3.2, Publication 1, Supplementary Data**), in agreement with other recent publications (Yu *et al.* 2007; Tretter *et al.* 2008), supports a subunit-specific role of gephyrin in the enrichment of post-synaptic sites with GABA(A)R.

While direct binding of GABA(A)R alpha2 to gephyrin has been demonstrated previously (Tretter *et al.* 2008), post-synaptic GABA(A)R alpha1 clustering is apparently gephyrin-independent (Kneussel *et al.* 2001; Levi *et al.* 2004; Yu *et al.* 2007). This fits a bigger picture, as GABA(A)R alpha2 are predominantly found at synapses of slow-spiking interneurons, while GABA(A)R alpha1 are preferentially associated with synapses of fast-spiking interneurons, which are involved in high frequency gamma network oscillatory activity (Freund and Katona 2007). Preponderant high frequency oscillatory activity in the hippocampal network in turn is known to precede epileptic seizures (Fisher *et al.* 1992; Bragin *et al.* 2007). Even small changes in overall hippocampal CA3 activity can commence the switch from gamma oscillations in a neuronal network to epileptiform bursts (Fisahn 2005). Accordingly, dentate gyrus granule cell to CA3 synapses are known as ‘conditional detonators’ and need to be tightly controlled, as they can easily discharge CA3 pyramidal cells and precipitate recurrent CA3 to CA3 activity (Henze *et al.* 2002).

4.2 GlyR

4.2.1 RNA-edited high affinity GlyR

As exemplified by the case of GluR mentioned above (see **4.1**; (Seifert *et al.* 2002)), abnormal RNA processing emerges as a pathogenic factor in TLE pathophysiology. Hence, this non-congenital mechanism may apply to a wider range of genes. In fact, the genetically encoded proline 185 of the mature signal-peptide cleaved GlyR alpha3 is subject to proline-to-leucine substitution upon C-to-U RNA editing via cytidin-deaminase, producing gain-of-function GlyR (Meier *et al.* 2005), that are associated with TLE pathology (**3.3, Publication 2**; also see (Eichler *et al.* 2008)). This proline is conserved in all GlyR subunits (amino acid 185 in alpha1 and 3, amino acid 192 in alpha2, respectively), and protein regions where the backbone has to make a sharp turn often feature proline or glycine residues, which apparently confer a high degree of local flexibility.

In contrast, GABA(A)R delta, alpha4 and alpha6 subunits, that are incorporated into receptors known to elicit tonic chloride currents in response to low neuronal ambient GABA concentrations (Mody 2001; Wisden *et al.* 2002; Caraiscos *et al.* 2004; Mody and Pearce 2004), exhibit aliphatic hydrophobic neutral amino acids such as valine, alanine or leucine in this position (Meier *et al.* 2005). It is thus manifest that substitution of leucine for proline 185 upon C-to-U editing of GlyR alpha subunit-coding RNA elevates the apparent agonist affinity of resulting receptor channels. Accordingly, the apparent affinity of all RNA edited GlyR alpha subunits is increased (see **3.3, Publication 2, Figure 2** and **4**), in fact in correlation to the size of ligands as determined with alpha3 (15- and 60-fold for glycine and taurine, respectively, and not calculable for GABA because it is not an agonist of non-RNA edited GlyR).

RNA-editing thus enables GlyR alpha3 to mediate tonic inhibition at ambient neuronal glycine and taurine levels (Meier *et al.* 2005). As elaborated on later (see **4.2.1.1**), this change in agonist affinity appears to emerge due to the conformational impact of amino acid residue 185 on the glycine binding pocket located at distance to the edited position in the F-loop, allowing for larger molecules such as GABA to bind to GlyR as well (see **3.3, Publication 2, Figure 3**). Nonetheless, size of agonists can not be an exclusive criterion since glutamate, a carboxylated variant of GABA, does not activate RNA-edited GlyR (personal communication, René Jüttner, MDC Berlin). Substitution of leucine for proline at corresponding positions 192 in GlyR alpha2 (Eichler *et al.* 2008) and 185 in alpha1 (**3.3, Publication 2, Figure 1**), respectively, has similar effects. Altogether, these observations indicate that the highly conserved proline residue at position 185 (alpha1 and 3) or 192 (alpha2) is a structurally relevant element that determines GlyR agonist affinity (see **3.3, Publication 2**).

4.2.1.1 Structural implications of GlyR RNA-editing

Using the crystal structure data derived from the acetylcholine binding protein (Celie *et al.* 2005), proline 185 in GlyR alpha1 and 3, as well as proline 192 in GlyR alpha2 are situated in the F-loop, at the beginning of beta sheet 9 (see **3.3, Publication 2, Figure 3**). The F-loop is positioned between beta sheets 8 and 9, which are connecting the amino acid groups G160, Y161 and K200, Y202, T204 that form the glycine binding pocket (Legendre 2001). As postulated above (**4.2.1**), proline-to-leucine substitution could effect a structural rearrangement, opening the ligand binding pocket and improving accessibility of GlyR agonists such as taurine and even GABA to the binding site. This notion is supported by the involvement of F-loop dynamics in benzodiazepine mediated GABA(A)R activation (Padgett and Lummis 2008), and a potential hinge function of the disulfide bridge connecting beta-sheets 6’

and 7 (Laube *et al.* 1993), to transmit conformational changes upon proline-to-leucine substitution to the glycine binding pocket.

4.2.1.2 Functional relevance of extra-synaptic high affinity GlyR

Glycine is known to be required for (NR1 subunit containing) NMDA receptor activation and therefore tightly controlled by glycine transporters (Gomeza *et al.* 2003). Under normal conditions extracellular glycine levels in the central nervous system are estimated to be close to 0.1µM (Roux and Supplisson 2000), but sustained pre-synaptic activity, i.e. precipitated by hyper-synchronous high frequency network activity in epileptic tissue (Fisher *et al.* 1992; Bragin *et al.* 2007), can temporarily elevate extracellular glycine (Roux and Supplisson 2000; Supplisson and Roux 2002), possibly as a result of astrocyte depolarisation due to abnormal GluR RNA splicing (see above **4.1**, (Seifert *et al.* 2002)) and/or due to reversal of glycine uptake. In deed, the potential impact of extracellular glycine on neuronal network activity in the hippocampus via non-synaptic GlyR-mediated tonic inhibition was reported recently (Zhang *et al.* 2008). Apart from astrocytes, pre-synaptic glutamatergic terminals are another possible source of glycine, as these terminals are known to contain glycine transporter 1 (Cubelos *et al.* 2005), and post-synaptic responses to hippocampal glutamatergic fibre stimulation include a recurrent small strychnine-sensitive component (Müller *et al.* 2007).

The exceptionally high agonist affinity of RNA-edited GlyR makes them well suited to respond to both, ambient neuronal extracellular glycine, mediating tonic inhibition of neuronal excitability, or glycine release from glutamatergic terminals. In fact, a glycine concentration of 0.3µM is sufficient to elicit single channel openings in receptors incorporating high affinity GlyR alpha3 and, accordingly, reduce membrane

resistance (see **3.3, Publication 2, Figure 4**). The diminution of membrane resistance upon activation of these receptors, irrespectively of a neuron's chloride equilibrium potential, can thus curb the propagation of action potentials and synaptic events, amounting to an inhibitory shunting mechanism (Eichler *et al.* 2008). Moreover, silenced hippocampal neurons with high intracellular chloride concentrations are susceptible to glutamatergic excitotoxicity mediated cell death (Eichler *et al.* 2008). In the light of this mechanism of neuronal inhibition, and the context of high chloride equilibrium potential as observed in TLE (Palma *et al.* 2006), the correlation between the amount of edited GlyR alpha2 and 3 mRNA and the severity of the disease in the hippocampus of patients suffering from intractable TLE gains pathophysiological relevance (Meier *et al.* 2005; Eichler *et al.* 2008; Eichler and Meier 2008). Akin to the histopathology of TLE (Loup *et al.* 2000; Stief *et al.* 2007), the ratio between glutamatergic and GABAergic nerve endings is up-regulated in tonically silenced neurons, and abnormal dendrite morphology reminiscent to TLE pathology arises under such conditions (Lohmann *et al.* 2005; Eichler *et al.* 2008).

Of course, all of this holds true only if RNA edited GlyR confer tonic inhibition. Despite recent evidence in favour of such a non-synaptic role for RNA edited GlyR (Chattipakorn and McMahon 2003; Song *et al.* 2006), this work (**3.4, Publication 3**) and others (Kubota *et al.* 2010), in concordance with unpublished results from the laboratory of Jochen Meier (MDC Berlin), indicate that hippocampal GlyR alpha2 (Kubota *et al.* 2010) and the long RNA splice variant of GlyR alpha3 (**3.4, Publication 3, Figure 3** and **5**) are targeted to pre-synaptic glutamatergic nerve endings, where they could rather facilitate glutamate release and favour TLE characteristic network activity (unpublished data & (Kubota *et al.* 2010)).

Given that the majority of patients with TLE express alpha3L (see **3.4, Publication 3, Figure 8**), it remains to be determined whether tonic inhibition of neuronal activity, facilitation of glutamatergic transmission, or both are relevant to TLE pathogenesis. Either way, RNA editing of *GLRA3* gene transcripts could facilitate epileptiform activity, when exon 8A is incorporated to produce the alpha3L splice variant, and contribute to neurodegeneration in a later stage of TLE (**3.4, Publication 3, Figure 8**), due to preferential GlyR alpha3K expression and resulting tonic inhibition of neuronal discharge in TLE specific conditions (Eichler *et al.* 2008).

4.2.2 GlyR alpha3 RNA splicing determines subcellular localisation

As elaborated on below (see **4.2.2.1**) this study documents a receptor intrinsic clustering mechanism of the GlyR alpha3L splice variant irrespective of gephyrin, as it shows that GlyR alpha3L produces clusters in transfected HEK293 cells and primary hippocampal rat neurons, while alpha3K exhibits a diffuse distribution in the plasma membrane (see **3.4, Publication 3, Figure 2** and **4**), despite the endogenous expression of gephyrin and GlyR beta in HEK293 cells (David-Watine 2001; Shaw *et al.* 2002) and primary hippocampal rat neurons (Meier and Grantyn 2004). GlyR alpha3L cluster size increases upon co-transfection with GlyR beta (see **3.4, Publication 3, Figure 7**), and alpha3K readily builds clusters when co-transfected with the beta subunit (**3.4, Publication 3, Figure 6**), indicating that HEK293 and neuronal endogenous GlyR beta expression is not sufficient to ensure efficient formation of heteromeric receptors upon over-expression of GlyR alpha3. If also over-expressed, GlyR beta increases the size of GlyR clusters in any case (**3.4, Publication 3, Figure 4** and unshown data) due to gephyrin binding.

However, smaller GlyR alpha3L clusters persisted even upon co-expression of the beta subunit, suggesting that GlyR beta assembles better with GlyR alpha3K than with alpha3L. Co-expressed with GlyR beta notwithstanding, GlyR alpha3L prefers glutamatergic nerve endings (see **3.4, Publication 3, Table 2, Figure 5** and **7**), suggesting that a gephyrin independent subcellular targeting mechanism of GlyR alpha3L exists, perhaps mediated via binding of the L-sequence to trafficking factors other than gephyrin.

4.2.2.1 Neuronal phenotypic promiscuity of hippocampal GlyR depends on RNA splicing

In agreement with previous reports (Kirsch *et al.* 1993; Meyer *et al.* 1995; Meier *et al.* 2001; Meier and Grantyn 2004), this work shows that GlyR clustering can be gephyrin-mediated, requiring the GlyR beta subunit and favouring association with GABAergic nerve terminals (see **3.4, Publication 3, Table 2, Figure 6** and **7**), or instead rely on gephyrin independent, receptor intrinsic mechanisms (Meier *et al.* 2000), conferring a preference for glutamatergic pre-synaptic terminals upon RNA splicing of exon 8A (**3.4, Publication 3, Table 2, Figure 5** and **7**, also see **4.2.1.2 §2**). Depending on the availability of GlyR alpha3K, the beta subunit and gephyrin variants without exon 6, GlyR can thus face GABAergic nerve endings (**3.4, Publication 3, Table 2**; also see (Meier and Grantyn 2004)), where they may be activated by high levels of >1mM GABA in the synaptic cleft, as the apparent affinity of GlyR alpha3K^{185L} for GABA is in the range of 2 to 3mM (**3.3, Publication 2, Figure 4**). Yet, a weak partial agonist of RNA edited GlyR alpha3K, such as GABA, should arguably inhibit GABAergic transmission ((Lu *et al.* 2008); **3.3, Publication 2**), due to competition of glycine and GABA for the same binding site. Consequently, the net effect of RNA edited GlyR alpha3K splice variants in neurons with a high chloride

equilibrium potential, as found in TLE (Palma *et al.* 2006), is expected to be inhibitory, due to diminution of depolarising GABAergic synaptic transmission and shunt inhibition of neuronal activity.

Nevertheless, the effect of synaptic GABAergic transmission on hippocampal network activity has to be interpreted against the backdrop of the actual membrane potential at a given time point during oscillatory network activity. Thus, even if the chloride equilibrium potential is decreased, GABAergic transmission can still cut off glutamatergic synaptic transmission if the actual membrane potential is lower than the chloride equilibrium potential, for example during oscillatory network activity. Furthermore, the type of GABAergic synapse that is concerned with GlyR alpha3^{185L} expression, *id est* a theta- or gamma-generating one, needs to be taken into consideration as preferential expression of these receptors at one of these two synapse-types will impact differently on hippocampal oscillatory network activity.

The preference of GlyR alpha3L receptor clusters for glutamatergic synapses in both hippocampus cryosections and primary hippocampal neurons suggests a novel pivotal role for GlyR alpha3L (see **3.4, Publication 3, Table 2, Figure 3** and **5**). The evocation of local GlyR mediated chloride currents in the vicinity of glutamatergic post-synapses could influence the efficacy of excitatory input (see **3.4, Publication 3, Table 2, Figure 5** and **7**). The agonist necessary for functional relevance of this mechanism might be co-released by hippocampal glutamatergic synapses, which are known to contain glycine transporter 1 (Cubelos *et al.* 2005). Provided that hippocampal GlyR are routed to pre-synaptic terminals of glutamatergic afferent synapses, as is the case for GlyR alpha2 (Kubota *et al.* 2010) and GlyR alpha3L *in vivo* (unpublished results, Jochen Meier, MDC, Berlin), the expression of RNA edited

GlyR would facilitate glutamate release (Turecek and Trussell 2001; Lee *et al.* 2009; Waseem and Fedorovich 2010) and sustain epileptiform neuronal network activity.

Therefore, at the time of this doctoral thesis, it is difficult to estimate the impact of GlyR RNA editing on TLE pathogenesis based on present experimental data, although both, GlyR alpha3K mediated tonic inhibition and GlyR alpha3L facilitated glutamatergic synaptic transmission clearly point to a pathophysiological role of GlyR C-to-U RNA editing.

4.3 Conclusion and outlook

Although this thesis can not answer the question whether irregular gephyrin RNA splicing affects GlyR RNA editing, recent experimental data from the laboratory of Jochen Meier (MDC Berlin), using the gephyrin RNA splice reporter (see **3.2, Publication 1, Supplementary Methods** and **Figure 9**), revealed that chronic neuronal silencing is another stressor that elicits exon skipping in gephyrin RNA (Winkelmann & Meier, unpublished), indicating that increased RNA editing of GlyR alpha3K-coding RNA can impact on gephyrin expression. Reiterating that postsynaptic gephyrin is a determinant of perisomatic GABA(A)R alpha2 dependent synaptic transmission and oscillatory network activity in the theta frequency range (see **4.1.2.3**), it follows, that RNA editing in TLE patients with a severe course of disease might exert a twofold role, by conferring neurodegeneration and impairing perisomatic synaptic GABAergic transmission, thence doubly contributing to TLE pathogenesis.

Thus, this work emphasises that many RNA processing events can contribute to ictogenesis in TLE patients and cooperation of RNA editing and splicing might be

even more efficient in TLE pathogenesis than the individual events separately. Many pieces of this puzzle have fallen into place in recent years, but there is yet much to learn about the mechanisms that evoke the initial emergence and contribute to the development of TLE. In the wake of a growing number of patients that develop pharmacoresistance against available drug therapies, the notion to simply apply more of a given drug to facilitate a more effective treatment of the phenotype of TLE has to be discarded as a concept of the past century. Thus a better understanding of the processes underlying aberrant neuronal network activity in TLE is required in order to reveal toeholds for new causatively-oriented therapeutic strategies.

4.3.1 Finding avenues to combat the disruptive effects of cellular stress on GABAergic post-synaptic domains

This work establishes that cellular stress, like rebound alkalosis secondary to seizure activity, is sufficient to cause dominant negative effects on GABAergic postsynaptic domains through inhibition of regular gephyrin RNA splicing and subsequent expression of TLE gephyrins. Exon skipping in gephyrin mRNA upon cellular stress, and it’s impact on post-synaptic gephyrin and GABA(A)R alpha2, could thus reduce the seizure threshold, making the network prone to further deregulation of gephyrin splicing in a self-propagating cycle.

Novel drug treatments that brace neurons against cellular stress could curb the progress of TLE by limiting the accumulation of dominant negative TLE gephyrins. Furthermore, the identification of gene expression with compensatory properties may reveal new drug targets for the medication of excitability diseases (Eichler and Meier 2008) and other neuronal impairments, like affective mood disorders and stroke (Tyagarajan *et al.* 2011). The novel splice-reporter construct introduced in this work

(see **3.2, Publication 1, Supplementary Methods** and **Figure 9**) presents an invaluable tool for drug screening in search of protective agents to counter cellular stress. The reporter construct can also be modified to investigate compensatory properties of gene expression, by inserting genes of interest in lieu, hence turning on gene expression upon cellular stress in a case-of-need-oriented way. Nouveau causally-oriented therapeutic approaches for the treatment of a wide range of disorders are now conceivable as neurons can defend themselves against cellular stress through conditional expression of multiple genes of interest.

5. Appendix

5.1 Abbreviations

AB/AM	Antimycotic/antibiotic
ACh	Acetylcholine
AMCA	Aminomethylcoumarin
AMP	Adenosine-mono-phosphate
ANOVA	Analysis of variance
AraC	Arabinofuranosyl Cytidine
BDNF	Brain-derived neurotrophic factor
BSA	Bovine serum albumin
$CaCl_2$	Calcium chlorice
cAMP	Cyclic adenosine-mono-phosphate
CAST	Calpastatin
CCD	charge couple device
CCK	Cholecystokinin
cDNA	Complementary desoxyribonucleic acid
CNS	Central nervous system
CA1-4	Cornu ammonis region 1 to 4
CMV	Cytomegalovirus
CO_2	Carbon dioxide
C-to-U RNA editing	Cytidin to uracil RNA-editing via cytidin-deaminase
Cy3 and Cy5	Carboxymethyl indocyanine 3 and 5
day E19	Day 19 of embryonal development
ddH_2O	Demineralised water
DEPC	Diethylpyrocarbonate
DG	Dentate gyrus
DL-APV	DL-2-Amino-5-phosphonopentanoic acid
DMEM	Dulbeco's modified Eagle's medium
DMF	N,N-Dimethyl formamide
DMSO	Dimethyl sulfoxide
DNA	Desoxyribonucleic acid
DNQX	6,7-Dinitroquinoxaline-2,3-dione
dNTPs	Deoxyribonucleotide triphosphates
DTT	Dithiothreitol
dTTPs	Deoxythymidin triphosphates
EC	Entorhinal cortex
EC_{50}	Half maximal effective concentration
ECL	Enhanced chemiluminescence

EDTA	Ethylenediaminetetraacetic acid
EGFP	Enhanced green fluorescent protein
FCS	Fetal calf serum
FITC	Fluorescein isothiocyanate
GABA	Gamma-amino butyric acid
GABA(A)R	Gamma-amino butyric acid (A) receptor
GABARAP	GABA(A)R-associated protein
GAD	Glutamic acid decarboxylase
GAPDH	Glyceraldehyde 3-phosphate dehydrogenase
GDPs	Giant depolarising potentials
GDP	Guanosine diphosphate
GLRA1-4	GlyR alpha1 to 4 encoding genes
GLRB	GlyR beta encoding gene
Glu	Glutamate
GluR	Glutamate receptor
Gly	Glycine
GlyR	Glycine Receptor
GlyT	Glycine transporters
GSK3beta	Glycogen synthase kinase 3beta
GSK3-IX	Specific inhibitor of GSK3beta
GTP	Guanosine triphosphate
HBS	HEPES buffered saline
HCl	Hydrochloric acid
HEK293	Human embryonic kidney cells line
HEPES	*N*-(2-hydroxyethyl)piperazine-*N*′-(2-ethanesulphonic acid)
5HT3	Serotonin receptor
IgG	Immunoglobulin G
IPSP	Inhibitory post-synaptic potential
KCC2	Potassium chloride co-transporter 2
KCl	Potassium chloride
KIF5	Conventional kinesin motor-proteins
LGIC superfamily	Ligand-gated ion channel superfamily
mAb	Monoclonal antibody
MDC	Max Delbrück Center for Molecular Medicine
MEM	Minimal essential medium
Mena/VASP	Mammalian enabled/vasodilator stimulated phosphoprotein
$MgCl_2$	Magnesium chloride
MoCo	Molybdenum co-factor
MPT	Molybdopterin
mRNA	Messanger RNA
NA	Noradrenalin

nAChR	Nicotinic acetylcholine receptor
NaCl	Sodium chloride
NB	Neurobasal medium
NH_4Cl	Ammonium chloride
NKCC1	Sodium potassium chloride co-transporter 1
NMDARs	N-Methyl-D-aspartate receptors
O-LM cell	Oriens-lacunosum moleculare cell
P	Significance level
pAb	Polyclonal antibody
PAGE	Polyacrylamid gel electrophoresis
PBS	Phosphate buffered saline (calcium and magnesium free)
pBSK	pBluescript II SK plasmide
PCR	Polymerase chain reaction
PFA	Paraform aldehyde
PEST	Proline (P), glutamic acid (E), serine (S) and threonine (T) rich peptide
Pin1	Peptidyl-prolyl isomerise NIMA interacting protein 1
PKA	cAMP-dependent protein kinase
PKC	Protein kinase C
PO	Poly-DL-ornithine hydrobromide
RAFT1	Rapamycin and FKBP12 target
RHC	Rat hippocampal neuron cell culture
RNA	Ribonucleic acid
ROI	Region of interest
SD	Standard deviation
SDS	Sodium dodecyl sulphate
SEM	Standard error of mean
SLC12A2	NKCC1 gene in human
Slc12a2	NKCC1 gene in mouse
SLC12A5	KCC2 gene in human
Slc12a5	KCC2 gene in mouse
SSS	Standard salt solution
Sub	Subiculum
TBS	Tris-buffered saline
TLE	Temporal lobe epilepsy
TM domain	Transmembrane domain
TRITC	Tetramethylrhodamine isothiocyanate
TrkB	Tyrosin kinase B
TTX	Tetrodotoxin
VIAAT	Vesicular inhibitory amino acid transporter
W0-4	Wyler classification grade 0 to 4

5.1.1 Units

bp	base pairs
^{o}C	Degrees Celsius
cm^2	Squarecentimeters
d	Days
d.i.v.	Days in vitro
g	Gram
h	Hour
kb	Kilobase
kDa	Kilodalton
kg	Kilogram
kHz	Kilohertz
l	Liter
mg	Milligram
ng	Nanogram
min	Minute
ml	Mililiter
mM	Millimolar
mm	Millimeter
MOhm	Megaohm
mosmol	Milliosmol
mV	Millivolt
rcf	Relative centrifugal force
rpm	Revolutions per minute
s	Second
U	Units of enzyme activity
µl	Microliter
µM	Micromolar
%	Percent

5.2 Index of Figures and Tables

Numbers in parentheses refer to page numbers in publications and supplementary data.

5. Appendix

5.3 Declaration to the publications

Publication 1 and Supplementary Material (see **3.1** and **3.2**):

Irregular RNA splicing curtails post-synaptic gephyrin in the *cornu ammonis* of patients with epilepsy.

Literature research and selection of references, first and final draft of the manuscript, table and figure design, design and execution of experiments excluding the contribution of co-authors stated below.

Experiments contributed by co-authors are indicated in **2. Material and Methods** and listed below in brief. Abdel Ali Belaidi contributed western blot analysis of patient material (**Publication 1, Figure 2A**) and the molybdenum co-factor synthesis assay (**Publication 1, Figure 5A and B**). René Jüttner provided the electrophysiological data presented in **Publication 1, Figure 7**. Carola Bernert contributed to molecular cloning in particular for the generation of the splice-reporter construct (see **Publication 1, Supplementary Methods**). Michael Tsokos provided hippocampal post-mortem control tissue. Surgery on TLE patients was performed by Thomas-Nicolas Lehmann and Peter Horn, and Christoph Dehnicke performed the presurgical evaluation of TLE patients.

Publication 2 (see **3.3**):

Glycine receptors caught between genome and proteome - Functional implications of RNA editing and splicing.

Participation in literature research and selection of references, figure design, first and final draft of the manuscript (~25%). Design of experiments and contribution of site-directed mutagenesis, cloning, cellculture and transfection for electrophysiological experiments corresponding to **Publication 2, Figure 1** and **2**. Electrophysiological experiments corresponding to **Publication 2, Figure 1** and **2** were performed by René Jüttner, electrophysiological data presented in **Publication 2, Figure 4** was contributed by Pascal Legendre.

Publication 3 (see **3.4**):

Splice-specific roles of glycine receptor alpha3 in the hippocampus.

Participation in literature research and selection of references, first and final draft of the manuscript (~5%). Contribution of semi-quantitative PCR analysis of GlyR beta expression in TLE patient and post-mortem control material and according figure design, as well as GlyR alpha3L and K expression in post-mortem control material (see **Publication 3, Figure 8**).

5.4 Summary

The main focus of this thesis is the involvement of the GABA(A) receptor alpha2 scaffolding protein gephyrin in hyperexcitability disorders. The recent observation of gradually declining hippocampal gephyrin immunoreactivity during epileptogenesis in an animal model of epilepsy (Fang *et al.* 2011) and a reduction of postsynaptic GABA(A) receptor alpha2 in the epileptic hippocampus (Bouilleret *et al.* 2000; Kneussel *et al.* 2001; Kumar and Buckmaster 2006) have linked gephyrin to temporal lobe epilepsy. Still, the mechanisms underlying reduced gephyrin immunoreactivity have remained enigmatic. Thus, aim of this PhD work was to identify and characterise cellular mechanisms responsible for loss of postsynaptic gephyrin in temporal lobe epilepsy. Immunohistochemical and western blot analyses unveiled aberrant gephyrin expression in the *cornu ammonis* of patients afflicted with temporal lobe epilepsy.

Four abnormally spliced gephyrin variants lacking several exons in the G-domain were isolated from patient RNA and characterised in HEK293 cells and primary hippocampal neurons via EGFP tagged expression constructs. All 4 identified temporal lobe epilepsy gephyrins were found to be oligomerisation-deficient and interact with regularly spliced gephyrins in a dominant negative way, thereby curbing hippocampal postsynaptic gephyrin and GABA(A) receptor alpha2. While gephyrin gene mutations were not detected by sequencing of genomic DNA, cellular stress like hyperthermia or alkalosis proved suitable and sufficient to induce inhibition of regular gephyrin RNA splicing and subsequent expression of dominant negative temporal lobe epilepsy gephyrins, leading to curtailed postsynaptic gephyrin and GABA(A) receptor alpha2 scaffolds in primary hippocampal neurons of a wild type background.

Thus, cellular stress, like rebound alkalosis occurring secondary to seizure activity, could facilitate the development of temporal lobe epilepsy by reducing GABA(A) receptor alpha2-mediated hippocampal synaptic transmission selectively in the cornu ammonis, and in turn reduce seizure threshold, making the network prone to further deregulation of gephyrin splicing and epileptogenesis in a self-propagating cycle. The novel RNA splice-reporter introduced in this work (see **3.2, Publication 1, Supplementary Methods** and **Figure 9**) presents an invaluable molecular tool in drug screening for protective agents to brace neurons against cellular stress and the search for gene expression with compensatory properties for the design of causally-oriented therapies for the treatment of excitability diseases (Eichler and Meier 2008) as well, as other neuronal impairments, like affective mood disorders and stroke (Tyagarajan *et al.* 2011).

5.5 Zusammenfassung

Der Hauptschwerpunkt dieser Dissertation liegt auf der Beteiligung des Alpha2 GABA(A) Rezeptor (GABA(A)R) Verankerungsproteins Gephyrin an Temporallappenepilepsie (TLE). Unlängst publizierte Beobachtungen eines graduellen Verlusts hippocampaler Gephyrinimmunoreaktivität während der Epileptogenese in einem Tiermodell der Epilepsie (Fang *et al.* 2011) und der Minderung postsynaptischer Alpha2 GABA(A)R im epileptischen Hippocampus (Bouilleret *et al.* 2000; Kneussel *et al.* 2001; Kumar and Buckmaster 2006) bringen Gephyrin in Verbindung mit TLE. Die Mechanismen, welche der verringerten Gephyrinimmunoreaktivität zugrunde liegen, blieben bislang rätselhaft. Ziel dieser Doktorarbeit war es daher, die zellulären Mechanismen des Verlusts postsynaptischen Gephyrins in TLE zu identifizieren und zu charakterisieren. Immunohistochemische und Westernblotuntersuchungen enthüllten abnormale Gephyrinexpression in der *Cornu Ammonis* (CA) Region von TLE Patienten.

Vier irregulär gespleißte Gephyrinvarianten, denen mehrere Exone in der G-Domäne fehlen, wurden aus Patienten-RNA isoliert und mittels EGFP-markierter Expressionskonstrukte in HEK293 Zellen und primären Hippocampusneuronen charakterisiert. Alle 4 fehlgespleißten Gephyrine wiesen Oligomerisationsdefizite auf und reduzierten mittels Interaktion mit regulärem Gephyrin in dominant-negativer Weise hippocampales postsynaptisches Gephyrin und Alpha2 GABA(A)R. Mutationen des Gephyringens bei der Sequenzierung genomischer DNA wurden nicht gefunden. Zellulärer Stress wie Hypertermie oder Alkalose, stellte sich hingegen als hinreichend heraus, reguläres Spleißen von Gephyrin RNA zu behindern und durch die resultierende Expression dominant-negativer Gephyrine postsynaptische Gephyrinaggregation und korrespondierende Alpha2 GABA(A)R-

Verankerung in primären Hippocampusneuronen mit Wildtyphintergrund einzuschränken.

Somit erweist sich zellulärer Stress, wie beispielsweise Alkalose infolge epileptischer Anfälle, als möglicher Verstärker in der Entwicklung von TLE, und zwar aufgrund einer selektiv in der CA Region eingeschränkten Verfügbarkeit postsynaptischer Alpha2 GABA(A)R. Die hieraus resultierende niedrigere Schwelle zur Auslösung epileptischer Aktivität kann das neuronale Netzwerk in einer selbstpropagierenden Schleife wiederum anfälliger für Deregulierung des Gephyrinspleißens machen. Der in dieser Arbeit vorgestellte neuartige Spleißreporter (**3.2, Publication 1, Supplementary Data**) stellt ein molekulares Werkzeug zur Identifkation potentiell protektiver Wirkstoffe gegen zellulären Stress dar und kann der Suche nach Genen mit kompensatorischen Eigenschaften gegenüber zellulärem Stress dienen, um Ansatzpunkte für die Entwickung neuer pharmakologischer Agenzien und ursachenorientierter Therapieformen nicht nur für die Behandlung von TLE (Eichler and Meier 2008) sondern auch von anderen neurodegenerativen Erkrankungen und affektiven Persönlichkeitsstörungen zu liefern (Tyagarajan *et al.* 2011).

6. References

Aguado F, Carmona MA, Pozas E, Aguilo A, Martinez-Guijarro FJ, Alcantara S *et al*. BDNF regulates spontaneous correlated activity at early developmental stages by increasing synaptogenesis and expression of the K(+)/Cl(-) co-transporter KCC2. Development 2003; 130: 1267-1280.

Alldred MJ, Mulder-Rosi J, Lingenfelter SE, Chen G, Luscher B. Distinct {gamma}2 Subunit Domains Mediate Clustering and Synaptic Function of Postsynaptic GABAA Receptors and Gephyrin. J Neurosci 2005; 25: 594-603.

Aram JA, Lodge D. Epileptiform activity induced by alkalosis in rat neocortical slices: block by antagonists of N-methyl-D-aspartate. Neurosci Lett 1987; 83: 345-350.

Arnett HA, Mason J, Marino M, Suzuki K, Matsushima GK, Ting JP. TNF alpha promotes proliferation of oligodendrocyte progenitors and remyelination. Nat Neurosci 2001; 4: 1116-1122.

Aubrey KR, Rossi FM, Ruivo R, Alboni S, Bellenchi GC, Le GA *et al*. The transporters GlyT2 and VIAAT cooperate to determine the vesicular glycinergic phenotype. J Neurosci 2007; 27: 6273-6281.

Balestrino M, Somjen GG. Concentration of carbon dioxide, interstitial pH and synaptic transmission in hippocampal formation of the rat. J Physiol 1988; 396: 247-266.

Barres BA. The mystery and magic of glia: a perspective on their roles in health and disease. Neuron 2008; 60: 430-440.

Baulac S, Huberfeld G, Gourfinkel-An I, Mitropoulou G, Beranger A, Prud'homme JF *et al*. First genetic evidence of GABA(A) receptor dysfunction in epilepsy: a mutation in the gamma2-subunit gene. Nat Genet 2001; 28: 46-48.

Bausen M, Fuhrmann JC, Betz H, O'Sullivan GA. The state of the actin cytoskeleton determines its association with gephyrin: role of ena/VASP family members. Mol Cell Neurosci 2006; 31: 376-386.

Bedet C, Bruusgaard JC, Vergo S, Groth-Pedersen L, Eimer S, Triller A *et al*. Regulation of gephyrin assembly and glycine receptor synaptic stability. J Biol Chem 2006; 281: 30046-30056.

Belizario JE, Alves J, Garay-Malpartida M, Occhiucci JM. Coupling caspase cleavage and proteasomal degradation of proteins carrying PEST motif. Curr Protein Pept Sci 2008; 9: 210-220.

Ben-Ari Y. Developing networks play a similar melody. Trends Neurosci 2001; 24: 353-360.

Ben-Ari Y, Gaiarsa JL, Tyzio R, Khazipov R. GABA: a pioneer transmitter that excites immature neurons and generates primitive oscillations. Physiol Rev 2007; 87: 1215-1284.

Betz H, Laube B. Glycine receptors: recent insights into their structural organization and functional diversity. J Neurochem 2006; 97: 1600-1610.

Blumcke I, Pauli E, Clusmann H, Schramm J, Becker A, Elger C *et al*. A new clinico-pathological classification system for mesial temporal sclerosis. Acta Neuropathol 2007; 113: 235-244.

Bouilleret V, Loup F, Kiener T, Marescaux C, Fritschy JM. Early loss of interneurons and delayed subunit-specific changes in GABA(A)-receptor expression in a mouse model of mesial temporal lobe epilepsy. Hippocampus 2000; 10: 305-324.

Bragin A, Claeys P, Vonck K, Van RD, Wilson C, Boon P *et al*. Analysis of initial slow waves (ISWs) at the seizure onset in patients with drug resistant temporal lobe epilepsy. Epilepsia 2007; 48: 1883-1894.

Breitinger HG, Becker CM. The inhibitory glycine receptor-simple views of a complicated channel. Chembiochem 2002; 3: 1042-1052.

Brewer GJ, Cotman CW. Survival and growth of hippocampal neurons in defined medium at low density: advantages of a sandwich culture technique or low oxygen. Brain Res 1989; 494: 65-74.

Brickley SG, Revilla V, Cull-Candy SG, Wisden W, Farrant M. Adaptive regulation of neuronal excitability by a voltage-independent potassium conductance. Nature 2001; 409: 88-92.

Brunig I, Suter A, Knuesel I, Luscher B, Fritschy JM. GABAergic terminals are required for postsynaptic clustering of dystrophin but not of GABA(A) receptors and gephyrin. J Neurosci 2002; 22: 4805-4813.

Brusa R, Zimmermann F, Koh DS, Feldmeyer D, Gass P, Seeburg PH *et al*. Early-onset epilepsy and postnatal lethality associated with an editing-deficient GluR-B allele in mice. Science 1995; 270: 1677-1680.

Bundgaard M, Abbott NJ. All vertebrates started out with a glial blood-brain barrier 4-500 million years ago. Glia 2008; 56: 699-708.

Buzsaki G. Hippocampal GABAergic interneurons: a physiological perspective. Neurochem Res 2001; 26: 899-905.

Caraiscos VB, Elliott EM, You T, Cheng VY, Belelli D, Newell JG *et al*. Tonic inhibition in mouse hippocampal CA1 pyramidal neurons is mediated by alpha5 subunit-containing gamma-aminobutyric acid type A receptors. Proc Natl Acad Sci U S A 2004; 101: 3662-3667.

Cardin JA, Carlen M, Meletis K, Knoblich U, Zhang F, Deisseroth K *et al*. Driving fast-spiking cells induces gamma rhythm and controls sensory responses. Nature 2009; 459: 663-667.

Cassel JC, Duconseille E, Jeltsch H, Will B. The fimbria-fornix/cingular bundle pathways: a review of neurochemical and behavioural approaches using lesions and transplantation techniques. Prog Neurobiol 1997; 51: 663-716.

Celie PH, Klaassen RV, Rossum-Fikkert SE, van Elk R, van Nierop P, Smit AB *et al*. Crystal structure of AChBP from Bulinus truncatus reveals the conserved structural scaffold and sites of variation in nicotinic acetylcholine receptors. J Biol Chem 2005; 280: 26457-26466.

Chattipakorn SC, McMahon LL. Pharmacological characterization of glycine-gated chloride currents recorded in rat hippocampal slices. J Neurophysiol 2002; 87: 1515-1525.

Chattipakorn SC, McMahon LL. Strychnine-sensitive glycine receptors depress hyperexcitability in rat dentate gyrus. J Neurophysiol 2003; 89: 1339-1342.

Chattipakorn SC, McMahon LL. Developmental expression of glycine-gated chloride channels in rat hippocampus: Functional and immunohistochemical studies. Abstract Viewer/Itinerary Planner Washington, DC: Society for Neuroscience 2004.

Chen ZW, Olsen RW. GABAA receptor associated proteins: a key factor regulating GABAA receptor function. J Neurochem 2007; 100: 279-294.

Christie SB, Miralles CP, De Blas AL. GABAergic Innervation Organizes Synaptic and Extrasynaptic GABAA Receptor Clustering in Cultured Hippocampal Neurons. J Neurosci 2002; 22: 684-697.

Church J, Baimbridge KG. Exposure to high-pH medium increases the incidence and extent of dye coupling between rat hippocampal CA1 pyramidal neurons in vitro. J Neurosci 1991; 11: 3289-3295.

Cossart R, Bernard C, Ben Ari Y. Multiple facets of GABAergic neurons and synapses: multiple fates of GABA signalling in epilepsies. Trends Neurosci 2005; 28: 108-115.

Cubelos B, Gimenez C, Zafra F. Localization of the GLYT1 glycine transporter at glutamatergic synapses in the rat brain. Cereb Cortex 2005; 15: 448-459.

David-Watine B. The human gephyrin (GPHN) gene: structure, chromosome localization and expression in non-neuronal cells. Gene 2001; 271: 239-245.

Deller T, Martinez A, Nitsch R, Frotscher M. A novel entorhinal projection to the rat dentate gyrus: direct innervation of proximal dendrites and cell bodies of granule cells and GABAergic neurons. J Neurosci 1996; 16: 3322-3333.

Dice JF. Molecular determinants of protein half-lives in eukaryotic cells. FASEB J 1987; 1: 349-357.

Dlugaiczyk J, Singer W, Schick B, Iro H, Becker K, Becker CM *et al*. Expression of glycine receptors and gephyrin in the rat cochlea. Histochem Cell Biol 2008; 129: 513-523.

Dugladze T, Vida I, Tort AB, Gross A, Otahal J, Heinemann U *et al*. Impaired hippocampal rhythmogenesis in a mouse model of mesial temporal lobe epilepsy. Proc Natl Acad Sci U S A 2007; 104: 17530-17535.

Dumoulin A, Triller A, Kneussel M. Cellular transport and membrane dynamics of the glycine receptor. Front Mol Neurosci 2009; 2: 28.

During MJ, Spencer DD. Extracellular hippocampal glutamate and spontaneous seizure in the conscious human brain. Lancet 1993; 341: 1607-1610.

Eichler SA, Kirischuk S, Jüttner R, Schäfermeier PK, Legendre P, Lehmann TN *et al*. Glycinergic Tonic Inhibition of Hippocampal Neurons with Depolarising GABAergic Transmission Elicits Histopathological Signs of Temporal Lobe Epilepsy. J Cell Mol Med 2008; 12: 2848-2866.

Eichler SA, Meier JC. E-I balance and human diseases - from molecules to networking. Front Mol Neurosci 2008; 1: 2.

Empson RM, Heinemann U. The perforant path projection to hippocampal area CA1 in the rat hippocampal-entorhinal cortex combined slice. J Physiol 1995; 484 (Pt 3): 707-720.

Essrich C, Lorez M, Benson JA, Fritschy JM, Luscher B. Postsynaptic clustering of major GABAA receptor subtypes requires the gamma 2 subunit and gephyrin. Nat Neurosci 1998; 1: 563-571.

Eugene E, Depienne C, Baulac S, Baulac M, Fritschy JM, Le GE *et al*. GABA(A) receptor gamma 2 subunit mutations linked to human epileptic syndromes differentially affect phasic and tonic inhibition. J Neurosci 2007; 27: 14108-14116.

Eulenburg V, Gomeza J. Neurotransmitter transporters expressed in glial cells as regulators of synapse function. Brain Res Rev 2010; 63: 103-112.

Evan GI, Lewis GK, Ramsay G, Bishop JM. Isolation of monoclonal antibodies specific for human c-myc proto-oncogene product. Mol Cell Biol 1985; 5: 3610-3616.

Fang M, Shen L, Yin H, Pan YM, Wang L, Chen D *et al*. Down-regulation of gephyrin in temporal lobe epilepsy neurons in humans and a rat model. Synapse 2011; 65: 1006-1014.

Feng G, Tintrup H, Kirsch J, Nichol MC, Kuhse J, Betz H *et al*. Dual requirement for gephyrin in glycine receptor clustering and molybdoenzyme activity. Science 1998; 282: 1321-1324.

Fisahn A. Kainate receptors and rhythmic activity in neuronal networks: hippocampal gamma oscillations as a tool. J Physiol 2005; 562: 65-72.

Fischer F, Kneussel M, Tintrup H, Haverkamp S, Rauen T, Betz H *et al*. Reduced synaptic clustering of GABA and glycine receptors in the retina of the gephyrin null mutant mouse. J Comp Neurol 2000; 427: 634-648.

Fisher RS, Webber WR, Lesser RP, Arroyo S, Uematsu S. High-frequency EEG activity at the start of seizures. J Clin Neurophysiol 1992; 9: 441-448.

Freund TF. Interneuron Diversity series: Rhythm and mood in perisomatic inhibition. Trends Neurosci 2003; 26: 489-495.

Freund TF, Katona I. Perisomatic inhibition. Neuron 2007; 56: 33-42.

Fritschy JM, Harvey RJ, Schwarz G. Gephyrin: where do we stand, where do we go? Trends Neurosci 2008; 31: 257-264.

Ganguly K, Schinder AF, Wong ST, Poo M. GABA itself promotes the developmental switch of neuronal GABAergic responses from excitation to inhibition. Cell 2001; 105: 521-532.

Gasnier B. The loading of neurotransmitters into synaptic vesicles. Biochimie 2000; 82: 327-337.

Giesemann T, Schwarz G, Nawrotzki R, Berhorster K, Rothkegel M, Schluter K *et al*. Complex Formation between the Postsynaptic Scaffolding Protein Gephyrin, Profilin, and Mena: A Possible Link to the Microfilament System. J Neurosci 2003; 23: 8330-8339.

Gloveli T, Dugladze T, Rotstein HG, Traub RD, Monyer H, Heinemann U *et al*. Orthogonal arrangement of rhythm-generating microcircuits in the hippocampus. Proc Natl Acad Sci U S A 2005a; 102: 13295-13300.

Gloveli T, Dugladze T, Saha S, Monyer H, Heinemann U, Traub RD *et al*. Differential involvement of oriens/pyramidale interneurones in hippocampal network oscillations in vitro. J Physiol 2005b; 562: 131-147.

Gomeza J, Ohno K, Betz H. Glycine transporter isoforms in the mammalian central nervous system: structures, functions and therapeutic promises. Curr Opin Drug Discov Devel 2003; 6: 675-682.

Grudzinska J, Schemm R, Haeger S, Nicke A, Schmalzing G, Betz H *et al*. The Beta subunit determines the ligand binding properties of synaptic glycine receptors. Neuron 2005; 45: 727-739.

Hamsikova E, Zavadova H, Zaoral M, Jezek J, Blaha K, Vonka V. Immunogenicity of a synthetic peptide corresponding to a portion of the heavy chain of H3N2 influenza virus haemagglutinin. J Gen Virol 1987; 68 (Pt 8): 2249-2252.

Hanus C, Vannier C, Triller A. Intracellular association of glycine receptor with gephyrin increases its plasma membrane accumulation rate. J Neurosci 2004; 24: 1119-1128.

Hartley Z, Dubinsky JM. Changes in intracellular pH associated with glutamate excitotoxicity. J Neurosci 1993; 13: 4690-4699.

Harvey RJ, Depner UB, Wassle H, Ahmadi S, Heindl C, Reinold H *et al*. GlyR alpha3: an essential target for spinal PGE2-mediated inflammatory pain sensitization. Science 2004; 304: 884-887.

Hauser WA. Incidence and prevalence. In: Engel J, Jr., Pedley TA, editors. Epilepsy: A Comprehensive Textbook. Philadelphia: Lippincott-Raven; 1997. p. 47-57.

Haverkamp S, Muller U, Harvey K, Harvey RJ, Betz H, Wassle H. Diversity of glycine receptors in the mouse retina: Localization of the alpha3 subunit. J Comp Neurol 2003; 465: 524-539.

Heinemann U, Schmitz D, Eder C, Gloveli T. Properties of entorhinal cortex projection cells to the hippocampal formation. Ann N Y Acad Sci 2000; 911: 112-126.

Heisler FF, Loebrich S, Pechmann Y, Maier N, Zivkovic AR, Tokito M *et al*. Muskelin regulates actin filament- and microtubule-based GABA(A) receptor transport in neurons. Neuron 2011; 70: 66-81.

Henze DA, Wittner L, Buzsaki G. Single granule cells reliably discharge targets in the hippocampal CA3 network in vivo. Nat Neurosci 2002; 5: 790-795.

Jarolimek W, Misgeld U, Lux HD. Activity dependent alkaline and acid transients in guinea pig hippocampal slices. Brain Res 1989; 505: 225-232.

Jonas P, Bischofberger J, Sandkuhler J. Corelease of two fast neurotransmitters at a central synapse. Science 1998; 281: 419-424.

Kaila K, Ransom BR. pH and Brain Function. Wiley-Liss, Inc., New York; 1998.

Kanematsu T, Mizokami A, Watanabe K, Hirata M. Regulation of GABA(A)-receptor surface expression with special reference to the involvement of GABARAP (GABA(A) receptor-associated protein) and PRIP (phospholipase C-related, but catalytically inactive protein). J Pharmacol Sci 2007; 104: 285-292.

Kang Y, Zhang X, Dobie F, Wu H, Craig AM. Induction of GABAergic postsynaptic differentiation by alpha-neurexins. J Biol Chem 2008; 283: 2323-2334.

Kasugai Y, Swinny JD, Roberts JD, Dalezios Y, Fukazawa Y, Sieghart W *et al*. Quantitative localisation of synaptic and extrasynaptic GABAA receptor subunits on hippocampal pyramidal cells by freeze-fracture replica immunolabelling. Eur J Neurosci 2010; 32: 1868-1888.

Kettenmann H, Verkhratsky A. Neuroglia: the 150 years after. Trends Neurosci 2008; 31: 653-659.

Kim EY, Schrader N, Smolinsky B, Bedet C, Vannier C, Schwarz G *et al*. Deciphering the structural framework of glycine receptor anchoring by gephyrin. EMBO J 2006; 25: 1385-1395.

Kins S, Betz H, Kirsch J. Collybistin, a newly identified brain-specific GEF, induces submembrane clustering of gephyrin. Nat Neurosci 2000; 3: 22-29.

Kirchner A, Breustedt J, Rosche B, Heinemann UF, Schmieden V. Effects of taurine and glycine on epileptiform activity induced by removal of Mg2+ in combined rat entorhinal cortex-hippocampal slices. Epilepsia 2003; 44: 1145-1152.

Kirsch J. Glycinergic transmission. Cell Tissue Res 2006; 326: 535-540.

Kirsch J, Langosch D, Prior P, Littauer UZ, Schmitt B, Betz H. The 93-kDa glycine receptor-associated protein binds to tubulin. J Biol Chem 1991; 266: 22242-22245.

Kirsch J, Wolters I, Triller A, Betz H. Gephyrin antisense oligonucleotides prevent glycine receptor clustering in spinal neurons. Nature 1993; 366: 745-748.

Kneussel M, Brandstatter JH, Laube B, Stahl S, Muller U, Betz H. Loss of postsynaptic GABA(A) receptor clustering in gephyrin-deficient mice. J Neurosci 1999; 19: 9289-9297.

Kneussel M, Helmut BJ, Gasnier B, Feng G, Sanes JR, Betz H. Gephyrin-independent clustering of postsynaptic gaba(a) receptor subtypes. Mol Cell Neurosci 2001; 17: 973-982.

Kneussel M, Loebrich S. Trafficking and synaptic anchoring of ionotropic inhibitory neurotransmitter receptors. Biol Cell 2007; 99: 297-309.

Knuesel I, Zuellig RA, Schaub MC, Fritschy JM. Alterations in dystrophin and utrophin expression parallel the reorganization of GABAergic synapses in a mouse model of temporal lobe epilepsy. Eur J Neurosci 2001; 13: 1113-1124.

Kohler C. A projection from the deep layers of the entorhinal area to the hippocampal formation in the rat brain. Neurosci Lett 1985a; 56: 13-19.

Kohler C. Intrinsic projections of the retrohippocampal region in the rat brain. I. The subicular complex. J Comp Neurol 1985b; 236: 504-522.

Kubota H, Alle H, Betz H, Geiger JR. Presynaptic glycine receptors on hippocampal mossy fibers. Biochem Biophys Res Commun 2010; 393: 587-591.

Kuhse J, Kuryatov A, Maulet Y, Malosio ML, Schmieden V, Betz H. Alternative splicing generates two isoforms of the alpha 2 subunit of the inhibitory glycine receptor. FEBS Lett 1991; 283: 73-77.

Kumar SS, Buckmaster PS. Hyperexcitability, interneurons, and loss of GABAergic synapses in entorhinal cortex in a model of temporal lobe epilepsy. J Neurosci 2006; 26: 4613-4623.

Lardi-Studler B, Smolinsky B, Petitjean CM, Koenig F, Sidler C, Meier JC *et al*. Vertebrate-specific sequences in the gephyrin E-domain regulate cytosolic aggregation and postsynaptic clustering. J Cell Sci 2007; 120: 1371-1382.

Laube B, Kuryatov A, Kuhse J, Betz H. Glycine-glutamate interactions at the NMDA receptor: role of cysteine residues. FEBS Lett 1993; 335: 331-334.

Lee EA, Cho JH, Choi IS, Nakamura M, Park HM, Lee JJ *et al*. Presynaptic glycine receptors facilitate spontaneous glutamate release onto hilar neurons in the rat hippocampus. J Neurochem 2009; 109: 275-286.

Lee J, Taira T, Pihlaja P, Ransom BR, Kaila K. Effects of CO2 on excitatory transmission apparently caused by changes in intracellular pH in the rat hippocampal slice. Brain Res 1996; 706: 210-216.

Legendre P. A reluctant gating mode of glycine receptor channels determines the time course of inhibitory miniature synaptic events in zebrafish hindbrain neurons. J Neurosci 1998; 18: 2856-2870.

Legendre P. The glycinergic inhibitory synapse. Cell Mol Life Sci 2001; 58: 760-793.

Levi S, Logan SM, Tovar KR, Craig AM. Gephyrin is critical for glycine receptor clustering but not for the formation of functional GABAergic synapses in hippocampal neurons. J Neurosci 2004; 24: 207-217.

Li RW, Yu W, Christie S, Miralles CP, Bai J, Loturco JJ *et al*. Disruption of postsynaptic GABA receptor clusters leads to decreased GABAergic innervation of pyramidal neurons. J Neurochem 2005; 95: 756-770.

Lohmann C, Finski A, Bonhoeffer T. Local calcium transients regulate the spontaneous motility of dendritic filopodia. Nat Neurosci 2005; 8: 305-312.

Loup F, Wieser HG, Yonekawa Y, Aguzzi A, Fritschy JM. Selective alterations in GABAA receptor subtypes in human temporal lobe epilepsy. J Neurosci 2000; 20: 5401-5419.

Lu T, Rubio ME, Trussell LO. Glycinergic transmission shaped by the corelease of GABA in a mammalian auditory synapse. Neuron 2008; 57: 524-535.

Luders HO, Burgess R, Noachtar S. Expanding the international classification of seizures to provide localization information. Neurology 1993; 43: 1650-1655.

Ludwig A, Li H, Saarma M, Kaila K, Rivera C. Developmental up-regulation of KCC2 in the absence of GABAergic and glutamatergic transmission. Eur J Neurosci 2003; 18: 3199-3206.

Lurton D, El Bahh B, Sundstrom L, Rougier A. Granule cell dispersion is correlated with early epileptic events in human temporal lobe epilepsy. J Neurol Sci 1998; 154: 133-136.

Luscher B, Keller CA. Regulation of GABAA receptor trafficking, channel activity, and functional plasticity of inhibitory synapses. Pharmacol Ther 2004; 102: 195-221.

Lynch JW. Native glycine receptor subtypes and their physiological roles. Neuropharmacology 2009; 56: 303-309.

Maas C, Tagnaouti N, Loebrich S, Behrend B, Lappe-Siefke C, Kneussel M. Neuronal cotransport of glycine receptor and the scaffold protein gephyrin. J Cell Biol 2006; 172: 441-451.

Magistretti PJ. Neuron-glia metabolic coupling and plasticity. J Exp Biol 2006; 209: 2304-2311.

Malosio ML, Grenningloh G, Kuhse J, Schmieden V, Schmitt B, Prior P *et al*. Alternative splicing generates two variants of the alpha 1 subunit of the inhibitory glycine receptor. J Biol Chem 1991a; 266: 2048-2053.

Malosio ML, Marqueze-Pouey B, Kuhse J, Betz H. Widespread expression of glycine receptor subunit mRNAs in the adult and developing rat brain. EMBO J 1991b; 10: 2401-2409.

Meier J. The enigma of transmitter-selective receptor accumulation at developing inhibitory synapses. Cell Tissue Res 2003; 311: 271-276.

Meier J, De Chaldee M, Triller A, Vannier C. Functional Heterogeneity of Gephyrins. Mol Cell Neurosci 2000a; 16: 566-577.

Meier J, Grantyn R. A gephyrin-related mechanism restraining glycine receptor anchoring at GABAergic synapses. J Neurosci 2004; 24: 1398-1405.

Meier J, Meunier-Durmort C, Forest C, Triller A, Vannier C. Formation of glycine receptor clusters and their accumulation at synapses. J Cell Sci 2000b; 113: 2783-2795.

Meier J, Vannier C, Serge A, Triller A, Choquet D. Fast and reversible trapping of surface glycine receptors by gephyrin. Nat Neurosci 2001; 4: 253-260.

Meier JC, Henneberger C, Melnick I, Racca C, Harvey RJ, Heinemann U *et al*. RNA editing produces glycine receptor α3P185L resulting in high agonist potency. Nat Neurosci 2005; 8: 736-744.

Meyer G, Kirsch J, Betz H, Langosch D. Identification of a gephyrin binding motif on the glycine receptor beta subunit. Neuron 1995; 15: 563-572.

Miller PS, Harvey RJ, Smart TG. Differential agonist sensitivity of glycine receptor alpha2 subunit splice variants. Br J Pharmacol 2004; 143: 19-26.

Mitchell SJ, Silver RA. Shunting inhibition modulates neuronal gain during synaptic excitation. Neuron 2003; 38: 433-445.

Mody I. Distinguishing between GABA(A) receptors responsible for tonic and phasic conductances. Neurochem Res 2001; 26: 907-913.

Mody I, Pearce RA. Diversity of inhibitory neurotransmission through GABA(A) receptors. Trends Neurosci 2004; 27: 569-575.

Monyer H, Markram H. Interneuron Diversity series: Molecular and genetic tools to study GABAergic interneuron diversity and function. Trends Neurosci 2004; 27: 90-97.

Moss SJ, Doherty CA, Huganir RL. Identification of the cAMP-dependent protein kinase and protein kinase C phosphorylation sites within the major intracellular domains of the beta 1, gamma 2S, and gamma 2L subunits of the gamma-aminobutyric acid type A receptor. J Biol Chem 1992; 267: 14470-14476.

Moss SJ, Smart TG. Constructing inhibitory synapses. Nat Rev Neurosci 2001; 2: 240-250.

Muir J, rancibia-Carcamo IL, Macaskill AF, Smith KR, Griffin LD, Kittler JT. NMDA receptors regulate GABAA receptor lateral mobility and clustering at inhibitory synapses through serine 327 on the gamma2 subunit. Proc Natl Acad Sci U S A 2010; 107: 16679-16684.

Müller E, Bakkar W, Legendre P, Bergeron R, Martina M. Site and mechanism of glycine release at glutamatergic synapse in mouse hippocampus. San Diego, CA: Society for Neuroscience 2007; Program No. 358.12/J20.

Mulligan SJ, MacVicar BA. Calcium transients in astrocyte endfeet cause cerebrovascular constrictions. Nature 2004; 431: 195-199.

Nason A, Lee KY, Pan SS, Ketchum PA, Lamberti A, DeVries J. Invitro formation of assimilatory reduced nicotinamide adenine dinucleotide phosphate: nitrate reductase from a Neurospora mutant and a component of molybdenum-enzymes. Proc Natl Acad Sci U S A 1971; 68: 3242-3246.

Navarro-Lerida I, Martinez MM, Roncal F, Gavilanes F, Albar JP, Rodriguez-Crespo I. Proteomic identification of brain proteins that interact with dynein light chain LC8. Proteomics 2004; 4: 339-346.

Neuhoff H, Sassoe-Pognetto M, Panzanelli P, Maas C, Witke W, Kneussel M. The actin-binding protein profilin I is localized at synaptic sites in an activity-regulated manner. Eur J Neurosci 2005; 21: 15-25.

Nikolic Z, Laube B, Weber RG, Lichter P, Kioschis P, Poustka A *et al*. The human glycine receptor subunit alpha3. Glra3 gene structure, chromosomal localization, and functional characterization of alternative transcripts. J Biol Chem 1998; 273: 19708-19714.

Nimmerjahn A, Kirchhoff F, Helmchen F. Resting microglial cells are highly dynamic surveillants of brain parenchyma in vivo. Science 2005; 308: 1314-1318.

O'Sullivan GA, Kneussel M, Elazar Z, Betz H. GABARAP is not essential for GABA receptor targeting to the synapse. Eur J Neurosci 2005; 22: 2644-2648.

Paarmann I, Schmitt B, Meyer B, Karas M, Betz H. Mass spectrometric analysis of glycine receptor-associated gephyrin splice variants. J Biol Chem 2006; 281: 34918-34925.

Padgett CL, Lummis SC. The F-loop of the GABA A receptor gamma2 subunit contributes to benzodiazepine modulation. J Biol Chem 2008; 283: 2702-2708.

Palma E, Amici M, Sobrero F, Spinelli G, Di AS, Ragozzino D *et al*. Anomalous levels of Cl- transporters in the hippocampal subiculum from temporal lobe epilepsy patients make GABA excitatory. Proc Natl Acad Sci U S A 2006; 103: 8465-8468.

Palma E, Spinelli G, Torchia G, Martinez-Torres A, Ragozzino D, Miledi R *et al*. Abnormal GABAA receptors from the human epileptic hippocampal subiculum microtransplanted to Xenopus oocytes. Proc Natl Acad Sci U S A 2005; 102: 2514-2518.

Papadopoulos T, Korte M, Eulenburg V, Kubota H, Retiounskaia M, Harvey RJ *et al*. Impaired GABAergic transmission and altered hippocampal synaptic plasticity in collybistin-deficient mice. EMBO J 2007; 26: 3888-3899.

Poulopoulos A, Aramuni G, Meyer G, Soykan T, Hoon M, Papadopoulos T *et al*. Neuroligin 2 drives postsynaptic assembly at perisomatic inhibitory synapses through gephyrin and collybistin. Neuron 2009; 63: 628-642.

Prior P, Schmitt B, Grenningloh G, Pribilla I, Multhaup G, Beyreuther K *et al*. Primary structure and alternative splice variants of gephyrin, a putative glycine receptor-tubulin linker protein. Neuron 1992; 8: 1161-1170.

Qu L, Leung LS. Mechanisms of hyperthermia-induced depression of GABAergic synaptic transmission in the immature rat hippocampus. J Neurochem 2008; 106: 2158-2169.

Qu L, Leung LS. Effects of temperature elevation on neuronal inhibition in hippocampal neurons of immature and mature rats. J Neurosci Res 2009; 87: 2773-2785.

Raiteri L, Raiteri M. Functional 'glial' GLYT1 glycine transporters expressed in neurons. J Neurochem 2010; 114: 647-653.

Ramming M, Kins S, Werner N, Hermann A, Betz H, Kirsch J. Diversity and phylogeny of gephyrin: Tissue-specific splice variants, gene structure, and sequence similarities to molybdenum cofactor-synthesizing and cytoskeleton-associated proteins. Proc Natl Acad Sci U S A 2000; 97: 10266-10271.

rancibia-Carcamo IL, Yuen EY, Muir J, Lumb MJ, Michels G, Saliba RS *et al*. Ubiquitin-dependent lysosomal targeting of GABA(A) receptors regulates neuronal inhibition. Proc Natl Acad Sci U S A 2009; 106: 17552-17557.

Reiss J, Gross-Hardt S, Christensen E, Schmidt P, Mendel RR, Schwarz G. A mutation in the gene for the neurotransmitter receptor-clustering protein gephyrin causes a novel form of molybdenum cofactor deficiency. Am J Hum Genet 2001; 68: 208-213.

Reiss J, Johnson JL. Mutations in the molybdenum cofactor biosynthetic genes MOCS1, MOCS2, and GEPH. Hum Mutat 2003; 21: 569-576.

Rivera C, Li H, Thomas-Crusells J, Lahtinen H, Viitanen T, Nanobashvili A *et al*. BDNF-induced TrkB activation down-regulates the K+-Cl- cotransporter KCC2 and impairs neuronal Cl- extrusion. J Cell Biol 2002; 159: 747-752.

Rivera C, Voipio J, Kaila K. Two developmental switches in GABAergic signalling: the K+-Cl- cotransporter KCC2 and carbonic anhydrase CAVII. J Physiol 2005; 562: 27-36.

Rivera C, Voipio J, Payne JA, Ruusuvuori E, Lahtinen H, Lamsa K *et al*. The K+/Cl- co-transporter KCC2 renders GABA hyperpolarizing during neuronal maturation. Nature 1999; 397: 251-255.

Rivera C, Voipio J, Thomas-Crusells J, Li H, Emri Z, Sipila S *et al*. Mechanism of activity-dependent downregulation of the neuron-specific K-Cl cotransporter KCC2. J Neurosci 2004; 24: 4683-4691.

Roux MJ, Supplisson S. Neuronal and glial glycine transporters have different stoichiometries. Neuron 2000; 25: 373-383.

Ruth RE, Collier TJ, Routtenberg A. Topography between the entorhinal cortex and the dentate septotemporal axis in rats: I. Medial and intermediate entorhinal projecting cells. J Comp Neurol 1982; 209: 69-78.

Ruth RE, Collier TJ, Routtenberg A. Topographical relationship between the entorhinal cortex and the septotemporal axis of the dentate gyrus in rats: II. Cells projecting from lateral entorhinal subdivisions. J Comp Neurol 1988; 270: 506-516.

Sabatini DM, Barrow RK, Blackshaw S, Burnett PE, Lai MM, Field ME *et al*. Interaction of RAFT1 with gephyrin required for rapamycin-sensitive signaling. Science 1999; 284: 1161-1164.

Saiepour L, Fuchs C, Patrizi A, Sassoe-Pognetto M, Harvey RJ, Harvey K. Complex role of collybistin and gephyrin in GABAA receptor clustering. J Biol Chem 2010; 285: 29623-29631.

Saiyed T, Paarmann I, Schmitt B, Haeger S, Sola M, Schmalzing G *et al*. Molecular basis of gephyrin clustering at inhibitory synapses: role of G- and E-domain interactions. J Biol Chem 2007; 282: 5625-5632.

Sanes JR, Lichtman JW. Can molecules explain long-term potentiation? Nat Neurosci 1999; 2: 597-604.

Santambrogio L, Belyanskaya SL, Fischer FR, Cipriani B, Brosnan CF, Ricciardi-Castagnoli P *et al*. Developmental plasticity of CNS microglia. Proc Natl Acad Sci U S A 2001; 98: 6295-6300.

Schrader N, Kim EY, Winking J, Paulukat J, Schindelin H, Schwarz G. Biochemical characterization of the high affinity binding between the glycine receptor and gephyrin. J Biol Chem 2004; 279: 18733-18741.

Schwarz G. Molybdenum cofactor biosynthesis and deficiency. Cell Mol Life Sci 2005; 62: 2792-2810.

Schwarz G, Mendel RR, Ribbe MW. Molybdenum cofactors, enzymes and pathways. Nature 2009; 460: 839-847.

Schwarz G, Schrader N, Mendel RR, Hecht HJ, Schindelin H. Crystal structures of human gephyrin and plant cnx1 g domains: comparative analysis and functional implications. J Mol Biol 2001; 312: 405-418.

Schweizer C, Balsiger S, Bluethmann H, Mansuy IM, Fritschy JM, Mohler H *et al*. The gamma2 subunit of GABA(A) receptors is required for maintenance of receptors at mature synapses. Mol Cell Neurosci 2003; 24: 442-450.

Seifert G, Schroder W, Hinterkeuser S, Schumacher T, Schramm J, Steinhauser C. Changes in flip/flop splicing of astroglial AMPA receptors in human temporal lobe epilepsy. Epilepsia 2002; 43 Suppl 5: 162-167.

Shaw G, Morse S, Ararat M, Graham FL. Preferential transformation of human neuronal cells by human adenoviruses and the origin of HEK 293 cells. FASEB J 2002; 16: 869-871.

Shulga A, Thomas-Crusells J, Sigl T, Blaesse A, Mestres P, Meyer M *et al*. Posttraumatic GABA(A)-mediated [Ca2+]i increase is essential for the induction of brain-derived neurotrophic factor-dependent survival of mature central neurons. J Neurosci 2008; 28: 6996-7005.

Simon J, Wakimoto H, Fujita N, Lalande M, Barnard EA. Analysis of the set of GABA(A) receptor genes in the human genome. J Biol Chem 2004; 279: 41422-41435.

Smith MJ, Pozo K, Brickley K, Stephenson FA. Mapping the GRIF-1 binding domain of the kinesin, KIF5C, substantiates a role for GRIF-1 as an adaptor protein in the anterograde trafficking of cargoes. J Biol Chem 2006; 281: 27216-27228.

Smolinsky B, Eichler SA, Buchmeier S, Meier JC, Schwarz G. Splice-specific functions of gephyrin in molybdenum cofactor biosynthesis. J Biol Chem 2008; 283: 17370-17379.

Sola M, Bavro VN, Timmins J, Franz T, Ricard-Blum S, Schoehn G *et al*. Structural basis of dynamic glycine receptor clustering by gephyrin. EMBO J 2004; 23: 2510-2519.

Sola M, Kneussel M, Heck IS, Betz H, Weissenhorn W. X-ray crystal structure of the trimeric N-terminal domain of gephyrin. J Biol Chem 2001; 276: 25294-25301.

Song W, Chattipakorn SC, McMahon LL. Glycine-gated chloride channels depress synaptic transmission in rat hippocampus. J Neurophysiol 2006; 95: 2366-2379.

Stallmeyer B, Nerlich A, Schiemann J, Brinkmann H, Mendel RR. Molybdenum co-factor biosynthesis: the Arabidopsis thaliana cDNA cnx1 encodes a multifunctional two-domain protein homologous to a mammalian neuroprotein, the insect protein Cinnamon and three Escherichia coli proteins. Plant J 1995; 8: 751-762.

Stallmeyer B, Schwarz G, Schulze J, Nerlich A, Reiss J, Kirsch J *et al*. The neurotransmitter receptor-anchoring protein gephyrin reconstitutes molybdenum cofactor biosynthesis in bacteria, plants, and mammalian cells. Proc Natl Acad Sci U S A 1999; 96: 1333-1338.

Steward O. Topographic organization of the projections from the entorhinal area to the hippocampal formation of the rat. J Comp Neurol 1976; 167: 285-314.

Steward O, Scoville SA. Cells of origin of entorhinal cortical afferents to the hippocampus and fascia dentata of the rat. J Comp Neurol 1976; 169: 347-370.

Stief F, Zuschratter W, Hartmann K, Schmitz D, Draguhn A. Enhanced synaptic excitation-inhibition ratio in hippocampal interneurons of rats with temporal lobe epilepsy. Eur J Neurosci 2007; 25: 519-528.

Supplisson S, Roux MJ. Why glycine transporters have different stoichiometries. FEBS Lett 2002; 529: 93-101.

Tang W, Ehrlich I, Wolff SB, Michalski AM, Wolfl S, Hasan MT *et al*. Faithful expression of multiple proteins via 2A-peptide self-processing: a versatile and reliable method for manipulating brain circuits. J Neurosci 2009; 29: 8621-8629.

Tao HW, Poo MM. Activity-dependent matching of excitatory and inhibitory inputs during refinement of visual receptive fields. Neuron 2005; 45: 829-836.

Thomas P, Mortensen M, Hosie AM, Smart TG. Dynamic mobility of functional GABAA receptors at inhibitory synapses. Nat Neurosci 2005; 8: 889-897.

Tretter V, Jacob TC, Mukherjee J, Fritschy JM, Pangalos MN, Moss SJ. The clustering of GABA(A) receptor subtypes at inhibitory synapses is facilitated via the direct binding of receptor alpha2 subunits to gephyrin. J Neurosci 2008; 28: 1356-1365.

Turecek R, Trussell LO. Presynaptic glycine receptors enhance transmitter release at a mammalian central synapse. Nature 2001; 411: 587-590.

Tyagarajan SK, Ghosh H, Yevenes GE, Nikonenko I, Ebeling C, Schwerdel C *et al*. Regulation of GABAergic synapse formation and plasticity by GSK3{beta}-dependent phosphorylation of gephyrin. Proc Natl Acad Sci U S A 2011; 108: 379-384.

Ule J, Jensen KB, Ruggiu M, Mele A, Ule A, Darnell RB. CLIP Identifies Nova-Regulated RNA Networks in the Brain. Science 2003; 302: 1212-1215.

van Zundert B, Alvarez FJ, Yevenes GE, Carcamo JG, Vera JC, Aguayo LG. Glycine Receptors Involved in Synaptic Transmission Are Selectively Regulated by the Cytoskeleton in Mouse Spinal Neurons. J Neurophysiol 2002; 87: 640-644.

Varley ZK, Pizzarelli R, Antonelli R, Stancheva SH, Kneussel M, Cherubini E *et al*. Gephyrin regulates GABAergic and glutamatergic synaptic transmission in hippocampal cell cultures. J Biol Chem 2011; 286: 20942-20951.

Vithlani M, Moss SJ. The role of GABAAR phosphorylation in the construction of inhibitory synapses and the efficacy of neuronal inhibition. Biochem Soc Trans 2009; 37: 1355-1358.

Vizi ES, Kiss JP. Neurochemistry and pharmacology of the major hippocampal transmitter systems: synaptic and nonsynaptic interactions. Hippocampus 1998; 8: 566-607.

Waseem TV, Fedorovich SV. Presynaptic glycine receptors influence plasma membrane potential and glutamate release. Neurochem Res 2010; 35: 1188-1195.

Wassle H. Parallel processing in the mammalian retina. Nat Rev Neurosci 2004; 5: 747-757.

Whiting P, McKernan RM, Iversen LL. Another mechanism for creating diversity in gamma-aminobutyrate type A receptors: RNA splicing directs expression of two forms of gamma 2 phosphorylation site. Proc Natl Acad Sci U S A 1990; 87: 9966-9970.

Wisden W, Cope D, Klausberger T, Hauer B, Sinkkonen ST, Tretter V *et al*. Ectopic expression of the GABA(A) receptor alpha6 subunit in hippocampal pyramidal neurons produces extrasynaptic receptors and an increased tonic inhibition. Neuropharmacology 2002; 43: 530-549.

Witter MP, Griffioen AW, Jorritsma-Byham B, Krijnen JL. Entorhinal projections to the hippocampal CA1 region in the rat: an underestimated pathway. Neurosci Lett 1988; 85: 193-198.

Witter MP, Groenewegen HJ, Lopes da Silva FH, Lohman AH. Functional organization of the extrinsic and intrinsic circuitry of the parahippocampal region. Prog Neurobiol 1989; 33: 161-253.

Wyler AR, Dohan FC, Jr., Schweitzer JB, Berry III AD. A grading system for mesial temporal pathology (hippocampal sclerosis) from anterior temporal lobectomy. J Epilepsy 1992; 5: 220-225.

Xiang S, Nichols J, Rajagopalan KV, Schindelin H. The crystal structure of Escherichia coli MoeA and its relationship to the multifunctional protein gephyrin. Structure (Camb) 2001; 9: 299-310.

Yu W, Jiang M, Miralles CP, Li RW, Chen G, De Blas AL. Gephyrin clustering is required for the stability of GABAergic synapses. Mol Cell Neurosci 2007; 36: 484-500.

Zhang LH, Gong N, Fei D, Xu L, Xu TL. Glycine Uptake Regulates Hippocampal Network Activity via Glycine Receptor-Mediated Tonic Inhibition. Neuropsychopharmacology 2008; 33: 701-711.

Zita MM, Marchionni I, Bottos E, Righi M, Del SG, Cherubini E *et al*. Post-phosphorylation prolyl isomerisation of gephyrin represents a mechanism to modulate glycine receptors function. EMBO J 2007; 26: 1761-1771.

Zonta M, Angulo MC, Gobbo S, Rosengarten B, Hossmann KA, Pozzan T *et al*. Neuron-to-astrocyte signaling is central to the dynamic control of brain microcirculation. Nat Neurosci 2003; 6: 43-50.

Curriculum Vitae

For reasons of data protection, the CV is not included in the online version.